1-15-2013 12:00 AM

Developing Electrochemical Biosensors for Point-of-care Diagnostics of Cardiovascular Biomarkers

Yang Cheng
The University of Western Ontario

Supervisor
Dr. Jun Yang
The University of Western Ontario

Graduate Program in Mechanical and Materials Engineering
A thesis submitted in partial fulfillment of the requirements for the degree in Master of Science

Developing Electrochemical Biosensors for Point-of-care Diagnostics of Cardiovascular Biomarkers

(Spine title: Design and Develop Amperometric Cardiac Troponin I Immunosensor)

(Thesis format: Monograph)

by

Yang Cheng

Department of Mechanical and Materials Engineering
Faculty of Engineering

Submitted in partial fulfillment
of the requirements for the degree of
Master of Engineering Science

The School of Graduate and Postdoctoral Studies
The University of Western Ontario
London, Ontario, Canada

THE UNIVERSITY OF WESTERN ONTARIO
School of Graduate and Postdoctoral Studies

CERTIFICATE OF EXAMINATION

Supervisor

_____
Dr. Jun Yang

Examiners

_____
Dr. Xunliang (Andy) Sun

_____
Dr. George K Knopf

_____
Dr. Ken Yeung

The thesis by

Yang Cheng

entitled:

Developing Electrochemical Biosensors for Point-of-care Diagnostics of Cardiovascular Biomarkers

is accepted in partial fulfillment of the
requirements for the degree of
Master of Engineering Science

_____ _____
Date Chair of the Thesis Examination Board

Abstract

Troponin is known as a type of reliable biomarker for the detection of cardiac disorders. Cardiac troponin I (cTnI), as a subunit of troponin, is highly sensitive to cardiac injury; therefore, the cTnI level is used as an index to diagnose myocardial damage, particularly acute myocardial infarction. It can be also used in cardiospecific diagnosis, risk stratification therapeutic treatment and post risk management. In this research, an amperometric immunosensor was developed based on planar electrode and sandwich ELISA format. The electrical response corresponding to biological information was obtained via four main procedures, including electrode modification, immunoreaction, signal amplifications and amperometric detection. Enzyme labels such as horseradish peroxide (HRP) and alkaline phosphatase (ALP) were used for signals amplification. Since alkaline phosphatase works better in low background current levels and has great reproducibility, it was used for nanomaterials, chitosan, gold nanoparticle, carbon nanotube as electrode modification investigation. The anti-cTnI antibody is detectable by electrochemical technology. Necessary conditions and interferences of the experiment were examined. Detection range was from 0.001 ng ml^{-1} to 300 ng ml^{-1} on PDDA-MWCNT sensor, and from 0.02 ng ml^{-1} to 200 ng ml^{-1} on chitosan-AuNPs sensor. The detection range was investigated using cyclic voltammetry. The signal behavior recorded was linear to cTnI concentration. This behavior makes the developed biosensor be able to widely use in clinical practice. Likewise, two liquid substrates were catalyzed by hydroquinone and 3, 3', 5, 5'-teteramethylbenzidine respectively. Hydrogen peroxide (H_2O_2) is a product of glucose oxidizes catalyzing the oxidation of β-D-glucose by oxygen. It is also used as an oxidizing agent in catalyzing HRP. Hence, an HRP-based immunosensor is important in integrating an immunosensor and an enzyme sensor for the purpose of achieving multianalyte detection compacted on one chip. The cTnI immunosensor developed here is rapid, easy-to-use, cost-efficient and robust.

Keywords

Cardiac biomarkers, cardiac troponin I (cTnI), point-of-care, electrochemical immunosensor, amperometric, sandwich ELISA, Horseradish peroxide, alkaline phosphatase.

Acknowledgments

It has been a wonderful and unforgettable experience that spending recent several years on completing my Master's thesis in the Department of Mechanical and Materials Engineering, Western University.

First of all, I would like to express my deepest gratitude to my supervisor Dr. Jun Yang for giving me such a great opportunity to work on this promising field. It has been a real pleasure to work with him, who taught me not only about solving the problems in study and research, but also how to deal with all the difficulties in the real world.

Furthermore, I am indebted to Dr. Qiuquan Guo and Dr. Tingjie Li. I learned a lot from them, such as sophisticated laboratory skills and the ability of developing new techniques to tackle the challenges in research. Their hard-working and high standard of self-management demonstrated as great examples in my research life. I am also very grateful to my other colleagues at Bionanotechnology Research Lab for all the informational and pleasant brainstorm time, which offered me plenty of new ideas.

I would like to thank my friends at Western. All the time we spent together in the lectures, study room and library will always be in my memory.

Special thanks to my significant other, Ran Xu, who has been supporting and encouraging me from the beginning till the end, especially in the time of difficulties.

Finally, I deeply appreciate the constant support from my family. Their belief and encouragement made me realize me how lucky I am as a member of them.

Table of Contents

CERTIFICATE OF EXAMINATION ii

Abstract iii

Acknowledgments iv

Table of Contents v

List of Tables viii

List of Figures ix

Chapter 1 1

1 Introduction 1

1.1 Cardiovascular disease 1

1.1.1 Cardiac biomarker detection: immunoassay 4

1.2 Cardiac biomarkers and application 4

1.2.1 Biomarkers of cardiac injury 5

1.2.2 Clinical application of cardiac biomarkers 9

1.3 Objective and outline of thesis 10

Chapter 2 12

2 Literature review 12

2.1 Point-of-care immunoassay 12

2.2 Immunosensor and nanomaterial enhancement 19

2.2.1 Nanomaterials: classification and application 19

2.2.2 State-of-the-art nanomaterials for cardiac immunosensors 22

2.3 Current commercialized cardiac point-of-care assays 25

2.4 Summary 34

Chapter 3 35

3 Sensor fabrication and biodetection 35

3.1 Introduction 35
3.2 Sensor fabrication 37
3.2.1 Materials and supplies 37
3.2.2 Fabrication procedure 37
3.3 Biodetection 41
3.3.1 Immunoassay 41
3.3.2 Working principle and classification 42
3.3.3 Procedures 44
3.4 Conclusion 45
Chapter 4 46
4 Electrode modification and optimization 46
4.1 Introduction 46
4.2 Experimental 48
4.2.1 Chemicals 48
4.2.2 Apparatus 49
4.2.3 Electrode preparation and pretreatment 51
4.2.4 Electrode modification and characterization 52
4.2.5 Preparation of antibody-enzyme conjugates 52
4.2.6 Immunoassay protocols 53
4.2.7 Electrochemical detection 54
4.3 Results and discussion 54
4.3.1 Electrochemical characteristics of bare electrode 54
4.3.2 Characteristics of CNT, AuNP 55
4.3.3 Cyclic voltammetry characterization of PDDA-MWCNT modified electrodes 56
4.3.4 Cyclic voltammetry characterization of PDDA-MWCNT and AuNPs modified electrodes 58

4.3.5 CV characterization of cTnI immunosensor 59
4.3.6 Optimization of immunoassay procedure 61
4.3.7 Calibration curve of the cTnI immunosensor 64
4.3.8 Stability and reproducibility of the cTnI immunosensor 69
4.3.9 Accuracy and clinical application 70
4.4 Conclusions 72
Chapter 5 73
5 HRP- and ALP-label enzyme comparison study 73
5.1 Introduction 73
5.2 Experimental 75
5.2.1 Materials and reagents 75
5.2.2 Preparation of antibody-enzyme conjugates 75
5.2.3 Construction of PB-PDDA-MWCNT Glucose Biosensor 76
5.2.4 Electrochemical and immunosensing experiments 78
5.3 Results and discussion 79
5.3.1 Principle of the glucose- cTnI immunosensor 79
5.3.2 Glucose deterimination 80
5.3.3 Feasibility study: HRP determination 84
5.3.4 Multimarker concept 87
5.4 Conclusion 87
Chapter 6 88
6 Summary and outlook 88
6.1 Summary 88
6.2 Thesis contributions 89
6.3 Recommendation for future work 89

List of Tables

Table 1.1: Clinical utilized cardiac biomarkers for diagnosing CVD. Adapted from (Mohammed and Desmulliez, 2011)..... 10

Table 2.1: Current Cardiac point-of-care available device. Adapted from (Christenson and Azzazy, 1998) 27

Table 3.1: Recommended coating parameters for LOR 5A (MicroChem Corp, 2001) 40

Table 3.2: Undercut size versus developing time. 41

Table 4.1: Characteristics of current cTnI POC assays. Adapted from (Christenson and Azzazy, 2009) 69

Table 4.2: Comparison of Measured cTnI levels between two methods. 71

List of Figures

Figure 1.1: Cardiac injury: the pathophysiology of acute coronary syndromes (ACS). Adapted from Ref. (Azzazy and Christenson, 2002). 2

Figure 1.2: ACS clinical classification regarding electrocardiogram. Adapted from Ref. (Azzazy and Christenson, 2002). 3

Figure 2.1: Central laboratories testing versus point-of-care testing in the clinical situation. 13

Figure 2.2: Schematics of typical POC testing. (a) An agglutination for HIV serology test. (b) Steps in rapid diagnostic test (lateral-flow test) for malaria antigen detection. (c) Classic light microscopy using Giemsa stain, results shown in both the thick and the thin smear. Figures adapted from Ref (Buhrer-Sekula et al., 2003; Kemp et al., 1988; Payne, 1988) 16

Figure 2.3: Gene-Z schematics and prototype. (a) An empty chip with four parallel reaction arrays. (b) Working principle and decomposition structure of the Gene-Z chip (c) Gene-Z prototype operated by an iPod set on the recharge port and the chip insertion door. Figures reprinted from Ref (Stedtfeld et al., 2012)..... 17

Figure 2.4: Schematics of various paper-based devices. Adapter from Ref (Zang, Ge et al., 2012; Cheng, Martinez et al., 2010; Ge, Wang et al., 2012) 18

Figure 2.5: Schematics of paper-based microfluidic electrochemiluminescence: fabrication and analysis. Figure adapted from Ref (Delaney et al., 2011)..... 18

Figure 2.6: An overview of various nanostructures (NSs) that are used in diagnostic assays. Reproduced from Ref. (Kurkina and Balasubramanian, 2012) 20

Figure 2.7: SiNW device demonstration: (a) SiNW microfluidics chip; (b) the layout of the SiNW device array; (c) SEM image of nanowires clusters. Adapted from (Chua et al., 2009). 23

Figure 2.8: Cardiac STATus™ Kit- Triple markers testing. Adapted with permission from Nanogen Inc. 28

Figure 2.9: Stratus® CS STAT fluorometric analyzer. Reprinted with permission from Siemens Medical Diagnostics. 29

Figure 2.10: Biosite's Triage flow-through detection technology. Reprinted with permission from Biosite. 30

Figure 2.11: RAMP cardiac marker system. Reprinted with permission from Response Biomedical Corporation. 31

Figure 2.12: i-STAT® system Portable cardiac analyzer and the explode view of the cartridge. Reprinted with permission from Abbott Point of Care Inc. 33

Figure 2.13 : Roche Cardiac Reader system and principle schematic. Reprinted with permission from Roche Diagnostics and Ref. (Collinson et al., 2001) 34

Figure 3.1: Schematic of the electrode layer structures. 37

Figure 3.2: Apparatus of main procedures for photolithography and metallization. 38

Figure 3.3: Spin speed versus thickness for Lift-off resist series. 39

Figure 3.4: The influence of soft bake time and temperature. 40

Figure 3.5: Working schematics of the traditional ELISA. 43

Figure 3.6: Schematics of the one-step electrochemical ELISA. 43

Figure 3.7: Configuration of cardiac troponin I immunosensor. 45

Figure 4.1: Planar electrode and preliminary design for immunosensor embedded in a microfluidic chip. 49

Figure 4.2: Illustration of antibody-ALP conjugates: (a) Attachment to antibody, (b) deprotection, and (c) reaction with ALP, (d) Conjugates. Adapted from (Life Technologies) 53

Figure 4.3: Electrochemical indication in 0.02 M PBS (pH 6.5) containing 5.0 mM $K_3[Fe(CN)_6]/K_4[Fe(CN)_6]$ (1:1) mixture and 0.1 M KCl from 0.6 to −0.2 V. 55

Figure 4.4: SEM images of (a) PDDA-MWCNT composite; (b) MWCNT without any treatment; (c) AuNP composite on the surfaces of gold electrodes. 56

Figure 4.5 (a) The cyclic voltammograms of PDDA-MWCNT-Au electrode at various scan rates from 10 to 500 mV s^{-1} in 0.02 M PBS (pH 6.5) containing 5.0 mM $K_3[Fe(CN)_6]/K_4[Fe(CN)_6]$ (1:1) mixture and 0.1 M KCl from 0.6 to −0.2 V. (b) The dependence the redox peak current over the square root of the various scan rates. 57

Figure 4.6: CVs of different modified electrodes in a 5 mM $K_3Fe(CN)_6$ solution containing 0.1M KCl (pH 6.5): (a) PDDA- MWCNT; (b) Chitosan- AuNP; (c) Bare electrode; (d) Chitosan. 59

Figure 4.7: Electrochemical behavior of various modified electrodes in immunoassay: (a) blank, (b) bare electrode, (c) chitosan-AuNPs electrode, (d) PDDA-MWCNT modified surface. 60

Figure 4.8: Influence of (a) pH value; (b) capture antibody concentration; (c) temperature; (d) incubation time on the immunosensor. 63

Figure 4.9: (a) The current-voltage response curves (b) calibration curve of bare gold electrodes. 65

Figure 4.10: (a) The current-voltage response curves (b) calibration curve of chitosan-AuNPs modified gold electrodes. 66

Figure 4.11: (a) The current-voltage response curves (b) calibration curve of PDDA-MWCNT modified gold electrodes. 67

Figure 4.12: Calibration curve of PDDA-MWCNT, AuNPs, and bare electrode. 68

Figure 4.13: Storage stability of the PDDA-MWCNT, AuNPs and bare electrodes. 70

Figure 4.14: Measurement of cTnI with spectrophotometric, the electrochemical with chitosan-AuNPs, PDDA-MWCNT methods in various concentration: 0, 1, 10, 20, 50 ng ml^{-1}. 71

Figure 5.1: Cyclic voltammograms of the electrode pretreatment and PB-glucose sensor construction. (a)Electrode cleaned and activated in 0.5M sulfuric acid; (b) Pb electropolymerization; (c) Pb activation; (d) Biosensor in the null and 5mM glucose. 77

Figure 5.2: Schematics and principle of the cTnI- glucose biosensor. Reprinted with permission from (Henares et al., 2010)..... 80

Figure 5.3: (a)Cyclic voltammograms of PB-PDDA-MWCNT electrodes at various scan rates from 30 to 300 Mv S in PBS (pH 6.78). (b) The dependence of the current of redox peaks over the square root of the scan rate. 81

Figure 5.4 (a) Glucose current-time current response curves (b) standard calibration curve. 83

Figure 5.5: Schematic of Horseradish peroxidase catalysis TMB. 84

Figure 5.6 : Cyclic voltammograms of 0.2 Mm TMB in citrate-phosphatase buffer (pH 5.0). (a) 10 mM glucose; (b) 5 mM glucose; (C) 0 mM glucose. 85

Figure 5.7: Cyclic voltammograms of 0.3 Mm HQ in PBS buffer (pH 7.0) + 0.1 M KCl. (a) PBS-KCl; (b) PBS-KCl-HQ; (c) PBS-KCl-HQ- glucose (5mM). 85

Chapter 1

1 Introduction

This chapter will introduce the background knowledge about cardiovascular disease, various cardiac biomarkers and their clinical applications. Motivation, objective, and outline of the thesis have also been addressed.

1.1 Cardiovascular disease

Regardless of enormous efforts and significant achievements in the precaution and treatment of cardiovascular disease (CVD), a severe medical condition, it still accounts for the majority of adult mortality in the present western world (McDonnell et al., 2009). The data and statistics from America's 2009 Centers for Disease Control and Prevention (CDC) showed that 599,413 Americans died from heart disease (195.2 deaths in every 100,000 people), over 30 million times visit to clinic, hospital or emergency department due to heart disease including primary diagnosis of ischemia heat disease, and up to 42.6% (635,000) cardiac condition patients residing in the nursing homes (CDC Home, 2009). In the European Union, the expense on cardiac condition is roughly 192 billion Euro annually (Allender S, 2008). Each year, countless patients pour in the emergency departments for medical care owning to chest pain syndrome or other forms of acute coronary syndrome (ACS), among which less than 10% are finally diagnosed as acute myocardial infarction (AMI) (Collinson PO, 1999; Lewandrowski et al., 2002). Through the ages, CVD conditions have crippled our human society in terms of health care services, medication and lost productivity.

The challenge is that symptoms, including chest pain, pressure, tightness, dyspnoea and heartburn sensations, are not adequate for correct diagnosis in primary medical clinic. Generally, panic disorder, stable angina, gastrointestinal disease, musculoskeletal pain and viral infection all can cause chest pain syndromes; however the critical suspects would be more severe cardiac conditions: heart failure (HF), thromboembolic events (TE)

and acute coronary syndromes (ACS), especially myocardial infarction (MI) (Brieger et al., 2004; Godfrey et al., 2006; Punukollu et al., 2005; Tomonaga et al., 2011). Figure 1.1 indicates the pathophysiology progression of acute coronary syndromes (ACS). When the fatty streaks accumulated to a certain extent to form plaques, the rupture of plaques and the thrombus will result in gradual deterioration, from unstable angina to heart failure (Azzazy and Christenson, 2002). Myocardial infarction (MI) can be defined as the non-reversible damage of cardiac myocytes caused by sustaining ischemia, resulting in necrosis of myocardial cells. Therefore, MI is recognized as the most life threatening cardiac condition requiring comprehensive, correct and quick diagnosis (Mohammed and Desmulliez, 2011).

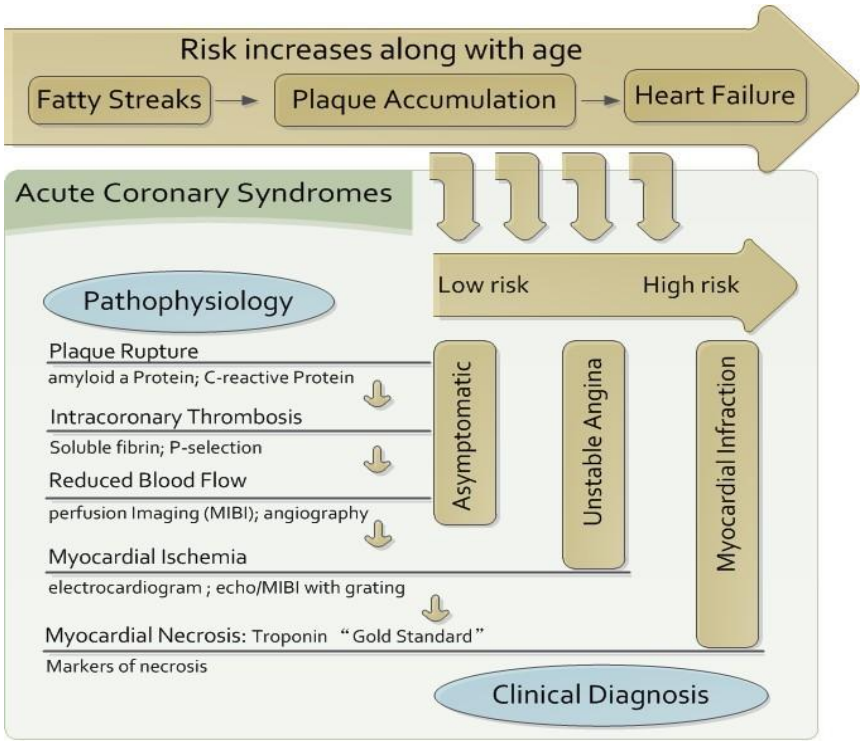

Figure 1.1: Cardiac injury: the pathophysiology of acute coronary syndromes (ACS). Adapted from Ref. (Azzazy and Christenson, 2002).

In 2002, the European Society of Cardiology (ESC) and the American College of Cardiology (ACC) reached consensus and redefined the diagnosis criteria of myocardial infarction: to conform or exclude AMI, it should meet no less than 2 conditions out of chest pain (typical and most common symptoms), elevation of cardiac biomarkers, or abnormal electrocardiogram (ECG) (Alpert et al., 2001; Lewandrowski et al., 2002). Figure 2.2 classifies the ASC patients on their ECG reading. The ECG is vital for treatment decision because patients with ST elevation usually have fibrin rich thrombus. On the other hand, most patients with non-ST elevation myocardial infarction have clots with abundant platelet (Azzazy and Christenson, 2002; Mizuno et al., 1992). Up to 50-70% hospital admissions with chest pain syndromes present normal or ambiguous ECG reading (Brogan and Bock, 1998; Morrow et al., 2007); thus, correct appraisal of elevated cardiac biomarkers is a reliable approach to a proper treatment for patients. Furthermore, the elevation of cardiac markers can indicate the type of ACS, the basic timeline since the initial onset, and even the location of damaged cells (Mohammed and Desmulliez, 2011).

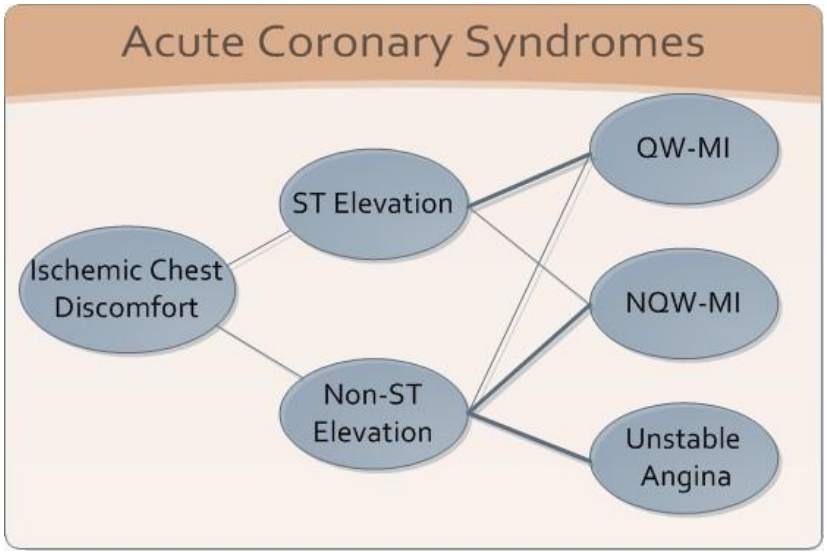

Figure 1.2: ACS clinical classification regarding electrocardiogram. Adapted from Ref. (Azzazy and Christenson, 2002).

1.1.1 Cardiac biomarker detection: immunoassay

Immunoassay is the interaction between antibody and antigen. Antibodies (Abs) are proteins generated by immune system of animals and human bodies in order to response to antigens (Ags), allochthonous substances. Every Ab has a unique structure to bind with the corresponding Ag in a "lock and key mechanism"; therefore, the binding between Ab and Ag is highly specific. To better utilize the benefits of antibody and antigen interaction, especially the sensitivity and specificity, immunoassays possess various formats. It provides the quantification and monitoring of the protein or biomolecules, for example nucleic acids, protein molecules, drugs and metabolites, and the pathogens (Lin et al., 2010b). Nowadays, immunoassay is a prevalent detection method used in food safety, environmental monitoring, biotechnological investigation, and clinical analysis. For cardiac biomarker determination and other biomarkers detection, immunoassay is believed to be the gold-standard technique (Lin et al., 2010b; Mohammed and Desmulliez, 2011). More details of immunoassay will be further discussed in Chapter 3.

1.2 Cardiac biomarkers and application

The history of cardiac biomarkers can be traced back to 1954; Ladue JS et al. reported the unusual elevation of glutamate oxaloacetic in serum after a few hours of acute myocardial infarction (AMI), the duration lasting for 4 to 6 days with a peak in 2 to 3 day (Ladue JS et al., 1954). An ideal biomarker would possess the following properties (Azzazy and Mansour, 2009; Braunwald, 2008):

- Small size: quick releasing from injured tissues
- Tissue specificity: exclusive in cardiac muscle
- High sensitivity: abundant in cardiac tissue
- Release: the concentration in plasma proportion to infarct sizing
- Stability: reach peak immediately after the injury and maintain for hours
- Clearance: cleared rapidly for recurrent injury diagnostic
- Application: Suitable for different stage of cardiac injury and cost effective

Even though, the parameters mentioned above are critical for monitoring ACS potential patients, there is no cardiac biomarker can meet all the requirements. Therefore, the knowledge regarding characteristics of biomarkers is vital for both research and clinical applications. Details about several cardiac biomarkers are discussed below.

1.2.1 Biomarkers of cardiac injury

1.2.1.1 Myoglobin

Myoglobin (MYO) (17.8kDa) is a small and single-chain hemeprotein of 153 amino acids, presenting high concentration in cardiac and red muscle tissue and playing a role as a storage site for transporting oxygen to various tissues or organs (Panteghini et al., 2004). Due to the small molecular size and weight, myoglobin will quickly release into the blood stream through cytoderm (cell wall), an hour or so after the onset of AMI, and then is elevated to the peak value in 4 to 12 hours, followed by a subsequent drop to baseline in 12 more hours (Adams et al., 1993; Gibler et al., 1990; Mair et al., 1992). Since Myoglobin distributed in almost all the tissues, the baseline value is measured over 30 ng/ml in peripheral circulation, normally. Either cardiac or skeletal damage will cause serum myoglobin elevated; therefore, myoglobin are used by hospitals as a negative predictive value (rule out the diagnosis of AMI) instead of conforming the diagnosis of AMI condition. (Lewandrowski et al., 2002; Sluss, 2006)

1.2.1.2 Creatine Kinases

Another well-known cardiac biomarker is Creatine Kinases. The measurements of CK (molecular weight 87kDa) and CK-MB (86kDa) for diagnosing AMI have a long history. Furthermore, the elevation of CK-MB was regarded as the traditional “gold standard” in 1980s for over two decades. CK has three subunits (three different types based on locating organs) including MM, MB, and BB, which present in both myocardium and skeletal tissues (Christenson and Azzazy, 1998; Lewandrowski et al., 2002). The concentration of CK-MM is dominant in skeletal muscle, 98% over total muscle CK. CK-MB presents only 2% to 5% in healthy skeletal muscle and higher level in patients with chronic myopathic injury and renal failure. Even though, CK-MB occupies over 20% in the myocardium over the total myocardial CK, still less than the concentration of CK-

MM in myocardial muscle. Therefore, the CK total elevation can be clinically applied in diagnosing skeletal muscle injury or disorders but not cardiac specific conditions (Lewandrowski et al., 2002). After cardiac injury, CK-MB starts to release into the bloodstream from the injured tissue in 4 to 9 hours of the occurrence of chest pain, reaches the peak at 24 hours and returns to normal value in 48 to 72 hours (Males et al., 2001). Therefore, CK-MB would not be a good candidate for AMI early stage, but be suitable for reinfarction diagnosis and critical aid tool in multimarker panel (Panteghini, 1998).

Since both myocardial and skeletal injury will cause total CK and CK-MB elevated, the ratio of CK-MB to total CK can be calculated for distinguishing cardiac specific conditions. Mostly, in the lab-based testing, when CK-MB is more than 5% of the total, it can be called as suggestive AMI (Lewandrowski et al., 2002). Furthermore, regardless of the emergence of troponin I, CK-MB remains high value in clinical application, such as decision making in ED department (Young et al., 1991), guidance of disposition decisions (Hedges et al., 1996), prognosis in patients with AMI symptoms and non-diagnostic ECGs (Hoekstra et al., 1994), and a valuable indicator in multiplex assays (Galla et al., 2006).

1.2.1.3 Cardiac Troponins

Cardiac troponins (low molecular weight 20- 25kDa) have significant sensitivity and specificity for myocardial muscle damage; therefore, they have been regarded as the "gold standard" for acute myocardial infarction diagnosis (Alpert et al., 2000; Martins et al., 1996). Even though, cardiac troponins only have been measurable for three decades, cTnT in 1989 (Katus et al., 1989) and cTnI in 1991(Bodor et al., 1992), the influence boosted tremendous advancement of the cardiac marker measurements. Troponin, as a regulatory complex, has three subunits on the thin filament combined with myocardial contractile muscle to control the calcium ions bindings: troponin C (the component for calcium binding), TnT (the tropomyosin-binding) and cTnI (the inhibitory component). The majority of troponins were stored in the sarcomeres; both TnI and TnT present in compartment distribution in the myocytes along with small trace in cytosolic pool (4%-6%). Therefore, both troponins have the analogous releasing kinetics after myocardial

damage: serum TnI and TnT elevated within 4 to 9 hours, reached the peak in 12 to 24 hours and remaining high level for up to 2 weeks. Besides the specificity and wide diagnostic window, the amino acid sequences of both TnI and TnT are suitable for monoclonal antibody-based immunoassay overcoming the cross-reactivity of similar proteins. Moreover, serum TnI and TnT are rarely presenting in peripheral circulation in healthy peoples; traditionally, both troponins are less than 0.1 and 0.4 ng/ml, respectively. Thus, tremendously rising troponin level will highly possibly indicate myocardial necrosis (Bertinchant et al., 1996; Lewandrowski et al., 2002; Sluss, 2006; Wu et al., 1999).

It takes several hours, similar to CK-MB, from the onset of AMI to serum troponins can be detectable, so TnI and TnT are not ideal candidates for early AMI assessment. While, among all the cardiac biomarkers, the superiority of cardiac TnI and TnT has been foreground by the highest cardiac-specific, the longest diagnostic window time (Martins et al., 1996), and the correlation is proximately proportional between peak values and the infarct size (Licka et al., 2002; Panteghini et al., 2002). Therefore, the evaluations of cardiac troponins have been crucial in cardiospecific diagnosis, risk stratification, prognostic risk assessment, and therapeutic choices (Babuin and Jaffe, 2005; Newby et al., 2003). Meanwhile, the reliability of troponins for diagnosing ACS has been constantly questioned as well, because of the false positive troponin level caused by other clinical situation instead of ACS, such like sepsis, renal failure, hypovolemia (severe blood loss) , and etc(Jeremias and Gibson, 2005; Yang and Zhou, 2006), which will need further investigation about the releasing mechanism.

1.2.1.4 Heart-type Fatty Acid Binding Protein (H-FABP)

Heart-type fatty acid binding protein (H-FABP) shares substantial similarity to myoglobin. In releasing kinetics (Table 1.1) perspective, the low molecular weight (15 kDa) makes H-FABP possible to release rapidly into the blood stream circulation right after (1 hour or so) myocardial infarction (Glatz et al., 2002). In terms of specificity and sensitivity of AMI diagnosis, plasma H-FABP has been proved to be more effective over myoglobin and equivalent potential in exclusion diagnosis (Chan et al., 2004; Pelsers et al., 2005). Furthermore, HFABP is expected to replace myoglobin to become a clinical

routine due to its performance in clinical application such as minor myocardial injury detection of heart failure and unstable angina, infarct size estimation, the success or failure of coronary reperfusion in AMI patients, and in-time detection of post-surgery myocardial tissue monitoring, especially patients through coronary bypass operation (Pelsers et al., 2005; Yang and Zhou, 2006).

1.2.1.5 C - reactive Protein

C-reactive protein (CRP) is an acute phase protein reactant, the release of which is corresponding to acute injury, infection, or inflammation stimuli, like hypersensitivity causes, inflammatory disease allograft rejection, necrosis, trauma, and malignancy. The elevated CRP could demonstrate inflammation instead of erythrocyte sedimentation rate, and respond to hormone change caused by pregnancy (Du Clos, 2000). The measurement of CRP at the hospital admission can be an independent predictor for diagnosing lately coronary events; AMI and mortality caused by ischemic heart disease were included as well (Liuzzo et al., 1994). Troponin and CRP can provide relatively effective treatment suggestion for patients with unstable angina and non-Q–wave AMI; the statistics indicated that the risk is only 1% for that patient presenting negative or ultralow levels of CRP died in 14 days. In contrast, for elevated CRP level over than 15 mg/L, the risk will increase up to 9% and remain the same in the following periods. Even though, it is still lack of consensuses in the right time to take CRP measurement and the CRP potential in emergency department(Liuzzo et al., 1994).

1.2.1.6 B-type Natriuretic Peptides (BNP) and NT-proBNP

Natriuretic peptides are small signal chain proteins, presenting in the cell of the cardiovascular system, including brain, heart and blood vessels. There are three types of natriuretic peptides: A, B, and C natriuretic peptides. B-type natriuretic peptide (BNP) is mainly synthesized in ventricular myocardium or arterial.

There have been fact proved that myocardial ischemia would cause BNP and NT-proBNP released into the blood stream circulation (Wu, 2005).

According to the American and European Cardiological Societies, the latest guidelines regarded that BNP is a valuable serum marker for diagnosing heart failure. De Lemos highlighted the prognostic value (de Lemos et al., 2001; Hunt et al., 2001; Remme et al., 2001). Even though, the clearance characteristics do not reach the agreement, the clinical data trials (FAST, GUSTO IV, and FRISC II) have strongly revealed the connection between patients' death with unstable coronary artery disease and the NT-proBNP level (Jernberg et al., 2004). Since both BNP and NT-proBNP have demonstrate clearly that their clinical value is precious in diagnosing and taking care of cardiac disease, BNP and NT-proBNP elevation testing should be added in the menu of clinical practice routine (Penney, 2005; Pfister and Schneider, 2004; Sluss, 2006).

1.2.2 Clinical application of cardiac biomarkers

The detection of cardiac markers elevated level is the fundamental procedure for patient with suspect ACS, which is critical for the following medical intervention such as assessment, diagnosis, risk stratification, status monitoring, decision making and prognosis. Generally, to rule in the AMI or a certain type of ACS, it may take the combination of various cardiac biomarkers; while, to rule out the AMI, one biomarker test present negative might be enough. For example, cTnT and cTnI have been the surrogates for cardiac necrosis: the data showed that cTnT and cTnI are the most convincing indicators of myocardial cell damage among all the current available cardiac biomarkers (Alpert et al., 2000). On the other hand, all the cardiac markers of various processes of the acute coronary syndromes are useful as well. For example, one of the common physiologic syndromes of ACS is plaque instability or disruption and platelet activation, the marker (still under investigation) corresponding to plaque stability will indicate such interruption. C-reactive protein, as discussed before, is the foremost biomarker demonstrating inflammation for assessment for quite long period risk evaluation along with auxiliary reference of ACS (Christenson and Azzazy, 1998). Cardiac ischemia and unstable angina are the initial physiologic process of ACS; therefore, the marker such as H-FABP would also be engaged in clinical evolution. Since the characteristics and releasing kinetics of troponin, CK-MB, and myoglobin have been

well established(Alpert et al., 2000; Christenson and Azzazy, 1998; Christenson et al., 2001), they are currently the core of clinical detection subjects.

Table 1.1: Clinical utilized cardiac biomarkers for diagnosing CVD. Adapted from (Mohammed and Desmulliez, 2011)

Cardiac biomarker	Clinical cut-off levels	Clinical cut-off (h)	Peak elevation (h)	Duration	CVD indicator type
Troponin I	0.01-0.1 ng ml^{-1}	4-6	18-24	4-7 days	Detection of MI and tool for risk stratification
Troponin T	0.05-0.1ng ml^{-1}	3-4	18-24	10-14 days	Detection of MI and tool for risk stratification
Myoglobin	70-200 ng ml^{-1}	1-3	6-12	12-24 h	Early detection of MI and reperfusion
CK-MB mass assay	10 U L^{-1}	3-4	12-24	24-36 h	Early detection of MI
H-FABP	6 ng ml^{-1}	1-3	6-8	24-36 h	Early detection of MI
C-Reactive Protein	No definitive or clinical consensus				CVD inflammatory
NT-proBNP					Ventricular overload or ischemia or necrosis

1.3 Objective and outline of thesis

The ultimate goal of this project is to develop a compact multiplex cardiac condition diagnostic panel for point-of-care testing based on electrochemical immunoassay technology. As discussed before, the combination of myoglobin, CK-MB and troponin I will help diagnose the exact stage of myocardial infarction; while the grouping of H-FABP, CRP and Troponin will define the certain type of cardiac condition, and more. As the first step of the whole project, we developed a highly sensitive immunosensor for Troponin I and investigated the related experimental condition. So, this dissertation is comprised of six chapters in the following orders:

Chapter 1, background introduction, covers the information of cardiovascular disease diagnostic and clinically utilized cardiac biomarkers. The research motivation, objective and outline are also presented.

Chapter 2, literature review, provides a review on the current situation of point-of-care diagnostics, update the study of nanomaterial-based electrochemical immunosensor, and present technology for cardiac biomarker detection from laboratory and clinical perspective.

Chapter 3, sensor fabrication and bio-detection, presents the principle and procedure of immunosensor fabrication and configuration. Photolithography in cleanroom using the lift-off technique, e-beam metallization, and sandwich enzyme-linked immunosorbent assay are described in detail.

Chapter 4, electrode modification, describes the electrochemistry of the biosensor enhanced by three nanomaterials, carbon nanotube, golden nanoparticle, and chitosan. As a promoter for signal amplification and electro transferring, the response signals of three nanomaterials biosensor are investigated and discussed.

Chapter 5, enzyme label and substrate comparison study and system optimization, compares the activities of two commonly used enzyme label, HRP (horseradish peroxidase) and ALP (Alkaline phosphatase) in different substrates. A concept of developing GOD biosensor and cTnI immunosensor, also the feasibility is investigated.

Chapter 6, conclusion and outlook, summarizes all the chapters of the thesis and emphasizes the contribution of this research project. Also, a few recommendations for future research have been addressed.

Chapter 2

2 Literature review

This chapter reviews the current status of point-of-care (POC) immunoassay testing, advanced nanomaterial technology for biosensor application, and up-to-date development of cardiac biomarker detection. The core of this project is to develop high-performance cardiac biomarker transducer for POC application based on electrochemical enzyme-linked immunosorbent assay (ELISA); thus, the review includes discussion of clinical application of innovative biosensor, the prospects and challenges in terms of point-of-care cardiac condition diagnostics.

2.1 Point-of-care immunoassay

Diagnostics is indispensable in health care for both developed word and the developing world. Accurate diagnostics can provide proper and timely care to patient, guarantee the safety of blood banking, surveil emergency public health intervention and evaluate long-term health strategies (Sluss, 2006; Yager et al., 2008). Nowadays, clinical diagnostics heads towards two opposite directions: consolidation and automation of testing in centralized laboratories (Blick, 1999) and near patient testing in decentralized format (St-Louis, 2000). Even though, the cost and the time involving have been reduced tremendously (Blick, 1999); in poor setting environment, the laboratories are not only hindered by physical constrains (including limited power supply, inconsistent refrigeration status, and poor water quality), but also be challenged by the following factors (Ridderhof et al., 2007; Stedtfeld et al., 2012):

- Laboratory facilities and capacities vary among countries and within one country
- Irregularly laboratory quality and management control
- Deficient fundamental equipment and unreliable experiment supplies
- Shortage of proficient personnel and restricted training occasions

Therefore, under the lack of financial and technical support circumstance, point-of-care (POC) platform has more significant utility potential for performing diagnostic due to its merits in clinical application over traditional lab-based procedures. For example, timely

diagnostic information provided by POC testing ensures the correct and proper treatment, shorten the duration of hospitalization and improve the quality of patient cares (Birkhahn et al., 2011). (Figure 2.1)

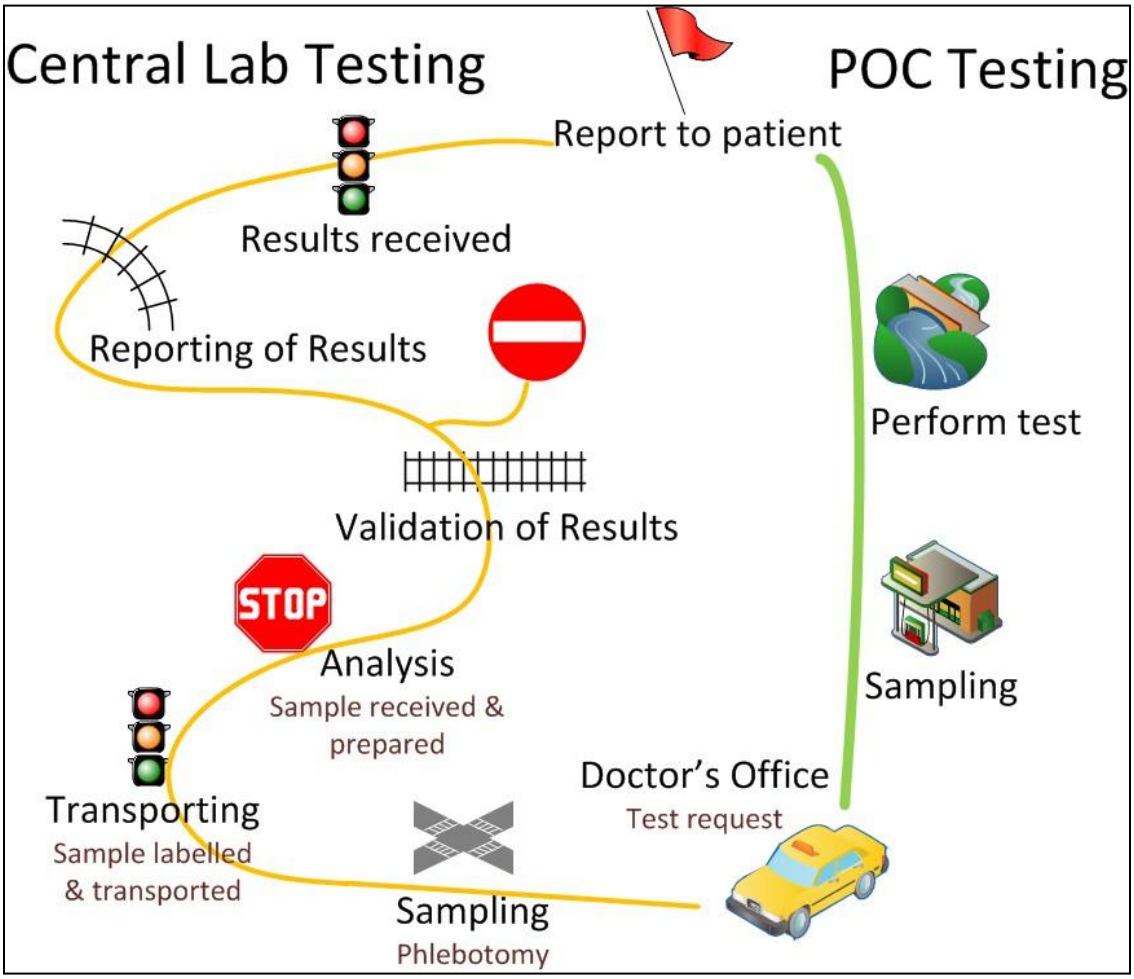

Figure 2.1: Central laboratories testing versus point-of-care testing in the clinical situation.

Generally, the definition of POCT is the testing performed near by the patients (St-Louis, 2000; von Lode, 2005), the performing location of which includes primary care facilities, hospital units, emergency department, mobile nursing practices, homes even peculiar situation like military or space shuttles etc. (von Lode, 2005). Even if the first rapid and easy-to-use immunoassay technology was realized by the pregnancy test over 43 years ago (Cabrera, 1969), the majority of present POCT applies to non-immunoassay analytes,

say glucose measurement. The perfection of POC technology allowed the immunoassay POCT for rapid growth within the last two decades.

In 2004, the World Health Organization (WHO) proposed an elemental guideline for the desirable POC device in less-developed areas, addressing from the cost, accuracy and feasibility perspective: (Mabey et al., 2004)

- Affordable for the high risk group and equipment-free
- Sensitivity (minimal falsely positive)
- Specificity (minimal falsely negative)
- User- Friendly (easy to operate and requiring little training program)
- Rapid (to ensure proper treatment at the initial visit) and robust
- Delivered to those who need it

However, for individual clinical applications, there are detailed, thorough, extensive and extraordinary requirements and specifications. The analytical performance requirements manifest two characteristics: practicability (as sample type, turn-around times, and operating skills) and reliability (e.g., limit of detection, interference, precision, accuracy, linearity and the measurement range) (Fraser, 2001). Differing from laboratory testing procedures, the main focus is on the practicability characteristic since the tests performed by unskilled personnel. Nevertheless, the accuracy of POCT is critical due to the closely connection to medical decision. In principle, the basic imprecision of a methodology cannot exceed fifteen percent for crucial treatment decision (Alpert et al., 2001).

Actually, the diagnostic situation in the physician's offices in a developed country is correspondent with the method utilized in limited resource environment. Under both circumstance, lateral-flow immunochromatographic immunoassay strip test is the absolutely dominant format, regardless of the low sensitivity levels (around 70%). In higher-income countries, the physician chose "simple" test over highly complicated but precise diagnostic based on clinical and social consideration: on the one hand, short turn-around times (TATs) about 15 to 20 min is desirable for timely medical decision; on the other hand, for the regulation of quality-control, only certain performing testts are approved by the Recommendations for Clinical Laboratory Improvement Amendments of

1988. The US Food and Drug Administration (FDA) describes the certain testing method "simple" with an "insignificant risk of an erroneous result."

According to the FDA, an ideal patient onsite diagnostic should have the following features: (Yager et al., 2008)

- Completely automated instrument or unitized, self-packed testing
- Utilize unprocessed specimens or capillary blood, nasal swabs, or urine
- No sophisticated operation requirement
- No intervention between analysis steps
- No equipment maintenance, calibration, interpretation or calculations
- No results analysis including data interpretation

With all the guidelines and regulations, POC immunotesting not only provides a multimillion dollars market but also is the fast growth part in the in-vitro diagnostics (IVD) business (Rosen S, 2004). Since then, great amounts of improvement in developing POC diagnostic platforms have been accomplished for both automated and manual approaches, which boost the introduction of POC diagnostic into the developing world.

Conventional straightforward manual assay has three primary assay formats, including agglutination assays, microscopy for direct detection of the analyte, and lateral flow tests (rapid diagnostic tests or RDTs) for detecting pathogen specific antigen or antibodies. (Figure 2.2) Even though the well-done performance of these tests can benefit both patients and health care resource, the quality will be considerably compromised by the poor source environmental setting. For instance, to a great extent, the accuracy of microscopes is influenced by high quality supplies, skilled staff, and the data interpretation. To solve this problem, scientists and researchers put enormous effort in investigating disease pathogenesis at a molecular level along with biomarker discovery and identification. The distinct benefits brought by molecular diagnostics (for example microfluidic technology and nanostructures sensing) can be summarized as: portability, the possible lowest detection limits, sensitivity improvement, and parallel recognition for multiplexing approach and etc. (Nam et al., 2004; Nam et al., 2003). All the benefits

coupled with small sample volumes contribute to a rising impact of micro-diagnostic technology in both the clinical and academic department.

Even though, great amount of papers published regarding POC device research, the POC device integrated using daily media (e.g mobile phones, mp4, and cameras) and paper-based microfluidic are the most creative and attractive for the widespread application. Stedtfeld et al. successfully developed genetic fluorescent microfluidic chip, called Gene-Z, for rapid quantitative detection of various biomarkers. This fully automated design featured in low cost, easy-to-operate, high sensitivity and specificity. The prototype (Figure 2.3) was connected with an iPod Touch for data reception and analysis, and then reported the result through Wi-Fi immediately.(Stedtfeld et al., 2012)

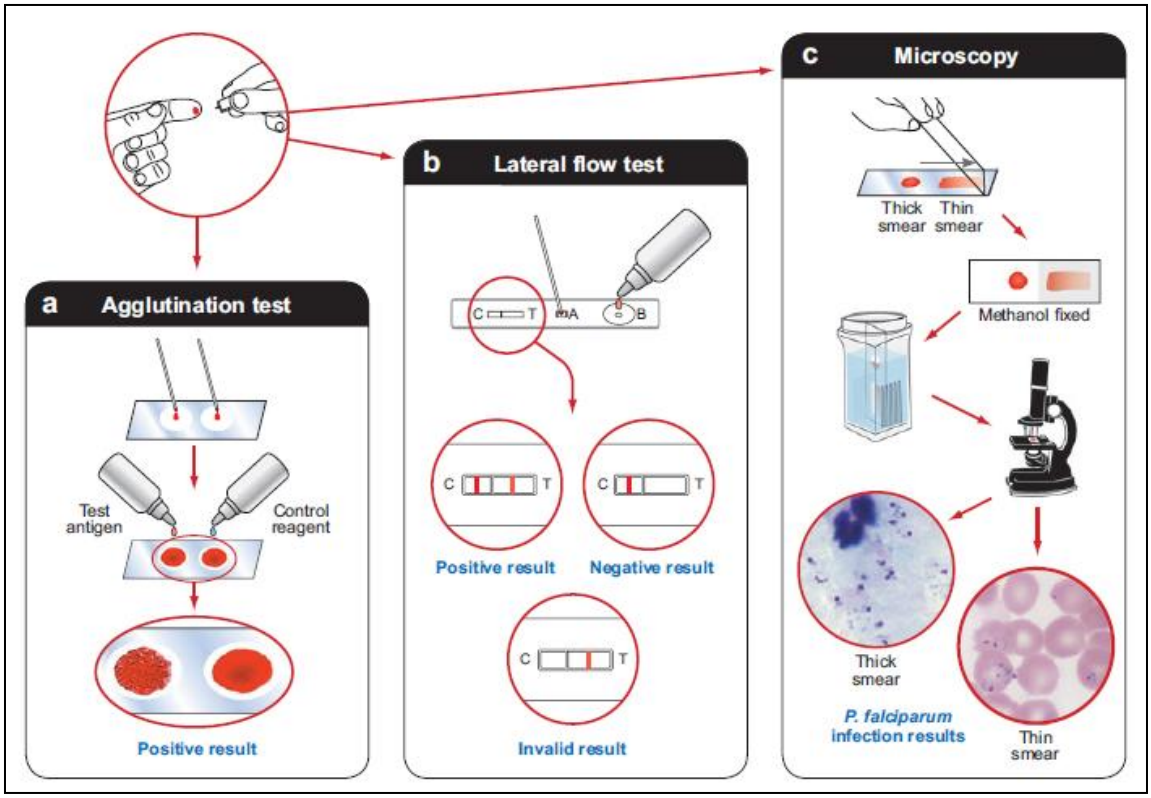

Figure 2.2: Schematics of typical POC testing. (a) An agglutination for HIV serology test. (b) Steps in rapid diagnostic test (lateral-flow test) for malaria antigen detection. (c) Classic light microscopy using Giemsa stain, results shown in both the thick and the thin smear. Figures adapted from Ref (Buhrer-Sekula et al., 2003; Kemp et al., 1988; Payne, 1988)

In addition, adding the attractiveness, Liu et al. and Ge et al. reported a three-dimensional paper microfluidic device based on origami principle. Liu et al. (Liu and Crooks, 2011) reported using classic lithography to create channels and reservoirs based on origami principle. (Figure 2.4(a)) Ge et al. (Ge et al., 2012) developed sandwich-type chemiluminescence immunosensor integrating with blood separation, automated rinsing and parallel immunoassay. For integrating ELISA with paper-based micro-sensor, Zang and Cheng approached in a different perspective. Zang et al (Zang et al., 2012) designed two pieces of paper, one fabricated with electrode pattern, the other immobilized with nanomaterials and antibody, and then overlapping to assemble the sensor. (Figure 2.4 (b))Cheng et al. (Cheng et al., 2010) fabricate the 96-microzone plate on paper for ELISA detection, high sensitivity, high specificity and less complexity(Figure 2.4 (c)). Lately, Delaney et al. (Delaney et al., 2011) constructed electrochemiluminescence detection on paper microfluidics utilizing cell phone camera for chemiluminescence emission. (Figure 2.5)

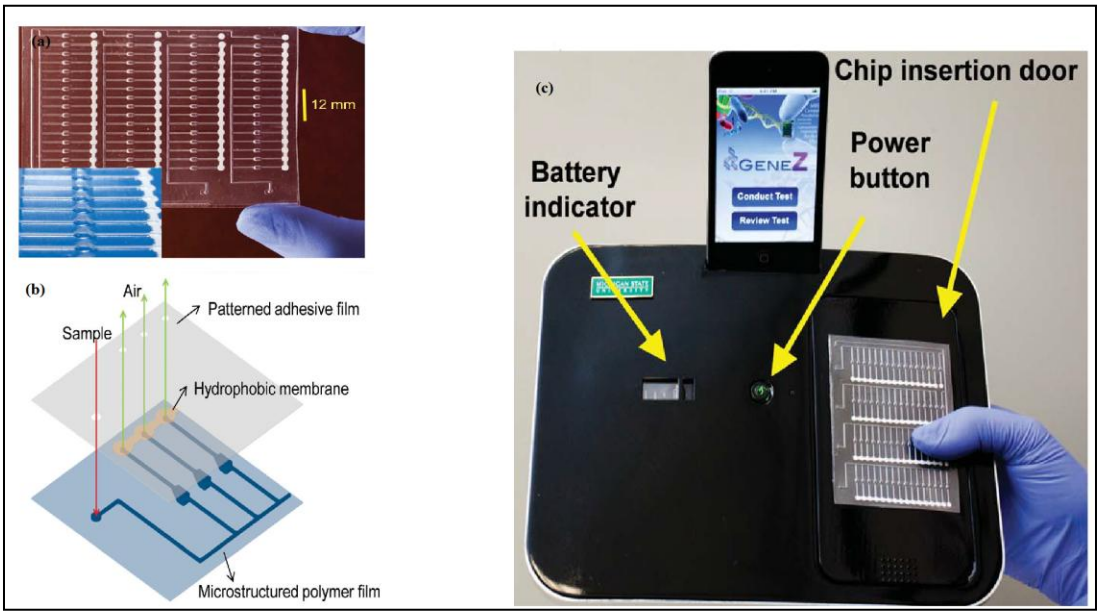

Figure 2.3: Gene-Z schematics and prototype. (a) An empty chip with four parallel reaction arrays. (b) Working principle and decomposition structure of the Gene-Z chip (c) Gene-Z prototype operated by an iPod set on the recharge port and the chip insertion door. Figures reprinted from Ref (Stedtfeld et al., 2012)

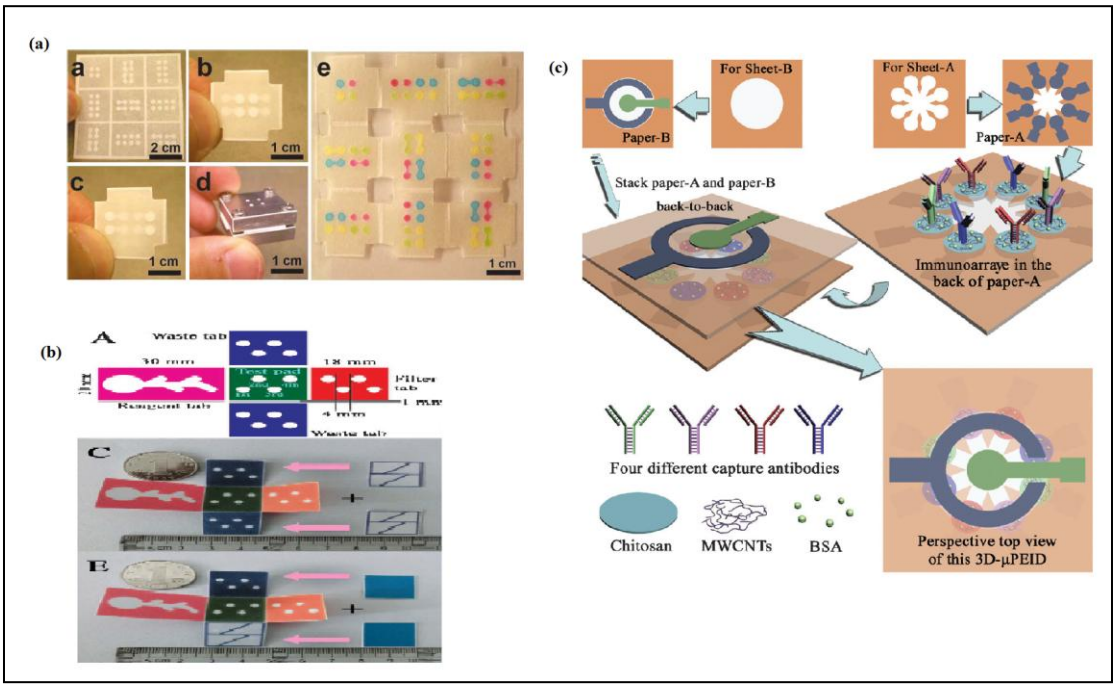

Figure 2.4: Schematics of various paper-based devices. Adapter from Ref (Zang, Ge et al., 2012; Cheng, Martinez et al., 2010; Ge, Wang et al., 2012)

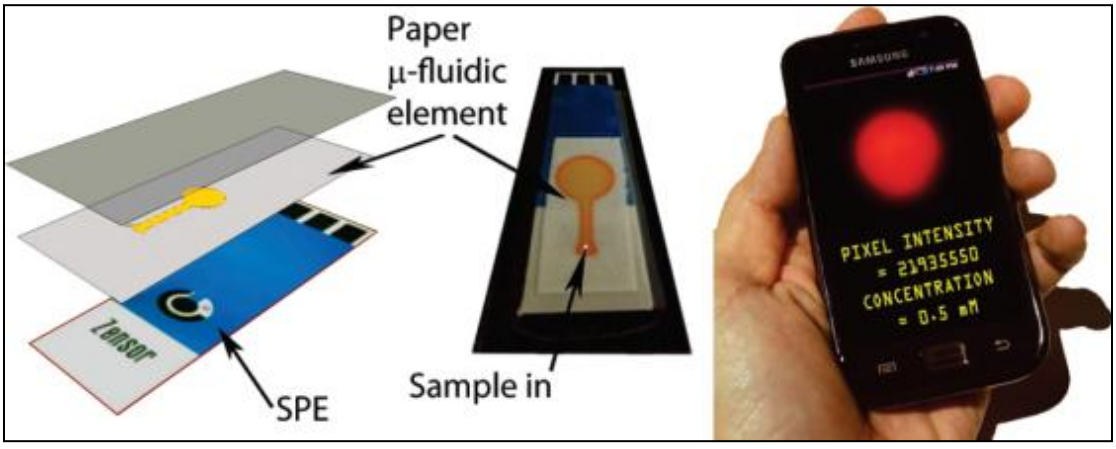

Figure 2.5: Schematics of paper-based microfluidic electrochemiluminescence: fabrication and analysis. Figure adapted from Ref (Delaney et al., 2011)

2.2 Immunosensor and nanomaterial enhancement

The device designed to qualify or quantify a certain biochemical molecule, say DNA sequence or protein molecule, is defined as biosensor. One of the most popular format biosensor is affinity-based biosensor, standing for using an immobilized capture probe to selectively bind the target molecule or analyte, the antigen in our case. Instead of sensing certain molecule in solution, affinity-based biosensor transfers the difficulty into detection a variation on the localized surface, which can be read out in various ways. Based on the detection methodology, the biosensor can be classified into optical, electrochemical, magnetical, and mass-loading immunosensor. (Bakker, 2004; Daniels and Pourmand, 2007; Drummond et al., 2003; Thevenot et al., 2001)

2.2.1 Nanomaterials: classification and application

The measureable size is less than 100 nm in any dimension; then this material can be defined as nanostructure. Based on the various dimensions, the materials can be divided into zero- (0D), one- (1D), and two-(2D) dimensional nanomaterials. Since we utilized zero- (0D), one- (1D), and two-(2D) dimensional nanomaterials in the electrodes surfaces modification, more details about zero- (0D), one- (1D), dimensional nanomaterials will be discussed later. Generally, in a diagnostic sensor requires one or multiple receptors for binding analytes along with signal generation function group, saying, a detectable label in the reacting event. The function of nanostructures in the molecules reaction can be varying with the physical, mechanical, or chemical properties. As a label of any biomolecules, it requires that the nanomaterials to meet these following criterias: stable in the corresponding buffer or fluids, detectable in the existence of required circumstance, and capable of conjugating the molecules with the functional groups. To achieve this objective, the surface usually is functionalized with ligands before spreading the dispersion of the nanoparticles aqueous on. As shown in Figure 2.6 illustrates the mainly applied nanostructures in the diagnostic assay device or technology development. In addation, a review about the properties, application and detection principles of the nanostructures are addressed as follows (Kurkina and Balasubramanian, 2012).

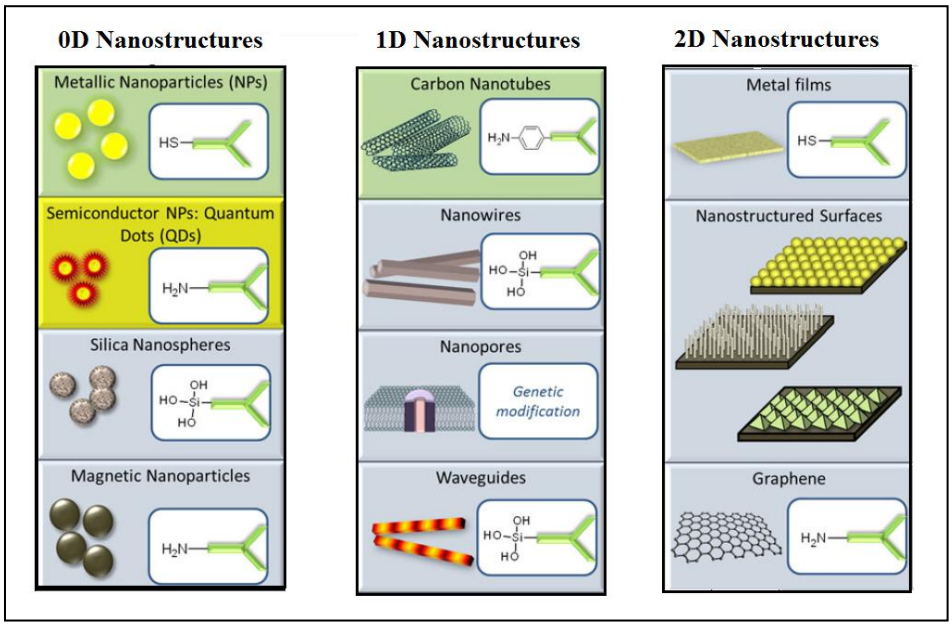

Figure 2.6: An overview of various nanostructures (NSs) that are used in diagnostic assays. Reproduced from Ref. (Kurkina and Balasubramanian, 2012)

2.2.1.1 0D nanostructures

As shown in Figure 2.6 -0D, the sizes of three dimensions are all less than 100 nm, then the materials are called as 0D nanostructure. A few classic representatives as shown in Figure 2.6-0D, includes nanoparticles and nanospheres, which can be divided into magnetic, metallic, semiconducting, or insulating nanoparticles based on the conductivity, saying, electrical properties. The basic function of nanoparticles can be essentially summarized as follows: immobilizing the biomolecules on certain surface, catalyzing electrochemical reaction, enhancing electron transferring, acting as a reactant or labelling biomolecules for further experiments, and etc.(Luo et al., 2006).

Speaking of nanoparticles for immobilizing biomolecules, gold nanoparticles (AuNPs), one of the most frequently used nanoparticles, can be utilized for both immobilization promoter and labels reactor in electrochemical immunosensing platforms, which has illustrating distinguish results in enhancing the signal response, lowering the detection limits in enzyme-based electrochemical biosensors, immunosensors, and DNA

hybridization detection (Kerman et al., 2008; Liu and Lin, 2007). AuNPs can be strongly attached to electrode surfaces through self assembled monolayer (SAM) of alkanethiol molecules due to the firm S–Au bonding, which creates plenty area for immobilizing biomolecules proximate to the surface of electrodes or biosensors (D'Orazio, 2011; Merkoci, 2007).

2.2.1.2 1D nanostructures

As shown in Figure 2.6—1D, 1D nanostructures stand for the size of these materials less than 100 nm in two dimensions, which can be considered as elongated version of nanoparticles, saying, tubes. Carbon nanotubes (CNTs), nanopores, nanowires and waveguides are all considered as 1D nanostructure.

Carbon nanotubes (CNTs), formed by rolling a thin layer of graphite to cylindrical structure, has the unique electrical properties such like metallic, semiconducting or superconducting electron transporting capability. CNTs, either single-wall carbon nanotubes (SWCNT) or multi-wall carbon nanotubes (MWCNT), can be produced in various synthesis ways, namely, chemical vapour deposition, laser evaporation, or carbon arc methods and most commercially available CNTs are in powder form (Kurkina and Balasubramanian, 2012). The average diameter of SWCNT is approximately 1 nm leading to high surface-to-volume ratio of such materials. Therefore, the unique electrical properties such like resistance display extremely high sensitivity in responding to the environmental changes in terms of chemical or biological variables. Furthermore, high surface-to-volume ratio and the indefinite conductivity contributes one of the most prevalent applications of CNTs to being the functional supporters electrical detectors in the label-free heterogeneous assays (Balasubramanian and Burghard, 2006; Kurkina and Balasubramanian, 2012; Wanekaya et al., 2006). Furthermore, CNTs can play a role in being utilized as optical labels, such like characterizing Raman signal, and being a carrier of payload labels (Duan and Lieber, 2000) such like the case of silica nanospheres (Kurkina and Balasubramanian, 2012).

Another extraordinary advantages of CNTs are acting as an immobilization matrix for biosensors, either biocatalytic or affinity biosensors, which are owing to the existence of

reactive groups on the surface, fast electron transfer kinetics (particularly beneficial for electrochemical biosensors) and the high surface to volume ratio (D'Orazio, 2011; Rivas et al., 2007).

The application of CNTs can enhance electron transferring of electrochemical biosensors, because the electron communication between immobilized proteins, mediators will lead to strong and sound signal response and lower the case of overpotentials to overcome the corresponding inference, which has been reported in the amperometric glucose biosensor applications (more discussion is in Chapter 5). Furthermore, the value of CNTs in electrochemical biosensor can also display by promoting sensitivity, shortening the assay time and elevating the clinical or analytical performance in terms of stability and precision and etc.(Justino et al., 2010).

2.2.2 State-of-the-art nanomaterials for cardiac immunosensors

Numerous literature manifest the benefit of utilizing nanotechnology in biosensors, for instance the ultrasensitive detection of cardiac biomarkers can be tremendous helping in provide accurate and timely information of diagnosis of acute myocardial infarction. Meanwhile, the present biomarker study has explored to unstable angina, coronary plaque and other types of cardiac disorder conditions. Lin's group has successfully developed deluxe cardiac biomarkers array of the nanostructure in the form of nanowells which were formed by biogenic nanoporous silica on the top of gold electrode. The silica was derived from Coscinodiscus wailesii, the eukaryotic unicellular photosynthetic algae, and then was overlayed on the top of gold substrate to form the structure of nanowells for detecting C-reactive protein (CRP) and myeloperoxidase (MPO), both of which are highly relevant to risk of coronary plaque rupture. The general diameter of each nanowell is 40 nm with a bottom of gold substrate electrode. The protein detection was implemented by quantifying the immunoreaction, namely the interaction between antibody and antigen, the affinity of which will disturb the regular charge distribution of the interface of the electrode and liquid. The shifted resistance can be measured by impedance spectroscopy and is proportional to the concentration of CRP and MPO. Compare to planar gold electrodes, the signal was cumulated and enhanced by the nanowells nanostructure with an exceedingly low limit of detection 10 pg mL^{-1} of CRP

and MPO in serum samples(Lin et al., 2010c). Chua et al succeeded in developing a real time, label-free, highly sensitive human cardiac troponin-T (cTnT) electrochemical immunosensor (Figure 2.7) by fabrication of oriented silicon nanowires (SiNW) clusters. The immunosensor utilizes the properties of complementary metal-oxide semiconductor (CMOS) and field effect transistor-compatible detection principle to characterize cTnT both in buffer solution or undiluted serum. The anti-cTnI antibody was immobilized on the functionalized nanowires on the surface, the conductivity of which will increase along with the amount of cTnT antigen binding to the antibody. This phenomena was based on the n-type semiconductor characterizations, namely, the impurity will results in free electron then increase the conductivity. The cTnT level can be detected as low as 30 fg mL^{-1} in undiluted serum and 1 fg mL^{-1} in buffer dilutes (Chua et al., 2009).

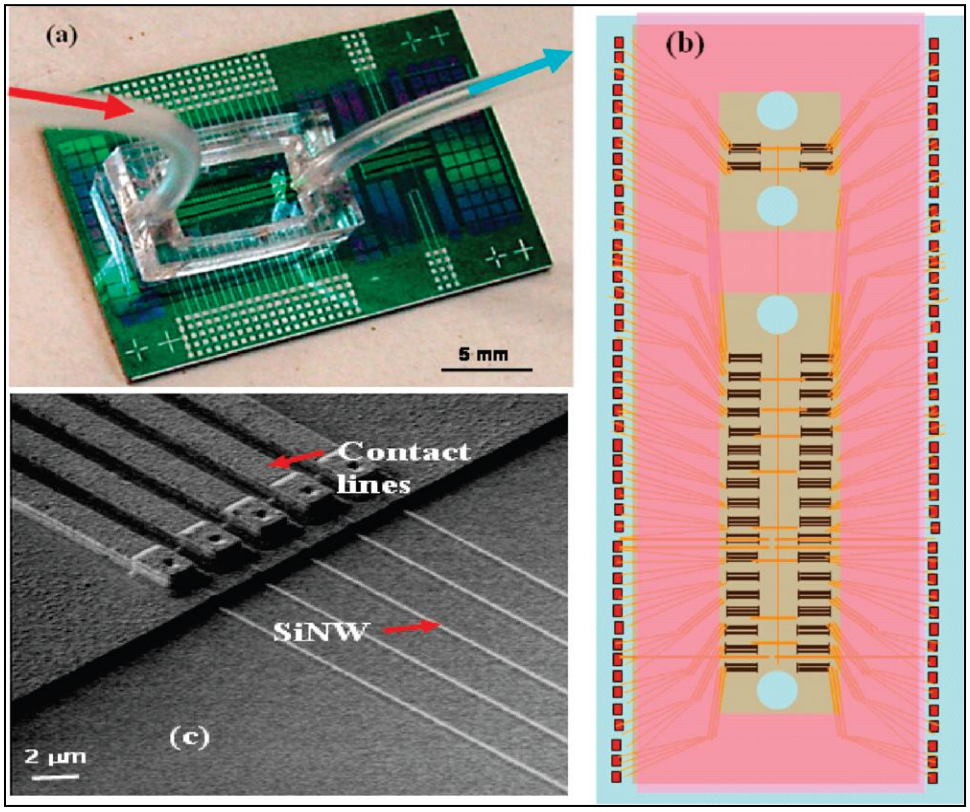

Figure 2.7: SiNW device demonstration: (a) SiNW microfluidics chip; (b) the layout of the SiNW device array; (c) SEM image of nanowires clusters. Adapted from (Chua et al., 2009).

The significance of CRP has been realized recently. Many literature published various novel CRP detection immunosensors for clinical application. An acoustic, highly sensitive immunosensor for the detection of CRP was presented by McBride JD, which testified the competitive sensitivity of CRP sandwich ELISA assay by the Resonant Acoustic Profiling (RAP™) biosensor (Akubio Ltd., Cambridge, UK). Applying a high frequency voltage on the piezoelectric crystal, it will induce oscillation and be monitoring the resonance frequency instantly. The immunosensor was operated on two different modes, direct and sandwich, on which the antibody along with the corresponding antigen bonded to the reading crystal by classic covalent bond and on the other crystal IgG immobilized as the control set to eliminate background signal. The specific binding reaction, immunoreaction between antibody and antigen, on the testing crystal will lead to a reduction of the frequency of the oscillation. The serum CRP detection limit of such immunosensor is 13 ng mL^{-1} of the direct mode and 3 ng mL^{-1} of the sandwich type, respectively. According to the statement of this literature, this immunosensor has immense potential for clinical application as the monitor for prediagnosis of cardiovascular disease, since the CRP assay requires the maximum low detection limit is 300 ng mL^{-1} (McBride JD, 2008).

Meanwhile, cardiac troponin-I (cTnI) remains the most popular biomarkers study projects. Both Wei's group and Masson's group developed a cTnI immunosensor based on s surface plasmon resonance technology. Wei et al can monitor the real time action of several and constant monoclonal antibodies and antigen cTnI, such as association, dissociation and affinity. The experimental system was build on a gold SPR chip for sandwich ELISA detection, and the optimized system has a low detection limit of 0.25 ng mL^{-1}, which is less than almost 90% of that of the direct SPR assay (Wei et al., 2003). Even though, the sensitivity of this immunosensor can be satisfy the practical standard for detecting sera cTnI from patients with suspect AMI. Still, the shortcoming of this immunosensor is low sensitivity and long processing time. Namely, nonspecific protein adsorption causing low sensitivity which can be solved by washing after each incubation, which calls for 40 minutes for the assay. Masson et al. tried to solve the same problem in their research. They used a self assembled monolayer, which is comprised of *N*-hydroxysuccinimide activated 16-mercaptohexadecanoic acid, to remove the nonspecific

binding responding of the serum protein for cTnI immunosensor utlizing SPR technology. However, it still needs more optimization or improvements before the application of AMI diagnosing since the detection limit is 0.7 ng mL^{-1} in undiluted serum in direct mode of immunoassay.

As discussed before, gold nanoparticles (AuNPs) show appreciable enhancement in fluorescence based biosensor. Hong and Kang reported a fiber optic based cTnI immunosensor by establishing- a self assembled monolayer through nanoparticles immobilization at a mediate distance from fluorophore. The immunosensor based on the sandwich type immunosensing using a second antibody labelled with a fluorescence enzyme. Because of the existence of AuNP, the quantitation of cTnI with a fairly low detection limit, down to several picomolar concentration (approximately 0.2 ng mL^{-1}). It can be explained by that free or self-quenching electron was attracted by AuNP and transfer to working zone, surface Plasmon polariton filed, and then the signal was significantly improved. This immunosensor still needs the washing steps to remove the nonspecific binding, which is the similar case with most optical based immunosensor (Hong and Kang, 2006).

2.3 Current commercialized cardiac point-of-care assays

The POCT devices for cardiac biomarkers are fundamentally based on immunoassay detection methods. A general principle of measuring various kinds of analytes using antibodies can be summarized in the following prospects: antibody binding to the analyte or antibody-antigen connection, isolation antibody-antigen complexes from excess regents or antibodies for the signal measuring, and calibration the corresponding relationship between signal response and the mass of analyte-antibody to establish standard curve. Currently, the commercialized cardiac POCT devices for clinical utilization can be divided into three categories: lateral–flow technology (LFT), flow-through immunoassay device, and sandwich immunometric methods (Sluss, 2006). Among all the analytes of POC immunotesing, the immunoassay for cardiac biomarkers, troponins in particular, grows the fastest, with an approximately 15-20% annual growth

(von Lode, 2005). In the current market, the qualitative and quantitative POCT devices are successfully commercialized for myoglobin, CK-MB, cTnT, and cTnI, as shown in Table 2.1.

All the assays shown in Table 2.1 are utilizing whole blood or anti-coagulated plasma within 20 minutes to generating results, which is portable, convenient, and rapid (Christenson and Azzazy, 2009; Di Serio et al., 2006; Kost and Tran, 2005; Lee-Lewandrowski et al., 2003; Storrow and Gibler, 1999). Comparing to qualitative testing, under the guidance from NACB POC, test results in quantitative ways offer unique power in risk stratification and ultralow sensitivity (Morrow, 2004; Pham et al., 2004). The 2-site antibody immunometric assays, also called sandwich immunometric assays, are suitable for highly specific protein level measurement, which is the dominant technology in measuring biomarkers in multimarkers assays, fully-automated and centralized laboratory instruments. Therefore, sandwich type immunoassay is the leading format of the detection method of the cardiac markers since they process various independent antigenic epitopes. Comparing to single antibody immunoassays, one of the most merits of the 2-site antibody immunometric assays are the degree of analyte specificity achieved by targeting 2 antigenic sites then along with high accuracy and precision of the test results. Miniaturization is the current trend for both centralized laboratory analysis and decentralized POC device (POCT device). A few POCT devices for cardiac detection are depicted in detail as follows.

Table 2.1: Current Cardiac point-of-care available device. Adapted from (Christenson and Azzazy, 1998)

Device	Cardiac marker	Suggested cut-off	Manufacture's claim	Assay Time (min)	Specimen (type and volume)
Roche cardiac T® rapid assay	cTnT	0.1 ng mL^{-1}*	Myocardial damage is detected	12	150 µL heparin whole blood
Nanogen cardiac STATus™ panel	CK-MB Myoglobin cTnl	5 ng mL^{-1} (Abbott method) 50 ng mL^{-1} (Behring Diagnostics method) 1.5 ng mL^{-1} (Dade Stratus method)	Aid in the diagnosis of cardiac ischemia	15	200 µL serum or heparinized whole blood or plasma
Stratus® CS STAT fluorometric analyzer (Dade Behring Inc)	CK-MB Myoglobin cTnl	3.5 ng mL^{-1} Male: 98 ng mL^{-1} Female: 56 ng mL^{-1} 0.06 ng mL^{-1}	All makers: Aid in the diagnosis of AMI cTnl: Risk stratification	14 min to the first result, 4 min for each additional result	Whole blood (lithium or sodium heparin): 3 mL^{-1} Plasma (lithium or sodium heparin): 200 µL for the first test, 100 µL for each additional test
Triage® cardiac panel (Biosite Diagnostics)	CK-MB Myoglobin cTnl	10.0 ng mL^{-1} 170.0 ng mL^{-1} 1.0 ng mL^{-1}	Aid in the diagnosis of MI	~15	250 µL heparinized whole blood or plasma
Response biomedical corporation	Myoglobin CK-MB cTnl	LLD 2.4 ng mL^{-1} (range 0~400 ng mL^{-1}) LLD 0.32 ng mL^{-1} (range 0-80 ng mL^{-1}) LLD 0.03 ng mL^{-1} (range 0-32 ng mL^{-1})	Aid in diagnosis of AMI	~15	Heparinized whole blood or plasma
iSTAT (Abbott Diagnostics)	cTnl	0.08 ng mL^{-1} (reportable range: 0-50 ng mL^{-1})	Help diagnose AMI	~10	16 µL whole blood

* TnT values indicating: <0.05 ng mL^{-1}, negative; between 0.05 to <0.1 ng mL^{-1}, low and repeat testing within one hour with freshly collected blood; between 0.1 and 2.0 ng mL^{-1}, myocardial damage; >2.0 ng mL^{-1}, massive myocardial damage.

2.3.1.1 Cardiac STATus™ device (Nanogen Inc., San Diego, CA)

The STATus™ assay system based on the principle of immunochromatographic solid-phase immunoassay; therefore, it can only provide the semi-quantitative results. For the accurate or precise reading of cTnI or CK-MB, it has a different device also commercially available. As shown in Figure 2.8, the testing panel includes myoglobin, CK-MB mass, and cTnI and the results were read and processed by LifeSign DXpress™ Reader. The device can be suitable for whole blood (heparinized), plasma or serum. The principle of the working schematics has shown in Figure 2.8 as well, which is the classic pregnancy testing style. After the sample was dispensed into the entrance well and was driven by the diffusion force to the testing zone. The sample was first mixed with the mouse monoclonal antibodies with a colour label and the complex react with the second antibody conjugated with a biotin. Then the sandwich complex flow through the display zone to react with the streptavidin, then the LifeSign DXpress™Reader can convert the intensity to a concentration (Christenson and Azzazy, 2009; Sluss, 2006).

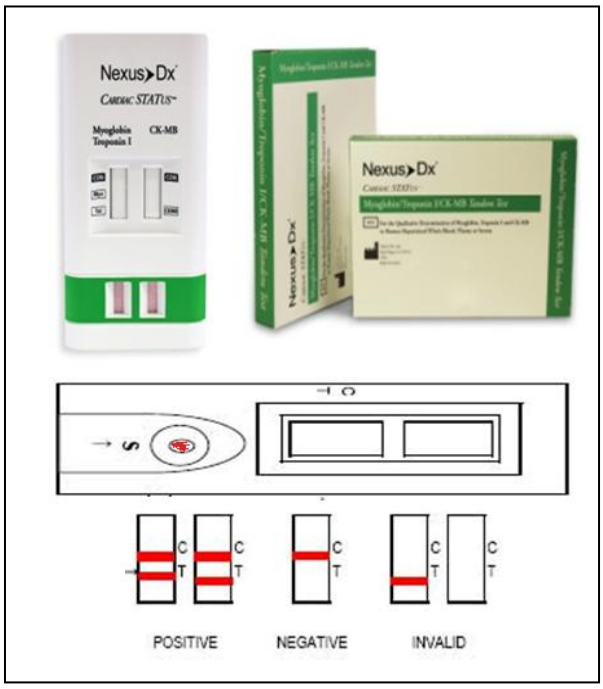

Figure 2.8: Cardiac STATus™ Kit- Triple markers testing. Adapted with permission from Nanogen Inc.

2.3.1.2 Stratus® CS STAT fluorometric analyzer (Siemens Medical Diagnostics, Glasgow, DE)

The Stratus CS (Figure 2.9) bases on sandwich immunoassay technology and fluorometric detection technology provides quantitative results of CK-MB, myoglobin, and cTnI, which can be suited for lithium heparin whole blood or plasma. The whole blood was processed first, centrifuging on-board to separate the blood cells from the plasma, and then the plasma was driven by centrifuge force to the capture antibody which were immobilized on a solid-phase glass fibre matrix. Like the i-STAT system, (details in section 2.3.1.6), then the second antibody conjugated with alkaline phosphatase reacts with the antigen to form a sandwich complex. To remove the nonspecific binding, the instrument followed by adding the washing buffer and clean the sample matrix, at the same time, there is a substrate can by catalyzed by alkaline phosphatase to generate a fluorescent signal which is proportional to the exist amount of myoglobin, cTnI and CK-MB (Christenson and Azzazy, 2009; Sluss, 2006).

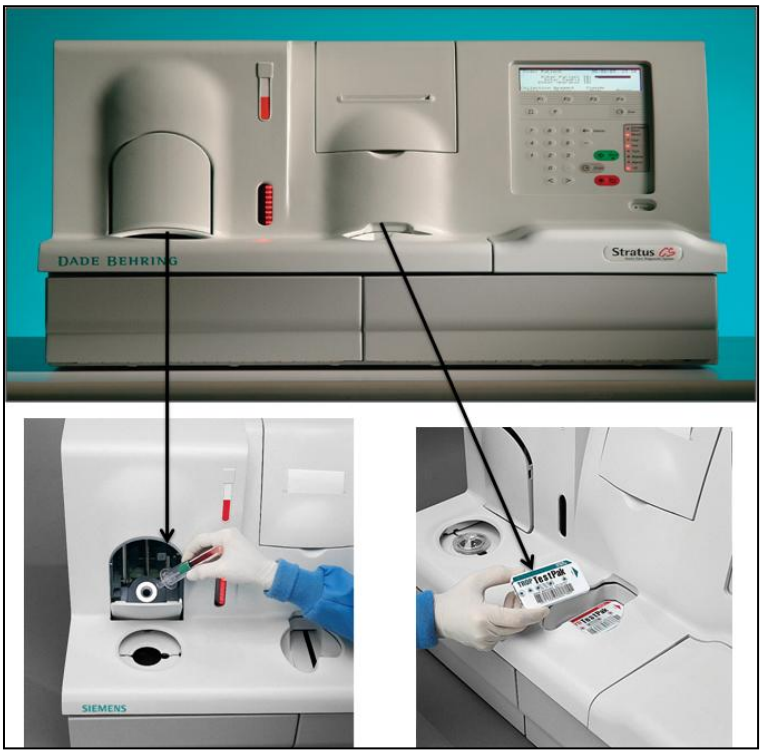

Figure 2.9: Stratus® CS STAT fluorometric analyzer. Reprinted with permission from Siemens Medical Diagnostics.

2.3.1.3 Triage® system for cardiac marker measurement (Biosite Diagnostics Inc., San Diego, CA)

The Triage® Cardiac system (Figure 2.10), based on microfluidics structure and immuno-fluorescence technology, has two basic components for detection triple cardiac markers at one reading, a cartridge containing all the structure and reagents and the data analyzer, the Triage® meter. The whole blood with anti-coagulation and plasma can be applied on the cartridge. When the sample enter the port, the blood cells were removed by filtration and the plasma flows through to the reaction well and reaction with the detection antibody labelled by fluorescent enzyme. When the complex (detection antibody- antigen) flows through the whole cartridge, the corresponding antibody can capture the specific complex, in this case are myoglobin, CK-MB, and cTnI, will "grab their owns complex" complex. Therefore, the three sandwich complexes were located in different zones, and detected by the Triage meter to get the fluorescent signal response (Christenson and Azzazy, 2009; Sluss, 2006).

Figure 2.10: Biosite's Triage flow-through detection technology. Reprinted with permission from Biosite.

2.3.1.4 RAMP™ cardiac marker testing (Response Biomedical Inc., Burnaby, B.C., Canada)

RAMP stands for the Rapid Analyte Measurement Platform (RAMP) (Figure 2.11) is based on quantitative immunochromatographic assay for cTnI and CK-MB detection. EDTA whole blood is the only specimen for this immunosensor, and must be combine with buffer to dilute before enter the analyzer. The analyzer contains capture and detection antibody is both monoclonal, indication this device has lightly robust but strong sensitivity. Like the rest of cardiac detecting devices, the antigen combining with detection antibody and the complex react with the capture antibody. Partial fluorescent-labelled latex particles were coated on the detection antibody to generate signal response in the working zone. The excess fluorescent-labelled were moved and immobilized in the other zone as the blank experiment. Then two working zones have been detected by the RAMP Clinical Reader, the differences between the two values are used to calculate the concentration of each analyte (Christenson and Azzazy, 2009; Sluss, 2006).

Figure 2.11: RAMP cardiac marker system. Reprinted with permission from Response Biomedical Corporation.

2.3.1.5 STAT® system cardiac Troponin I (Abbott Point of Care Inc., East Windsor, NJ)

CTnI test cartridge of i-STAT (Figure 2.12) is based on classic sandwich ELISA detection method, which can be utilized for whole blood (either lithium or sodium heparinized), plasma or non-anticoagulated whole blood (freshly drawn blood samples with any anticoagulated treatment). Because the cartridge itself contains all necessary and sufficient reagent to dilute, capture, wash or conjugate the blood sample; however, for the freshly drawn blood, it requires to apply in the cartridge before the blood started to clot (usually 1 minute). I-STAT cardiac system can also be called as a simultaneous detection system, since the capture and detection antibody was forming as a complex at the same time and the washing buffer also plays a role of detection substrates. The anti-cTnI human antibody (monoclonal capture antibody) was immobilized on the silicon based electrochemical sensor surface during the fabrication. A polyclonal second antibody is firstly conjugated with alkaline phosphatase (ALP) and reacts with antigen (cTnI) when the sample was added in the cartridge, since the conjugated detection antibody was placed closed to the sample entry well. Then the complex of antigen-antibody-alkaline phosphatase label was driven by capillary force and pneumatic pressure flowing through within the cartridge to the surface of the electrochemical sensor coated with capture antibody. Then a washing buffer remove all the unbinding enzyme conjugate, non-specific binding, which is the biggest influence in the sandwich ELISA type immunoassay. This washing buffer also contains liquid substrate which can be catalyzed by alkaline phosphatase to generate an electrochemically detectable substrate and then generate proportional response (current) to the amount of the cTnI within the sample, which was processed by a hand-hold analyser to generate the critical analysis results.

The i-STAT cardiac marker detection system (cTnI in particular) has a low detection limit of 0.02ng mL^{-1}, and a relative narrow linear range between 1ng mL^{-1} to 50ng mL^{-1}. However, the design of the i-STAT is one of the most successful examples and the only electrochemical based POCT cardiac device (Christenson and Azzazy, 2009; Sluss, 2006).

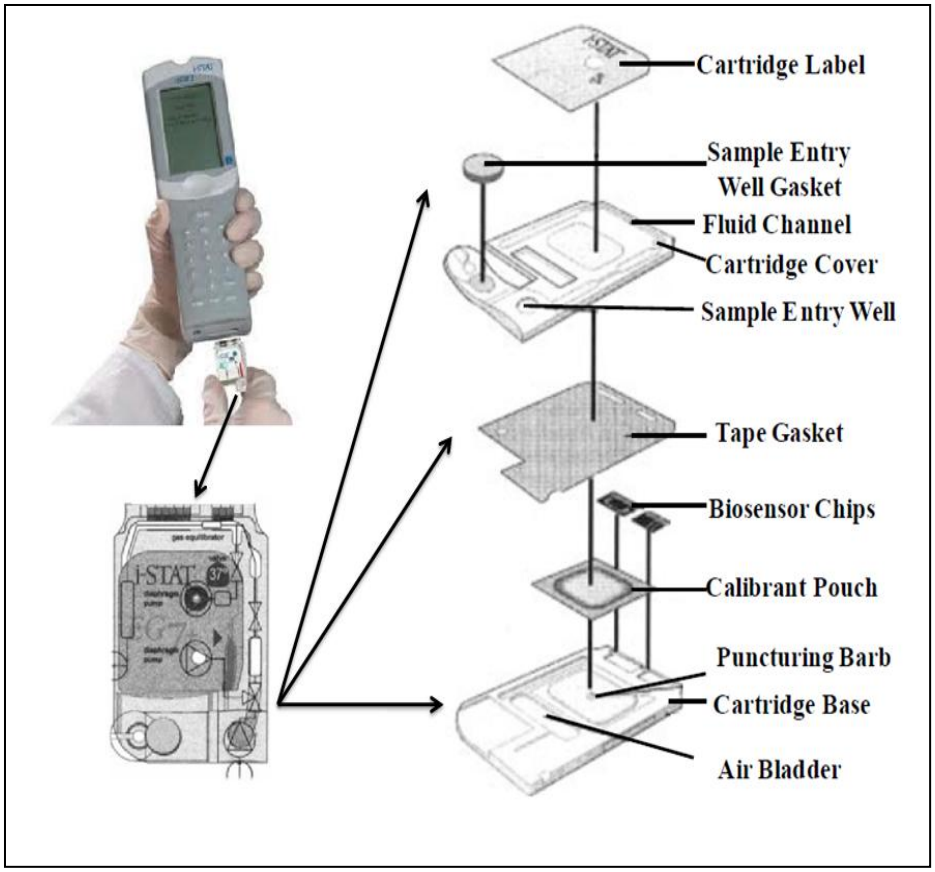

Figure 2.12: i-STAT® system Portable cardiac analyzer and the explode view of the cartridge. Reprinted with permission from Abbott Point of Care Inc.

2.3.1.6 Roche cardiac reader (Roche Diagnostics, Indianapolis)

The cartridge of Roche Cardiac Reader (Figure 2.13) is based sandwich type ELISA and immunochromatography for measuring cTnT or myoglobin. EDTA whole blood or plasma can be used in the cartridge. The principle of Roche Cartridge has many similarities with Biosite's Triage. The blood cells were removed by filtration before the reaction starts. Both the antibodies were solubilised by the sample: the capture antibody was bound with biotin, and the detection antibody was bound with gold particles. The complex flow to the streptavidin immobilized zone, detection zone, the gold-label sandwich complex will concentrate to be visibly observed. The excess labelled antibody will bind with anti- IgG as a control. Then the cartridge can read visibly for qualification measurement or use cardiac reader analyzer for quantities measurement.

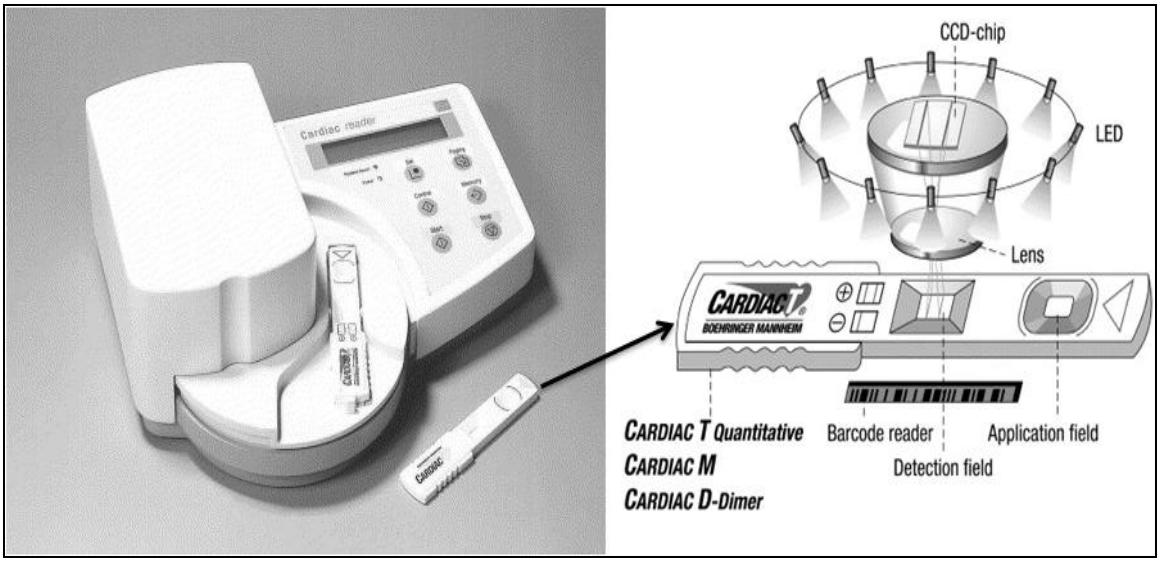

Figure 2.13 : Roche Cardiac Reader system and principle schematic. Reprinted with permission from Roche Diagnostics and Ref. (Collinson et al., 2001)

2.4 Summary

We have reviewed the update developments in diagnosing criteria and device innovation in cardiovascular disease, AMI in particular. The proposed research information from various laboratory groups not only offers critical research perspectives, but still many challenges remain to be solved. The current commercialized available cardiac detection kit, the majority of which is based on the optical detection methodology, can provide results within 20 minutes near the patients with satisfying accuracy and sensitivity. However, the apparatus for optical detection kit is expensive and hulking, which can not realize portable then will not be suitable for frequently mobile circumstances. While, comparing to the majority, i-STAT is the sole electrochemical based immunosensor with excellent portability, but with narrow detection range (0 to 50 ng/ml) and less rebuts.

Chapter 3

3 Sensor fabrication and biodetection

This chapter will present the principle and procedure of immunosensor fabrication and configuration. A particular description includes photolithography in cleanroom using the lift-off technique, e-beam metallization, and sandwich enzyme-linked immunosorbent assay (ELISA).

3.1 Introduction

In the early 1990s, microfluidic technology was successfully developed and introduce to the world, since then, countless attentions and efforts were poured into this novel and promising technology. Particularly, to integrate immunoassay with microfluidic technology to realize high specific antibody-antigen reaction comes with great benefits along with substantial challenges. The on-chip devices can ameliorate the immunosensing performance through the automated operation significantly in terms of shortening the assay time, economising the consumption of reagents and sample, improving the reliability and sensitivity, and coordinating parallel or sequential assays in one platform (Bange et al., 2007; Kurita et al., 2006; Zaytseva et al., 2005). Basically, the critical aspects to construct a microfluidic immunosensor include device microfabrication, capture antibody (probe) immobilization, immunoreaction, and signal detection scheme (Dong et al., 2007).

Lift-off and etching are the most common approach to fabricate metal or oxide microstructures the surface of semiconductors. Lift-off performs as an additive process during the microstructure fabrication, in contrast, the etching presents subtractive process. During the etching process, firstly fabricate a metallic pattern directly coating on the substrate with metal or oxide surface, followed by using photoresist to overlay the desired pattern of the mask, and then, the etching process will remove the metal or oxide which is not being covered by the photoresist, which can be classified as wet chemical etching or dry etching. Wet chemical etching is the more popular in the etching process,

but it will cause the isotropy of the whole process and or overcut/undercut the photoresist. On the other hand, dry etching is an optional choice but requires sophisticated and expensive machine to generate reactive ion plasma. The post-etching process usually involves residue removing in a solvent bath (Golden et al., 2009).

During the lift-off process, it requires an inverse mask pattern to print a sacrificial photoresist layer. The pattern of the substrate, metallic or oxide, is generated by blanked coating by the photoresist and the sacrificial layer was washed off as well. Meanwhile, the materials deposited on the top of the sacrificial layer was washed off which has been indirectly contacted with the substrate surface. The lift-off technique can be classified into many types, all of which will be suitable for metallization by e-beam and sputtering techniques. But there are several defects will occur during the process, such as retention, “tails”, “tears”, “flagging” or “fencing”, which is not quite relevant to the types of the materials. Retention stands for the pattern of the substrate showing undesired and residue metal pattern, which might be caused by the insufficient lifting time or solution resulting in the excess metal left on the substrate. The circumstances mostly happened when the metal coved the photoresist thoroughly and without any gaps during the metal deposition during the photoresist being penetrated and dissolved by the solvent. Flagging or fencing presents the defect in the certain gap happening between the metal layer and the photoresist top surface with a extremely thinner metallization layer (Carpenter et al., 2004). When the situation happened, the metal will dissolve along with the photoresist and leaving a “flag” behind, a ragged pattern, which will cause uneven surface and the failure of device fabrication (Golden et al., 2009; Roesch and Hamada, 2004).

In this chapter, we will describe the procedures for obtaining gold electrodes or interconnects in detail. These electrodes can be used for electrokinetic manipulation, local application of voltage or current, DNA immobilization, and so on. (benjamin Y. part)

3.2 Sensor fabrication

3.2.1 Materials and supplies

Ultraviolet (UV) flood exposure machine, evaporation machine, photoresist spinner, two hot plates. Thermal Oxide coated (1 micron) silicon [Si] wafer, Lift-off Resist (LOR-5a), Shipley 1827 positive photoresist, photoresist developer Microposit MF 319, Remover PG, and Nano-Strip were used as receive in cleanroom.

3.2.2 Fabrication procedure

To fabricate the biosensor utilizing lift-off techniques, traditionally, the lift-off resist (LOR) will be coated on the surface of the wafer firstly, and then the photoresist is spread on. The chemical properties of LOR lead to no interacting or intermixing between these two layers, LOR and photoresist. After exposed for patterning, the wafer coated with both LOR and photoresist is immersed in develop solution. When the photoresist is thoroughly developed, the developer will keep on dissolve off the LOR layer at the open area. Thus, a small amount of standard photoresist developing time increase will contribute to the LOR undercut properly for the following steps. The process of developer dissolving LOR can be both isotropical and well-controled, which attributes the high standard of precise undercut control of lift-off techniques (Golden et al., 2009). The procedures and apparatus of fabricating electrodes can be summarized as Figure 3.1 and Figure 3.2, respectively.

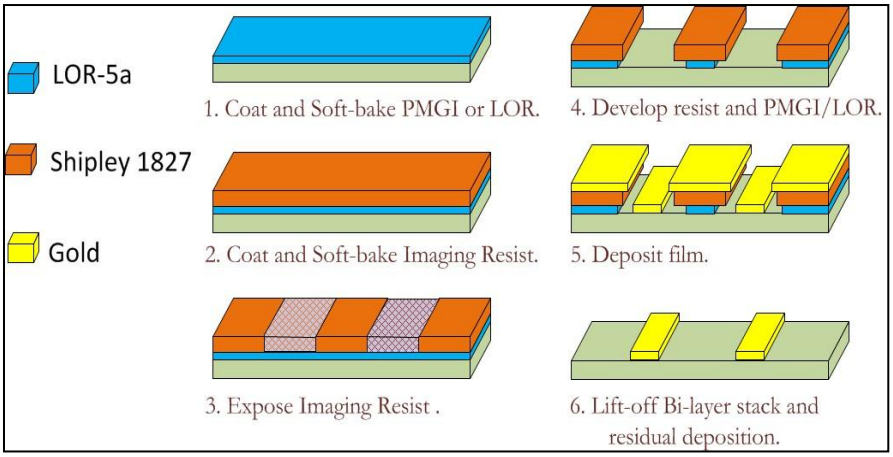

Figure 3.1: Schematic of the electrode layer structures.

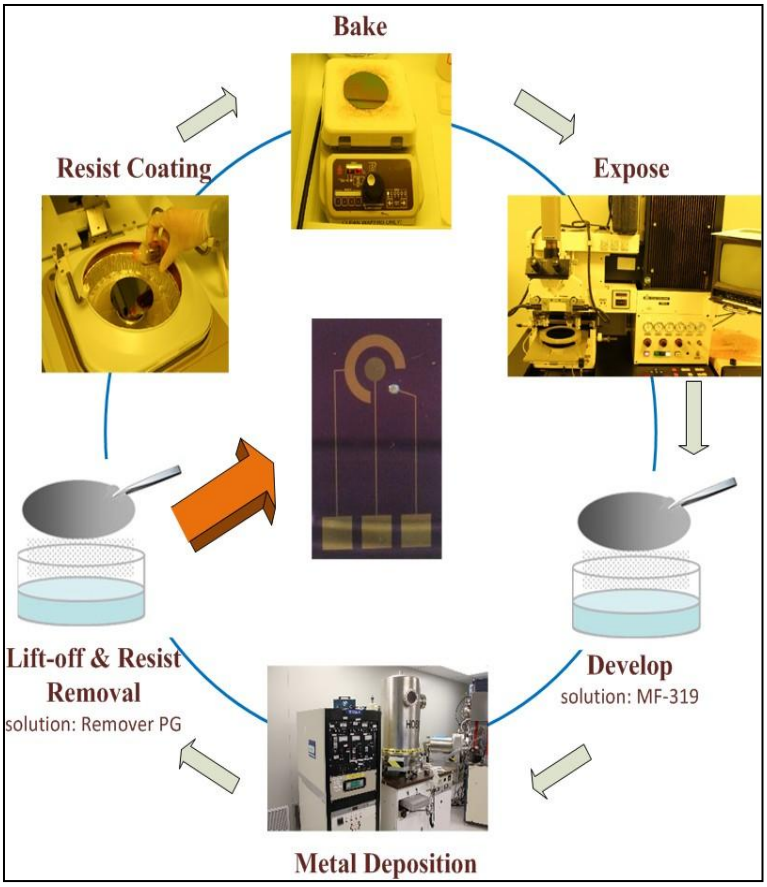

Figure 3.2: Apparatus of main procedures for photolithography and metallization.

3.2.2.1 Substrate pretreatment

Before applying lift off resist (LOR) and photoresist, the substrate was clean and dried in order to maximize process reliability. The wafer cleaning began with Nano-strip solvent to wash off surface organic material, followed by de-ionized (DI) water rinse, and then nitrogen blow dry. Afterwards, to completely dehydrate surface, the wafer was baking on a hotplate at 200°C for 5 minutes. Due to outstanding adhesion of LOR to most semiconductors (SiO_2 in our case), HMDS (hexamethyldisilazane) primer is not necessarily applied as adhesion promoter (MicroChem Corp, 2001).

3.2.2.2 Lift-off resist coating

According to the data sheet of LOR resists, LOR resists is a great candidate for producing various film thicknesses with different spin-coat condition with minimum defect generating. The dependence of the film thickness on spin speed is displayed in Figure 3.3, which provides necessary information about the LOR spin-coating conditions. For better lift-off results, the thickness of the LOR film should be thicker than the metal deposition thickness; typically the thickness of the metal film is about 1.33 to 1.5 times. The range of LOR spin speed is between 2,500 and 4,500 rpm without coating defect generation but statistic uniformity. The spin-coating speed will adjust along with the area of the substrates such as higher speeds suitable for smaller substrate and vice versa. The coating parameter suited for LOR 5a best is listed in Table 3.1(MicroChem Corp, 2001).

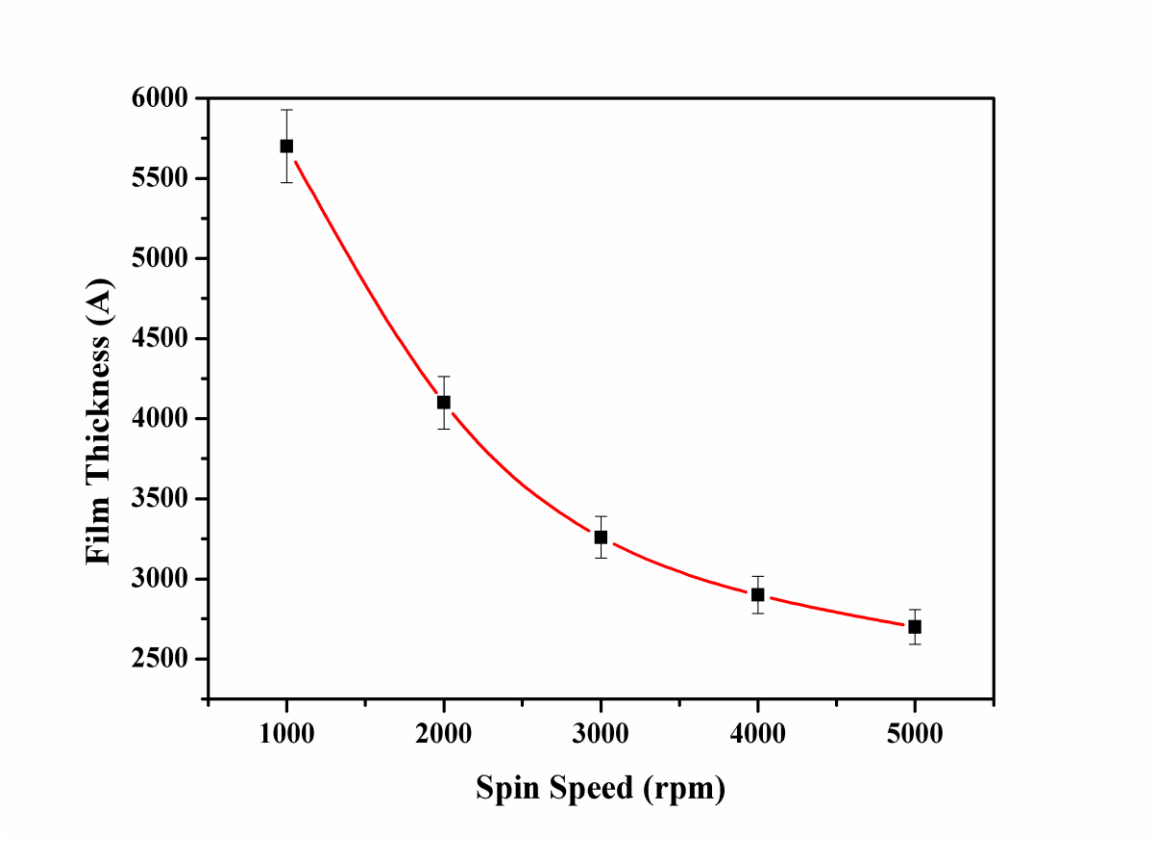

Figure 3.3: Spin speed versus thickness for Lift-off resist series.

Table 3.1: Recommended coating parameters for LOR 5A (MicroChem Corp, 2001)

Process Step	**Process Parameters**
Dispense volume	3ml (100-mm Si wafer)
Dispense mode	Dynamic 3-5 seconds
Dispense spin speed	200-500 rpm
Acceleration	10,000 (rpm) per second
Terminal spin speed	3,000 (rpm)
Spin time	45 seconds
Edge bead remover	EBR PG

3.2.2.3 Soft bake

The primary purpose of the soft is to remove the solvent and dehydrated the LOR film and control the undercut rate during the development process. In this process, temperature and bake time is critical. As shown in Figure 3.4 (a) and (b), the temperature shows greater influences over the baking time. The parameters in our experiment are bake at 160 ℃ for 5mins.

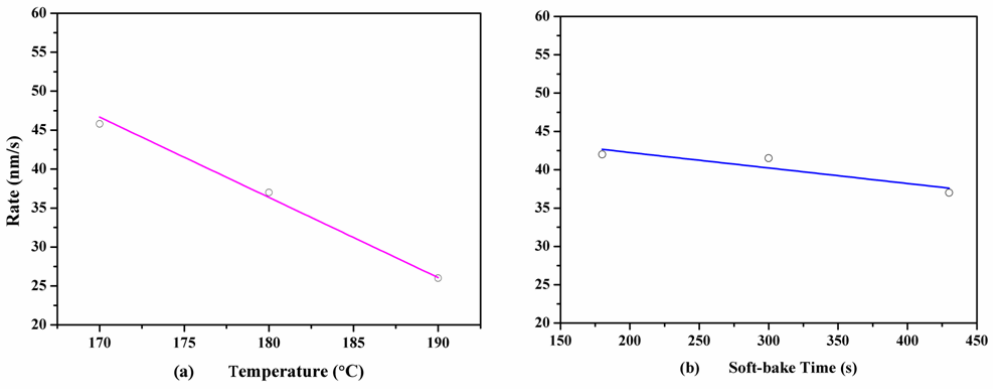

Figure 3.4: The influence of soft bake time and temperature.

3.2.2.4 Development process

In our case, we chose MF-319 for the developing solution. The experimental condition was listed in Table 3.2. The whole process was performed on the automated machine set the parameter as follow: rinsing for 30s, develop for 6 mins and rinsing and blow dry.

Table 3.2: Undercut size versus developing time.

Develop Time	**1.5 – 2 mins**	**2 – 3 mins**	**3 – 4 mins**
Undercut (2000 rpm and 200°C soft bake)	0 -2 μm	2 -5 μm	5 -7 μm

3.2.2.5 O_2 Descum

In order to get the best experimental results, before metal deposition, the wafer is optional to clean by oxygen plasma etch, which is call oxygen plasma de-scum. The de-scum is a short-time (2-3 minutes) etching by oxygen plasma to eliminate residue photoresist leading to poor metal contact or adhesion.

3.2.2.6 Lift-off Process

The bottom layer is LOR, then it will require sufficient time to stripping of the LOR layer and soaking in Remover PG overnight has the best results.

3.3 Biodetection

3.3.1 Immunoassay

As introduced in Chapter 1, immunoassay is the interaction between antibody and antigen, which is the gold standard technique for cardiac biomarker detection and determination, and is one of the most prevalent detection methods used in food safety, environmental monitoring, biotechnological investigation, and clinical analysis (Lin et al., 2010b; Mohammed and Desmulliez, 2011) .

3.3.2 Working principle and classification

One of the immunoassay formats is that divided into heterogeneous and homogeneous type. (Ha et al., 2009) When the antibody and antigen are immobilized on a solid substrate forming the complex without further separation, the immunoassay is called heterogeneous format. Because the immunoreaction happens on the surface of the substrate, heterogeneous immunoassay has high surface area/volume ratio and excellent analytical sensitivity. But immobilizing antibody or antigen on the solid substrate is inextricable and sophisticated, for instance, hydrophilic protein molecules are difficult to absorb on the hydrophobic polymer substrate without pretreatment. In contrast, when the conjugation of antibody and antigen happens in the solution, the immunoassay is the homogeneous format. Homogeneous style brings the multiplexing and fast electrophoretic separations up to immunoassay, but being constrained by antibody or antigen solution preconcentration (Lin et al., 2010a).

Traditional ELISA usually takes several hours and complicated process to get the final results. As shown in Figure 3.10. However, the one-step electrochemical ELISA (Figure 3.11) can be simplifies the whole process into four steps without comprising the benefits of the ELISA. Both detection systems are classic sandwich immunoassay principle, which includes the following steps: monoclonal antibody coating on the surface and antigen–detection antibody complex react with the capture antibody with a detectable label.

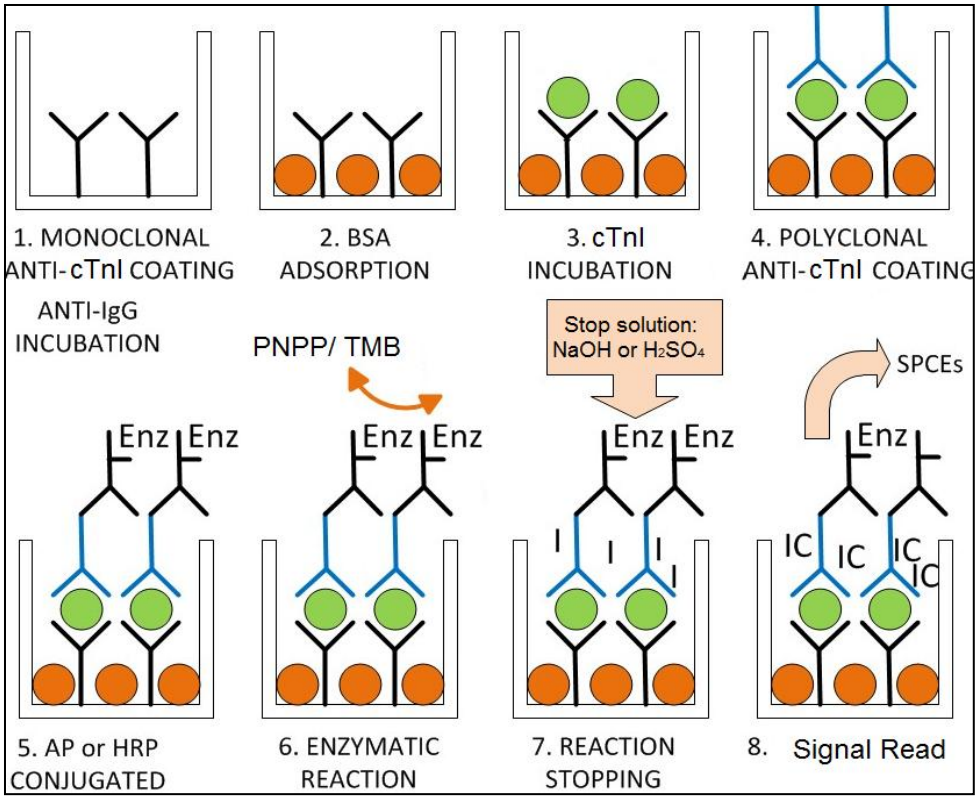

Figure 3.5: Working schematics of the traditional ELISA.

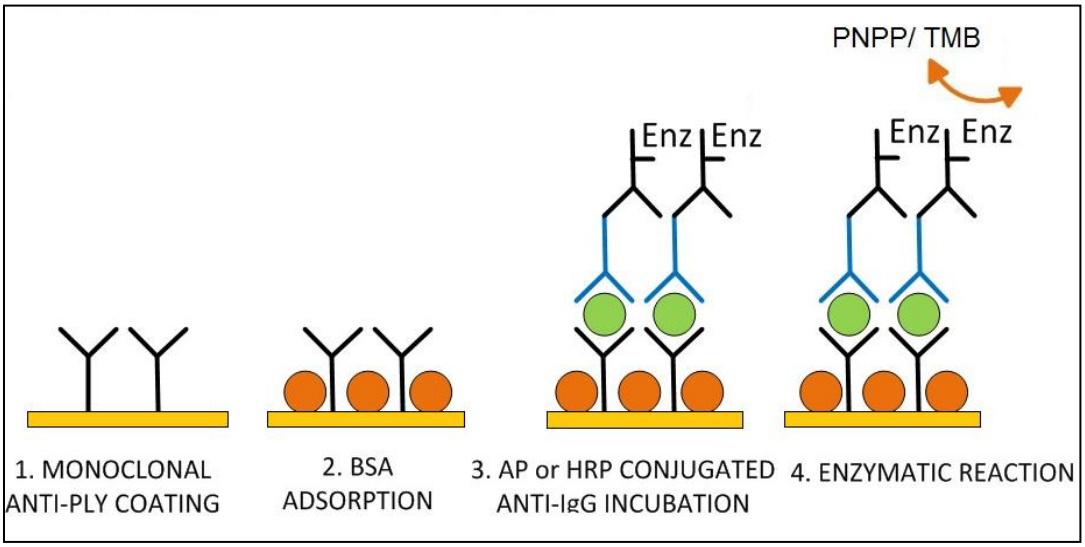

Figure 3.6: Schematics of the one-step electrochemical ELISA.

3.3.3 Procedures

3.3.3.1 Immobilization of cTnI capture antibody

One of the most critical steps is to immobilize the capture antibody on the surface of the immunosensor. The response may present high background noise or poorly reactive of the reaction of the probe, which will result in decreasing significantly the sensitivity or the ratio of signal to noise of the immunosensor, due to the inappropriate binding of the capture antibody (Corgier et al., 2005; Corgier et al., 2007; Lahann et al., 2003; Mao et al., 2002).

3.3.3.2 Configuration of the immunosensor

As shown in Figure 3.12, the configuration of the immunosensor can be divvied into base, which including the substrate, metal layer, and the mediator; immunoreaction, BSA, capture antibody and detection antibody labeled with enzyme; and the signal generation, which was catalyzed by the enzyme and generation free electron to obtain the amperometric response.

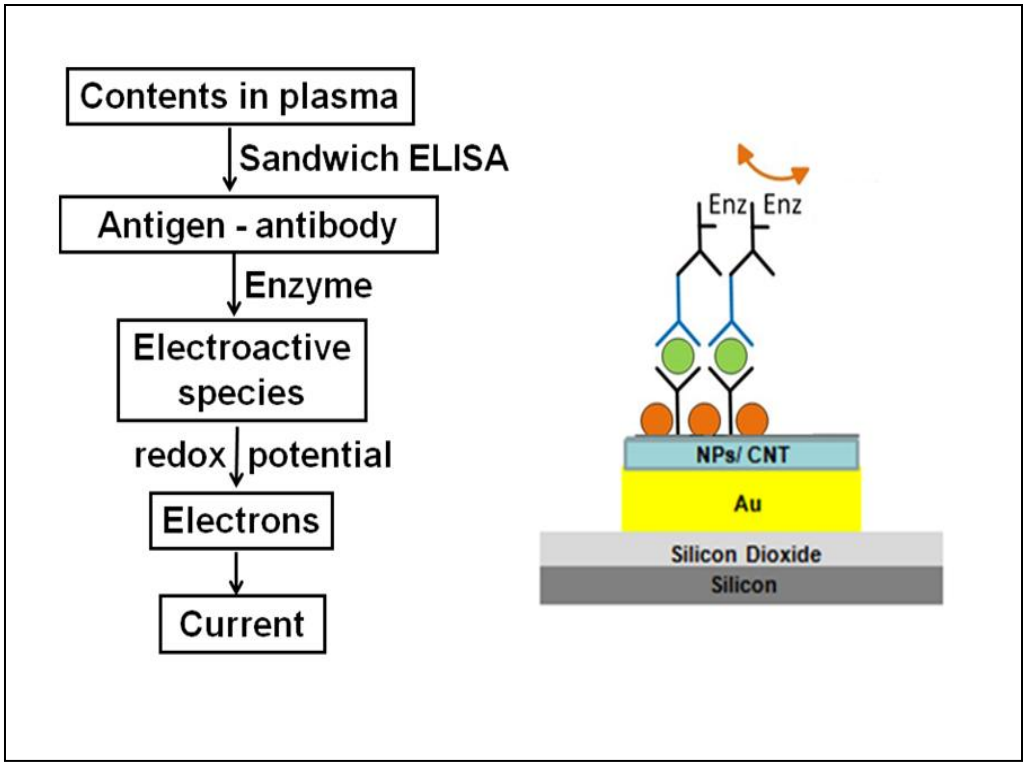

Figure 3.7: Configuration of cardiac troponin I immunosensor.

3.4 Conclusion

In this chapter, we have discussed about the fabrication process and configuration of the immunosensor. The pattern from the mask was transferred to the substrate by lift-off technique, in which lift-off resist and positive photoresist Shipley1827 was involved in the photolithography process. Shipley1827 as the sacrificial layer was indirect contacted with the substrate. Meanwhile, the fabrication process was being controlled by temperature, developing time, exposing dose and other factor. The immunosensor was constructed by classic sandwich ELISA: the complex of antigen and detection antibody labeled with signal generating enzyme was captured by immobilized first antibody, and BSA acting as a blocking membrane to eliminating non-specific binding interference.

Chapter 4

4 Electrode modification and optimization

Electrochemical immunosensor brought tremendous interest for point-of-care diagnostics, such as small sample volume, high sensitivity, and time efficiency. In this chapter, nanomaterials modified immunosensor, carbon nanotube, and gold nanoparticles, were designed, investigated, and optimized.

4.1 Introduction

As discussed before, troponin I (cTnI) plays a critical role in diagnosis and management, prognosis of myocardial infarction. It is well known that electrochemical immunosensor possesses tremendous promising properties such like specificity and detection simplicity, cost efficiency, short assay time, and highly adaptable for miniaturization, has recently drawn considerable attention. Various format immunosensors combined with electrochemical techniques such as potentiometry, amperometry, or piezoelectry, have been developed for electrochemical assays of the cTnI level (Ahammad et al., 2011; Kurkina and Balasubramanian, 2012; Lin et al., 2011; Tang et al., 2011; Zhou et al., 2010). For example, a multiplex cancer electrochemical immunosensor was recently reported by Guo et al., which was a flow injection device as the screen-printed glassy carbon electrode modified chitosan matrix to enhance molecular immobilization. The cancer biomarker arrays were developed to determine several tumor markers simultaneously without comprising experimental performance such as low detection limit and high throughput (Guo et al., 2010).

Lately, the development of advanced materials and the utilization of nanomaterials in biosensor gain more and more attentions from various research groups. Carbon nanotube (CNT) possesses unique properties in terms of remarkable mechanical, electrical, chemical and structural performance. CNT, the largest elastic materials among the world, can play as metallic ions, semi-conductive materials with excellent electron

transportation, and be suitable as a host for storing guest biomolecules as well (Davis et al., 2003; Wang, 2005). Furthermore, CNT demonstrates substantial prospects in sensor fabrication, both biosensor and immunosensor, in terms of excellent chemical stability, extraordinary electronic properties, strong mechanical performance, and high surface-area-to volume ratio(Lin et al., 2011). However, the CNT application was constrained by the poor liquid dispersibility, particularly in DI water; therefore, introducing Poly (diallydimethylammonium) chloride, a water-soluble quaternary ammonium polyelectrolyte, also called PDDA is used to improve the dispersibility of CNT. PDDA was commonly used in water treatment, the mining industry operation, paper manufacturing process and biological application (Rochette et al., 2005), and was found to be capable of improving the homogeneity of CNT film by helping CNT disperse in the water(Kim et al., 2003; Kim and Sigmund, 2003; Wen et al., 2007). There are two types of CNT based on the production process: single-wall carbon nanotube (SWCNT) and multi-wall carbon nanotube (SWCNT). We use MWCNT in all the following experiments.

In electrochemical application, gold nanoparticles (AuNPs) can have various functions, which can be classifies as: biomolecules immobilization, electron transfer enhancement, catalyzing the reaction, function as biomolecules label and even act as a reactant (Luo et al., 2006). Furthermore, AuNPs is also notable biocompatible materials, which can create a native environment for bioconjugates or biomolecules. Therefore, AuNPs can be the perfect candidate for the immobilization matrix because it can absorb biomolecules firmly due to its large specific surface area along with high surface free energy without destroying the biological activity of the antibody or antigens (Luckham and Brennan, 2010; Luo et al., 2006). However, the absorption capacity of AuNPs on the electrode surface is not sufficient. Therefore, we introduce AuNPs doped with chitosan for electro modification. On the one hand, chitosan is a natural biopolymer comprised of rich hydroxyl function groups and active amino, which is one of the most popular candidates for immobilization matrix (Cavalcanti et al., 2012). On the other hand, the poor conductivity leads chitosan to combining with other materials such like CNT, metal nanoparticles, or redox mediators for biosensing in electrochemical platforms (Yang et al., 2011).

In this current work, we using PDDA-MWCNT and chitosan- AuNPs as the electrode modification, for capture antibody immobilization and electron transfer enhancement to construct a sensitive immunosensor for cTnI determination. In addition, based on such a configuration, the experimental conditions were optimized and the linearity and sensitivity were investigated.

4.2 Experimental

4.2.1 Chemicals

Troponin I from the human heart, the rabbit anti-human cTnI polyclonal antibody, and the mouse anti-human cTnI monoclonal antibody were purchased from Sigma-Aldrich. 4-Aminophenyl phosphate monosodium salt hydrate was obtained from Gold Biotechnology (St. Louis, USA). Maleimide alkaline phosphatase and maleimide horseradish peroxide were received from Innova Bioscience (Cambridge, UK). N-Succinimidyl S-acetylthioacetate (SATA), alkaline phosphatase stabilizing buffer, sodium aside, diethanolamine (DEA), dimethylsufoxide (DMSO), bovine serum albumin (BSA), p-nitrophenyl phosphate (p-NPP) liquid substrate, Trizma® base (tris-(hydroxylmethyl)-aminomethane(Tris)), hydroquinone, potassium ferricyanide (III), polyoxyethylenesorbitan manolaurate (Tween™ 20), and PDDA (20 wt % in water) were all purchased from Sigma-Aldrich.

All these buffers. such like phosphate buffer solution (PBS), blocking buffer (1% BSA in PBS) and etc., were prepared every week. The MWCNT (cylindrical with diameter range in 5-15nm) with 95% purity was purchased from US Research Nanomaterials, Inc.

All the reagents and chemicals were analytical-reagent grade or better without any further purification. Deionized (DI) water, with resistivity higher than 18 MΩ (Milli-Q, USA), was used throughout.

4.2.2 Apparatus

Hitachi S-4500 field emission scanning electron microscope (SEM) along with the energy dispersive X-ray spectroscope (EDX) was the equipment performed to characterize the microstructure of the modified electrodes and all images were taken at 5 kV. The Varian UV-visible spectrophotometer were engaged to provide the control experiment reference of cTnI in serum using a standard troponin I kit purchased from GenWay Biotech, San Diego.

All electrochemical experiments were performed by a computer-interfaced CHI1200a (CHI Instruments, Inc., USA). For traditional electrochemical cell, the bulk gold working electrode (2 mm diameter), a platinum wire counter electrode, Ag/AgCl reference electrode immersed in saturated KCl solution were incorporated into a classic three-electrode electrochemical cell. All the electrodes and cell stand were all obtained from CHI instruments, Inc., USA. For the planar electrode, as mention in chapter 3, three electrodes along with leads and contact pads were fabricated on the silicon wafer with 100 nm silicon oxide layer. All the modifications only were applied on working electrode (diameter 3mm). A dot of Ag/AgCl ink (AG-500, conductive compounds) was dropped on the reference electrode, as shown in Figure 4.1.

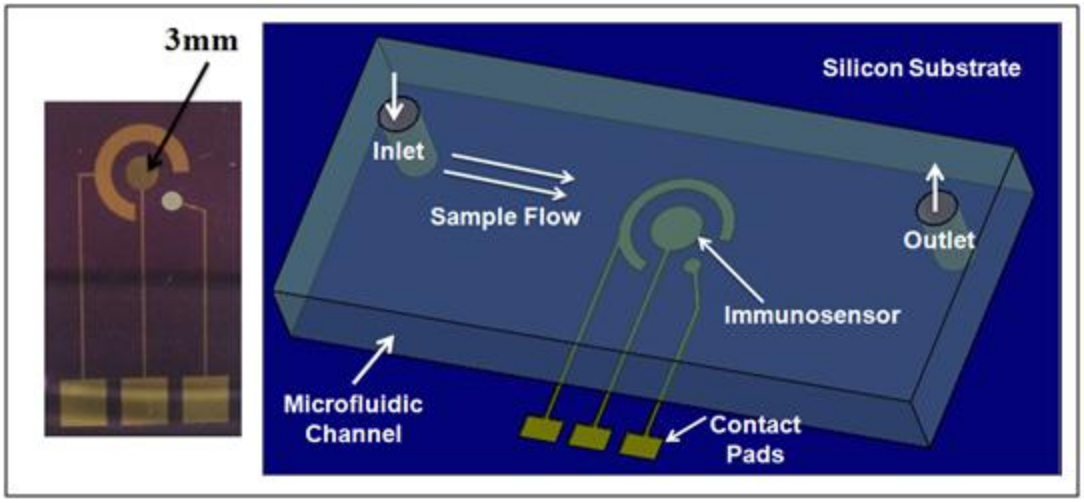

Figure 4.1: Planar electrode and preliminary design for immunosensor embedded in a microfluidic chip.

4.2.2.1 Carbon nanotube preparation

In general, carbon nanotube needs to be immersed in strong acids, e.g. HNO_3 or H_2SO_4, to functionalize and purify. Hydrogen ion (H^+) will cause carbon nanotubes rich in carboxyl group (-COOH), which are vital for not only conjugate with biomolecules but also absorb in the hydrophilic surface. Therefore, the MWCNT was firstly added into the mixture of H_2SO_4 (98%) and HNO_3 (60%) (3:1 (v/v)) for hydrophilic treatment for eight hours (Kannan et al., 2009; Piao et al., 2009; Saito et al., 2002). Then the acid mixture solution was removed from the supernatant and adds NaOH into MWCNT solution till pH value reach 7 to neutralize the solution. Then to remove the residue $NaNO_3$ and Na_2SO_4 the following procedures were repeated several times: adding DI water to the MWCNT solution, centrifugation the mixture and removing the supernatant. To form MWCNT-PDDA composite, in 10 ml vial, adding 2 ml 8% PDDA and 2 mg MWCNT, and the mixture was ultrasonicated for 1.5 h. The excess PDDA was removed by centrifugation (higher speed) and washed with DI water till the mixture is stable. Then the MWCNT-PDDA was ready for the following experiments. (Bi et al., 2009; Manesh et al., 2008; Wang et al., 2011).

4.2.2.2 Preparation of chitosan-AuNPs

The gold nanoparticles were prepared using the protocols according to the literature (Doron et al., 1995; Xue et al., 2006), by adding 2.5 mL of 1.0% trisodium citrate to the 100 mL of boiling $HAuCl_4$, the concentration of which is 0.01 % (w/w). Keep the mixture boiling and stirring for 10 minutes. Then pour the solution into a dark glass bottle and use it in a week to prevent the AuNPs from agglomerating.

1% (wt%) chitosan solution was prepared, in a 15 mL vial, by adding chitosan powder into 0.05 M acetic acid solution, and then ultrasonicated until the chitosan powder was completely dissolved (Xue et al., 2006). Then mix the AuNPs solution with chitosan solution together in volume ratio 1:1 to form the chitosan-AuNPs composite.

4.2.3 Electrode preparation and pretreatment

For the bulk electrode, the Au electrode was polished with 0.1 and 0.1 μm alumina slurry on microcloth pads sequentially to physically remove the oxide layer, followed by rinsing with double dilute water. Then the electrode was immersed in freshly prepared Piranha solution (30% H_2O_2: H_2SO_4 = 1:3 (v/v)) to remove organic residue. Then the electrode was ultrasonicated in DI water, acetone, and DI water for 5 minutes, respectively. To further clean and activation, the electrode was immersed in 0.1 M sulfuric acid under a cyclic voltage from 0.6 to 1.5 V with the scan rate of 50 mV s^{-1} till a stable voltammogram established (Figure 4.1), then the electrode has been fully ready for further electrochemical experiments (Elliott et al., 1999). For planar electrode, it will only require the last step for cleaning and activating the working electrode.

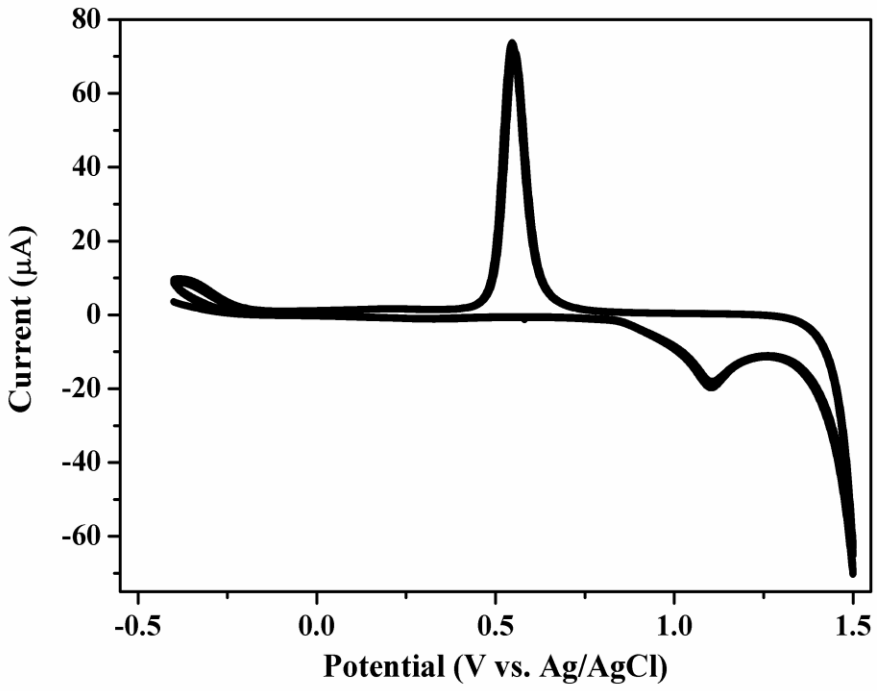

Figure 4.2: Electrochemical cleaning and activation of electrodes in 0. 1 M sulfuric acid by cycling between 0.6 V and 1.5 V at a sweep rate of 50 mV s-1.

4.2.4 Electrode modification and characterization

To modify the electrodes, spread 5 μL of the MWCNT-PDDA solution or chitosan-AuNPs solution over the Au electrode surface, and then set it at the room temperature to evaporate the solvent. After that, on the surface of the electrode, a film will form, which can be visually observed.

4.2.5 Preparation of antibody-enzyme conjugates

The process was established through SATA as a crosslink to form a thiol function group and then react with maleimide activated alkaline phosphatase (ALP). The schematic is shown in Figure 4.2. The antibody-enzyme conjugation process is depicted as follows (O'Regan et al., 2003; O'Regan et al., 2002).

(1) Prepare antibody stock solution. In 2 mL vial, adding 100 μL anti-cTnI polyclonal antibody (1 mg/mL) and then adding 100 μL sodium phosphate buffer (50 mM NaH_2PO_4 and 1mM EDTA, pH 7.5).

(2) Prepare SATA stock solution (1.5 mg/mL in DMSO).

(3) Add 5 μL SATA stock solution to antibody stock solution, and then gently shake the vial and set at room temperature for 45 min.

(4) To remove the by-product (residue SATA) by centrifugation using a 30 kDa cut-off ultracentrifuge filter (Sigma) against sodium phosphate buffer.

(5) Prepare deacetylation solution, 20 mL (50 mM NaH_2PO_4, 25 mM EDTA, 0.5 M hydroxylamine– HCl, pH 7.5).

(6) Add to the antibody mixture and let it incubate for 2 hours at room temperature to reveal the thoil group.

(7) Dialyse the solution against DPBS (137 mM NaCl, 2.6 mM KCl, 8 mM Na_2HPO_4, 1.5 mM NaH_2PO_4, 1 mM EDTA, pH 6.6) at room temperature for 12 h/ overnight.

(8) Add maleimide activated ALP to antibody solution based on molar ration 2:1 (1:1(w/w)) and then left in 4 °C for 12 hours.

(9) Dialyze conjugates against Tris buffer (50 mM Trizma base, 50 mM NaCl, 1 mM $MgCl_2$, pH 7.4) for overnight at room temperature.

(10) Add ALP stabilizing buffer (Tris buffer, pH 8.0, 1% (w/v) BSA and 0.05% (w/v) sodium azide) to adjusted to a final volume of 500 mL. Then store the conjugates at 4 ^{0}C.

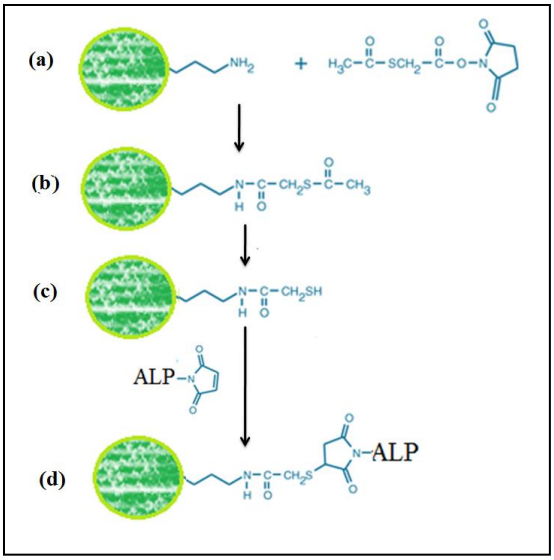

Figure 4.2: Illustration of antibody-ALP conjugates: (a) Attachment to antibody, (b) deprotection, and (c) reaction with ALP, (d) Conjugates. Adapted from (Life Technologies)

4.2.6 Immunoassay protocols

The immunoassay utilized in the current work is 2-site enzyme-linked-immunosorbent serologic assay (ELISA), also called as sandwich type ELISA. Therefore, the immunoassay protocols include three principal procedures: incubate first antibody, blocking, and incubation antigen-antibody-ALP. First, incubate the capture antibody. Add 5 µL capture antibody solution (anti-cTnI monoclonal in carbonate buffer, pH 9.5) and incubate for 60 minutes at 37 °C, and then rinsing thoroughly with washing buffer (0.05% Tween® in PBS, pH 7.4) to remove the unbound antibodies. Then add a drop of 5 µL 10% (w/v) BSA in PBS (pH 7.4) and incubate for 60 minutes at 37 °C, to block the non-specific bounding. Afterwards, repeat washing by 0.05% Tween® in PBS. Finally, incubate the premixed antigen-antibody-ALP a drop of 5 µL, incubate for 60 minutes at 37 °C. Then the electrode would be ready to move on the electrochemical experiments. For the bulk electrodes, after each immunoassay run, immerse the electrode into 0.1 M glycine-HCl (pH 2.0) for 5 min and rinse by double dilute water. Then start from electrode pre-treatment to carry out another sensing cycle (Gao et al., 2003).

4.2.7 Electrochemical detection

Electrochemical measurements were done in a conventional electrochemical cell or on a flat chip, which is the macroscale prototype of at the room temperature. Firstly, Cyclic voltammograms (CVs) were performed 2 mM PBS (pH 6.5) containing 5.0 mM $K_3[Fe(CN)_6]/K_4[Fe(CN)_6]$ (1:1) mixture and 0.1 M KCl from 0.6 to −0.2 V (vs. Ag/AgCl) at the scan rate of 50 mV s^{-1} to monitor the current variation (ΔI) before or after nanomaterial modification because PDDA-MWCNT and chitosan-AuNPs will increase the electron transferring and lead to current response enlarged (Gao et al., 2003). Secondly, the immunoreaction was monitored by cyclic voltammograms performed in PNPP (p-nitrophenyl phosphate) liquid substrate (pH 9.0) purchased from Sigma. When the antigen has bound with both antibodies: capture antibody helping coated on the surface of the electrode and the second antibody (labelled with ALP) catalyzing the substrate to generating current response, then there is current response of the immunoreactions. All the electrochemical experiments were carried at the room temperature.

4.3 Results and discussion

4.3.1 Electrochemical characteristics of bare electrode

After polished, ultrasound, and strong acid clean, to clarify that the electrode is ready for experiment: Cyclic voltammograms (CVs) were performed in 0.02 M PBS (pH 6.5) containing 5.0 mM $K_3[Fe(CN)_6]/K_4[Fe(CN)_6]$ (1:1) mixture and 0.1 M KCl from 0.6 to −0.2 V. The ideal difference between redox peak should be 67 mV (Tang et al., 1988), which is barely happening in the realistic. As long as the difference ranges between 60 mV to 100 mV, then the electrode can perform well. If the potential difference of the peak of redox current is over 100 mV, then the electrode needs further clean which may start from the electrode pre-treatment. Here, Figure 4.2 shows the cleaned electrode with 71 mV difference, indicating the electrode been cleaned, activated and ready for the following experiments.

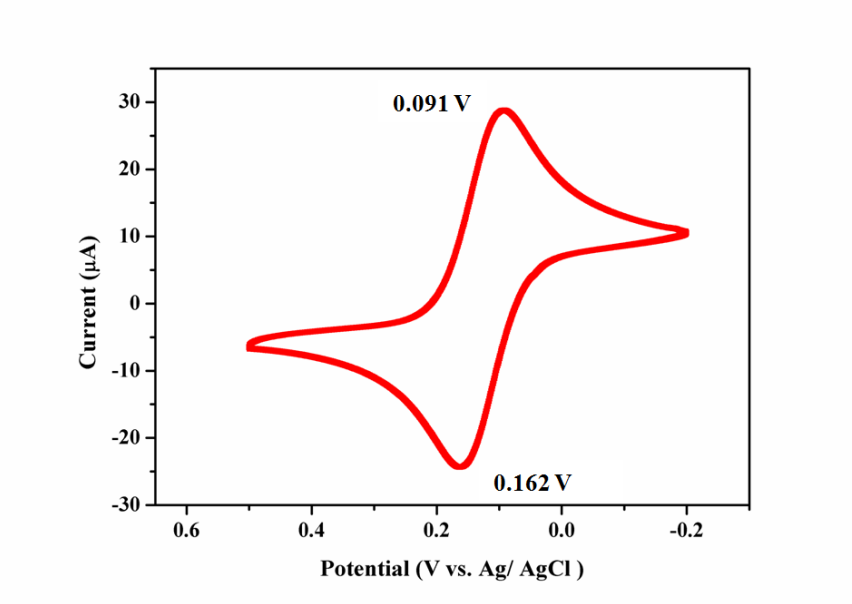

Figure 4.3: Electrochemical indication in 0.02 M PBS (pH 6.5) containing 5.0 mM $K_3[Fe(CN)_6]/K_4[Fe(CN)_6]$ (1:1) mixture and 0.1 M KCl from 0.6 to −0.2 V.

4.3.2 Characteristics of CNT, AuNP

Adding PDDA into MWCNT solution leads to phenomenal improvement of the dispersibility of MWCNT in water. In addition, the stability has been remarkably enhanced, for example the homogeneous, well-soluble suspension of PDDA-MWCNT could be stored stably for months. The characterization of the PDDA-MWCNT composite, morphology and structure were shown in Figure 4.4. Figure 4.4 (a) shows the homogeneous and porous film comprised of PDDA-MWCNT (Suprun et al., 2011), which is evenly spread on the surface of the working electrode. On the contrary, Figure 4.4 (b), the inset of Figure 4.4 (a), demonstrated conglobation comprised by MWCNT without treatment, ending up with a uniform surface, indicating the enormous value of PDDA in dispersing MWCNT (Wen et al., 2007). Figure 4.4 (c) displays the characterization of gold nanoparticles (AuNPs), which would significantly increase the coverage of capture antibody anti-cTnI due to large surface-to-volume ration of the nanospheres structure (Suprun et al., 2010).

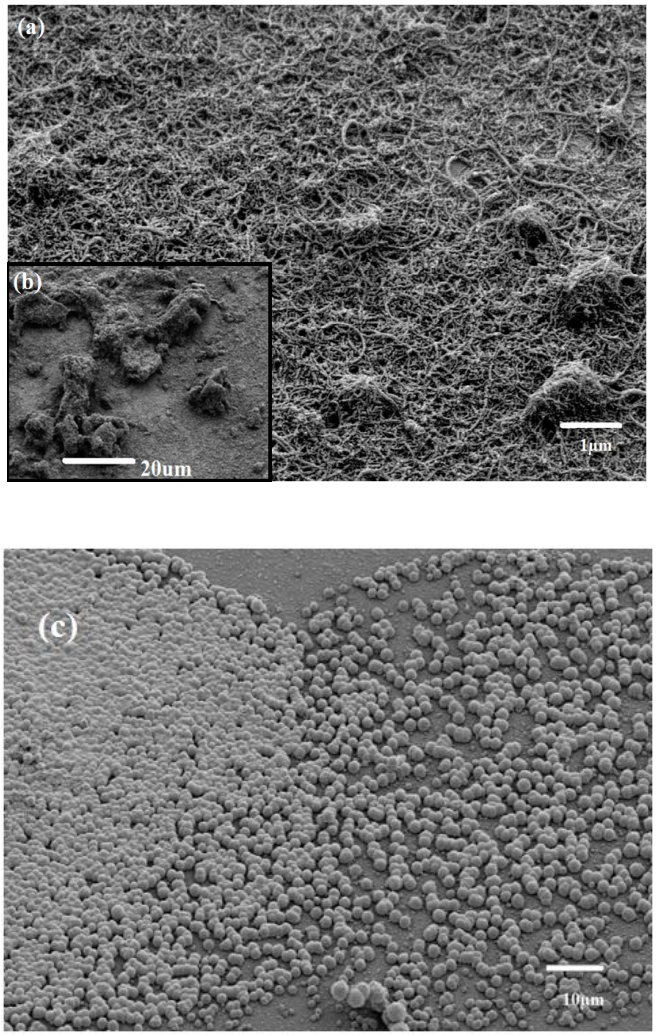

Figure 4.4: SEM images of (a) PDDA-MWCNT composite; (b) MWCNT without any treatment; (c) AuNP composite on the surfaces of gold electrodes.

4.3.3 Cyclic voltammetry characterization of PDDA-MWCNT modified electrodes

The cyclic voltammetry in various scan rates was shown in Figure 4.5. It can be observed that both the peak currents of anode and cathode were increased with the scan rate. In addition, the difference between peak currents of anode and cathode was enlarged as well. Both the anodic and cathodic currents were proportional to the square roots of scan rate, from 10 mV s^{-1} to 500 mV s^{-1} , indicating that the redox process is diffusion controllable.

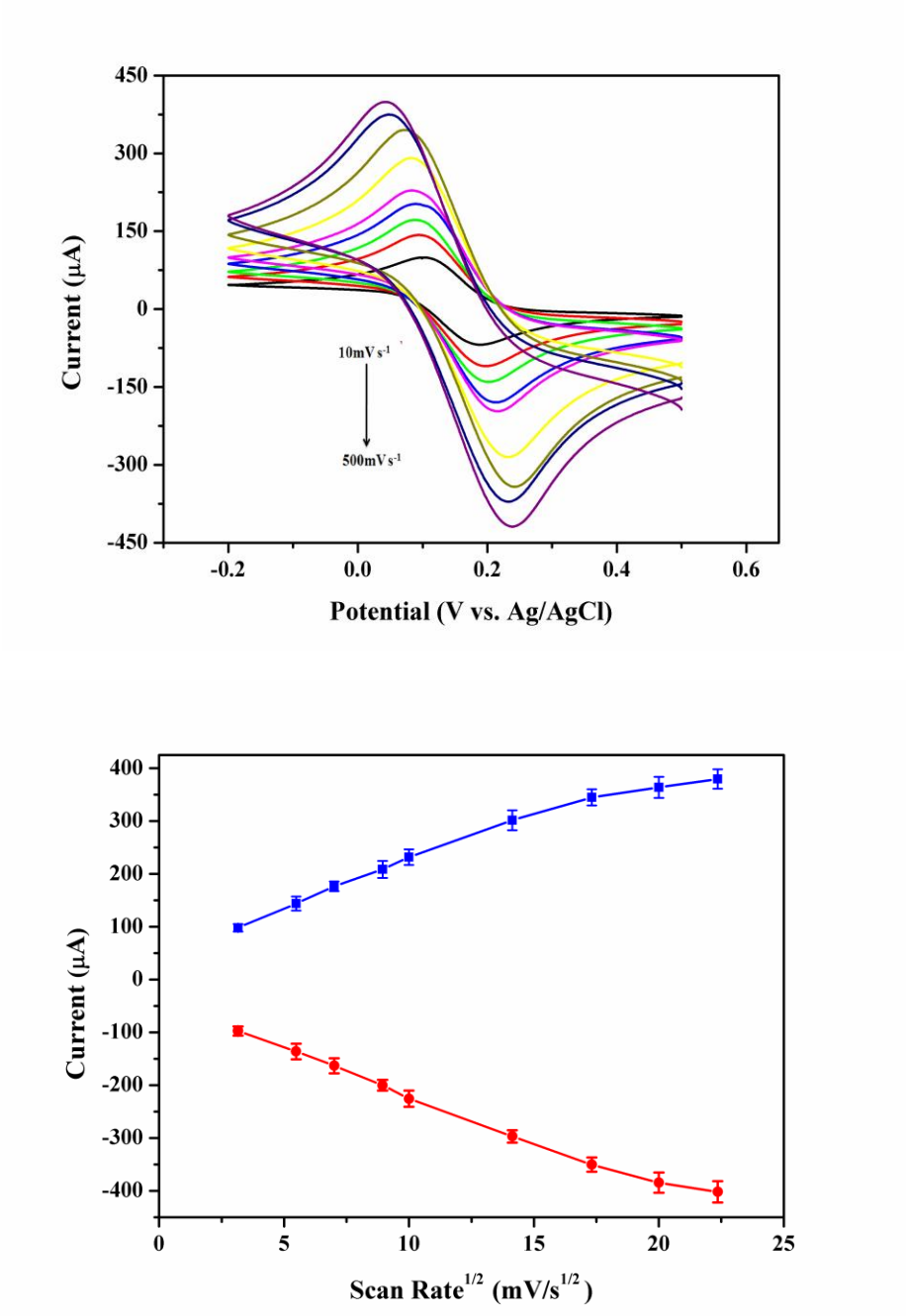

Figure 4.5 (a) The cyclic voltammograms of PDDA-MWCNT-Au electrode at various scan rates from 10 to 500 mV s^{-1} in 0.02 M PBS (pH 6.5) containing 5.0 mM $K_3[Fe(CN)_6]/K_4[Fe(CN)_6]$ (1:1) mixture and 0.1 M KCl from 0.6 to −0.2 V. (b) The dependence the redox peak current over the square root of the various scan rates.

4.3.4 Cyclic voltammetry characterization of PDDA-MWCNT and AuNPs modified electrodes

Utilizing cyclic voltammetry (CV) to characterize the modified PDDA-MWCNT and chitosan-AuNPs electrodes are based on the redox reaction of ferricyanide, as shown in equation (4.1). Herein, we choose 5 mM $K_3Fe(CN)_6$ along with 0.1M KCl solution to probe the reduction or oxidation on the surface of the electrodes. Figure 4.6 shows various modifications of the electrodes in the probing solution.

$$Fe(CN)_6^{4-} \leftrightarrow Fe(CN)_6^{3-} + e^- \quad (4.1)$$

In figure 4.6, curve a stands for the PDDA-NWCNT, which we can observe a smooth curve with a couple of well-formed redox peaks and compare with the rest three curves, the redox peaks are the largest, indication that the PDDA- MWCNT has the strongest ability of enhancing electron transfer among the other three. Curve c shows the bare electrode response of ferricyanide redox reation. Curve d displays the electrode after modified by chitosan without AuNPs, both the peaks shrunk dramatically suggesting that the chitosan molecules act as a blocking layer for the electron and mass transfer and stop the diffusion of ferricyanide (Wen et al., 2007). The blocking effect of the film can be caused by the poor conductivity of pure chitosan, the result of which agrees with the insulation of curve b. As curve b shows, the current response (curve b) increases significantly when the AuNPs were entrapped with chitosan. That is might be the AuNPs increase the conductivity of the film by facilitating the electron transferring. However, the result of electron transfer enhancement is not as good as PDDA-MWCNT, which may cause by the poor conductivity of pure chitosan as well.

Accordingly, the cyclic voltammetry (CV) characterization confirms the theory that modifying the electrode surface by PDDA-MWCNT and chitosan-AuNPs could facilitating the electro transfer for better electrochemical performance.

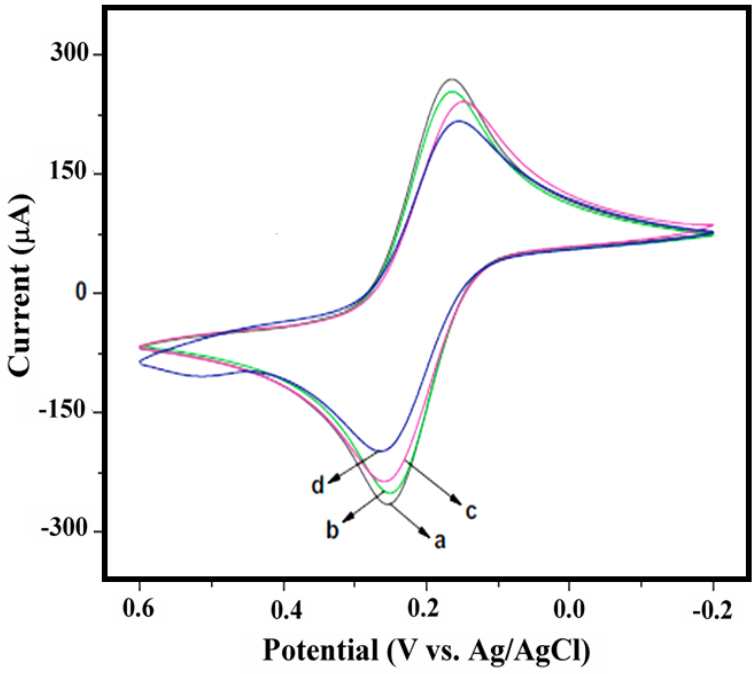

Figure 4.6: CVs of different modified electrodes in a 5 mM $K_3Fe(CN)_6$ solution containing 0.1M KCl (pH 6.5): (a) PDDA- MWCNT; (b) Chitosan- AuNP; (c) Bare electrode; (d) Chitosan.

4.3.5 CV characterization of cTnI immunosensor

To investigate the PDDA-MWCNT and chitosan-AuNPs electrochemical behaviour in the immunosensors, modified electrode along with bare electrode followed the immunoassay protocol to incubate with cTnI antigen (50 ng/mL) and alkaline phosphatase (ALP) labelled second antibody. Then all the sensors were characterized by CV scan in PNPP liquid substrate (5mM, pH 9.0). Since the existence of antibody label ALP in the solution, it will catalyze the PNPP hydrolyzing into PNP, which leads to tense electron transferring to form a well-defined oxidation peak. The scan potential range is from -0.8 to 1.2 V, and the current peak appears at about 1.0V. The amperometric response should be proportional to the amount of ALP, which were labelled with the second antibody. Since sandwich ELISA is highly sensitive and specific reaction, theoretically, the current response would be proportionally related to the antigen concentration, saying, cTnI. Figure 4.9(a), 4.10 (a) and 4.11(a) display the various current response of different concentration of the cardiac troponin I.

As shown in figure 4.7, various modifications have distinct peak value of the oxidation. Curve (a) stands for blank curve: No cTnI involved in the immunoreaction, therefore, no current response or peak value. Curve (b) indicates the bare electrode current varies on potential shifts. Curve (c) and (d) demonstrate the bare electrode current varies on potential shifts on chitosan-AuNPs and PDDA-MWCNT. As shown in figures, the peak current value of PDDA-MWCNT is twice larger than chitosan-AuNPs, and three times bigger than bare electrode, which can be explained by the following causes: First, the roughness on the electrode surface is from high to low: PDDA-MWCNT, chitosan-AuNPs, bare electrode. The rougher surface and the easier to immobilize the capture antibody, which is a key step for signal generation. Second, as discussed before, the poor conductivity of pure chitosan hinders the electron transfer to a certain extent, especially compared to the great electron transfer prompter, PDDA-MWCNT.

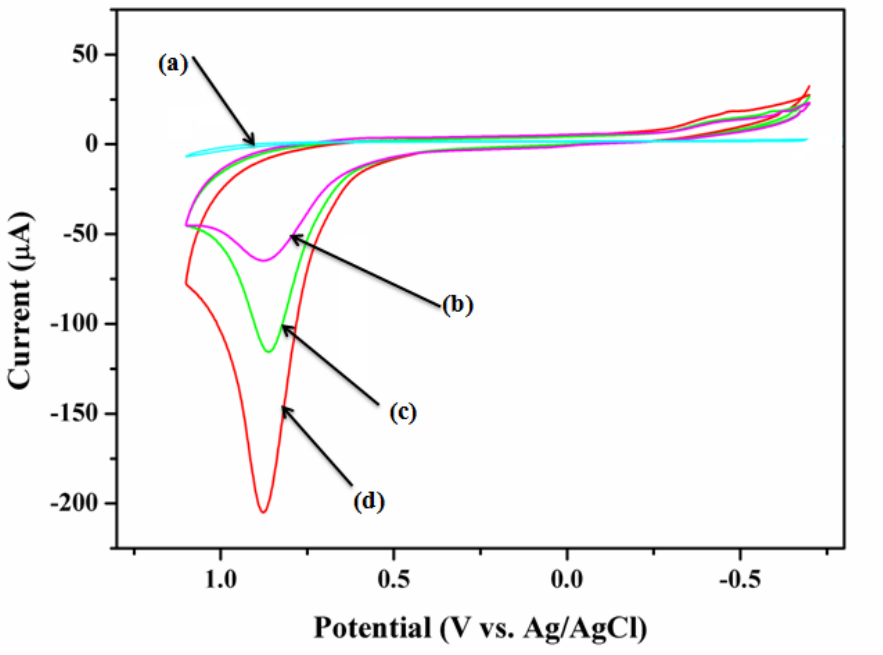

Figure 4.7: Electrochemical behavior of various modified electrodes in immunoassay: (a) blank, (b) bare electrode, (c) chitosan-AuNPs electrode, (d) PDDA-MWCNT modified surface.

4.3.6 Optimization of immunoassay procedure

There have been many factors capable of obstructing the performance of the immunosensor such like the pH value of the liquid substrate, the amount of immobilized cTnI antibody, the temperature and the incubation time etc.. Herein, the experimental condition optimization was implemented on unmodified electrodes. The amount of the capture antibody on the immunosensor to grab antigen-antibody-ALP is critical and influential for the overall performance of either PDDA-MWCNT or chitosan-AuNPs immunosensor. Then, all the experiments of optimizing experimental conditions were carried on bare electrode except other specifically addressed. The influence caused by different substrates will be addressed in the next chapter. Herein, the substrate, PNPP liquid substrate, was used as directly purchased from sigma. The concentration of the analyte, cTnI, is 30 ng ml^{-1}. Figure 4.8 (a) illustrates that the relationship between the pH value and the sensitivity. The results the sensitivity increases along with the elevated pH value from 6.1 to 10.0, and then followed by a significant drop. Therefore, take both stability and bioactivity into consideration, the pH value 9.0 was used in the following experiments. Figure 4.8 (b) presents the capture antibody concentration influence of the experiment results. As shown in the figure, the currents response increases sharply before the immobilized antibody concentration reached 20 μg ml^{-1} and then the rate of increased has been slowing down. After 40 μg ml^{-1} the response tends to be decreased, which might be caused the blocking effect of excess antibody. Therefore, the antibody concentration was as 20 μg ml^{-1} due the cost and the sensitivity. Figure 4.8 (c) demonstrates that the temperature effect on the immunosensor performance. Herein, we only take four different temperatures tested in the identical experiments: 4°C, 20°C, 37°C, and 50°C, due to the limit of the experiment conditions. The experiment response reached the peak when the temperature was 37°C, which is consisted with most literature, it might be caused by the protein reaction, antigen and antibody, reached the high bioactivity leads to the better conjugates. Figure 4.8 (d) incubation time stands for different incubation time for two different concentrations of cTnI, 10ng ml^{-1} and 50ng ml^{-1}. When the incubating time reached 20 minutes, the reaction was almost 70% finished and reached the stable till 45 min. Therefore, the incubation time was set as 20 mins.

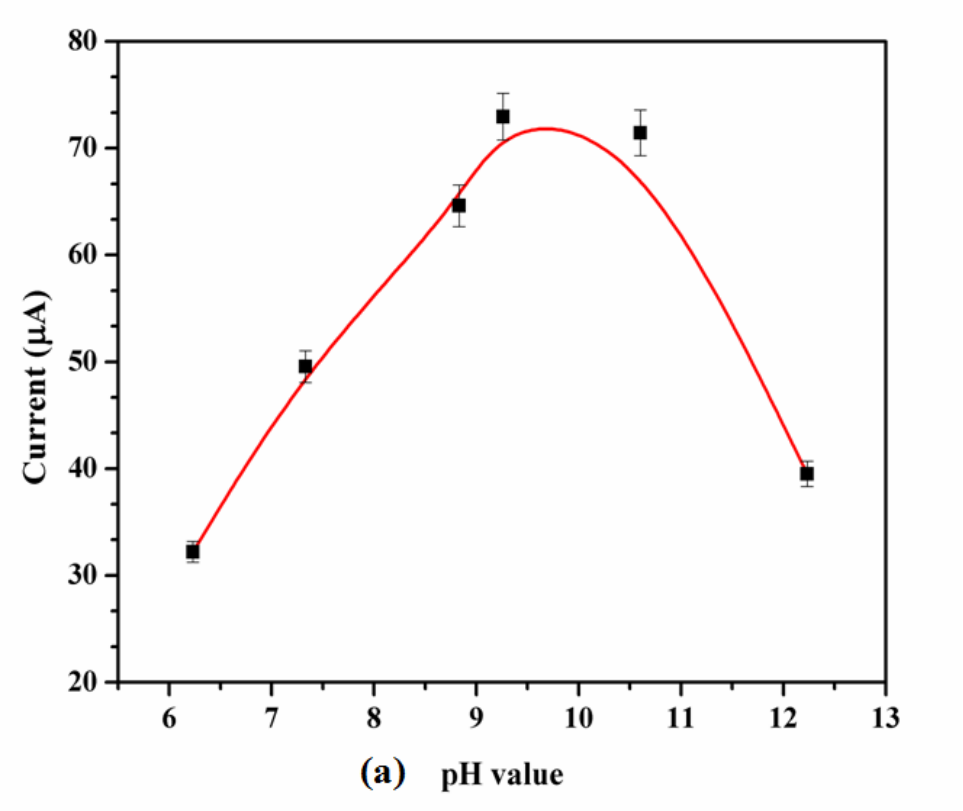
Current (μA)
80
70
60
50
40
30
20
6
7
8
9
10
11
12
13
(a) pH value

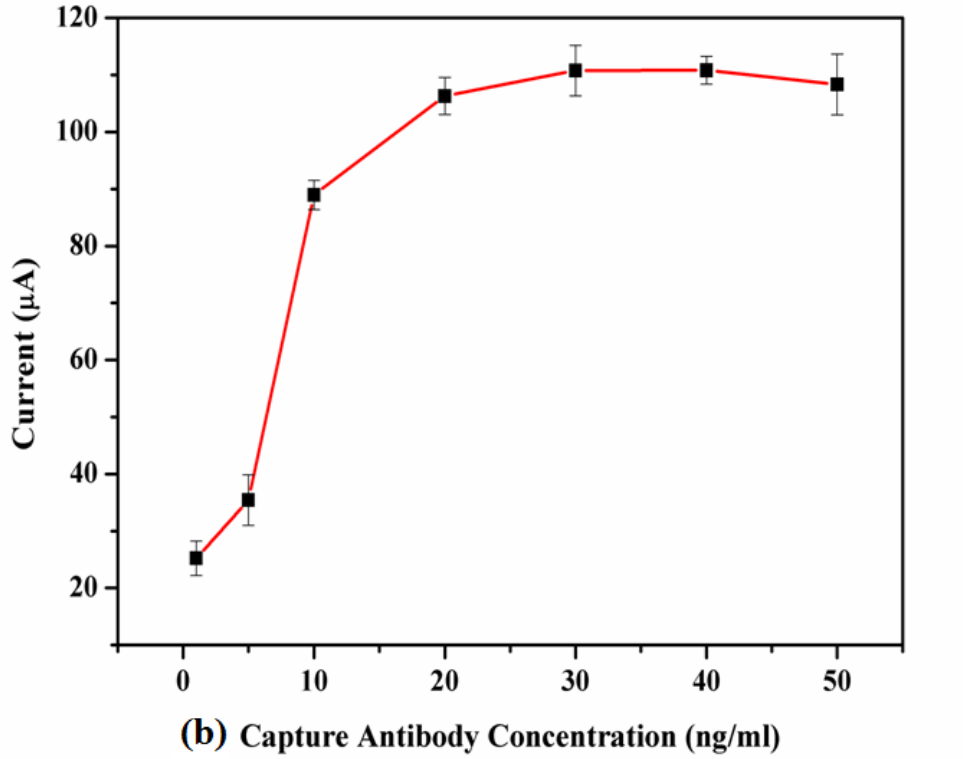
Current (μA)
120
100
80
60
40
20
0
10
20
30
40
50
(b) Capture Antibody Concentration (ng/ml)

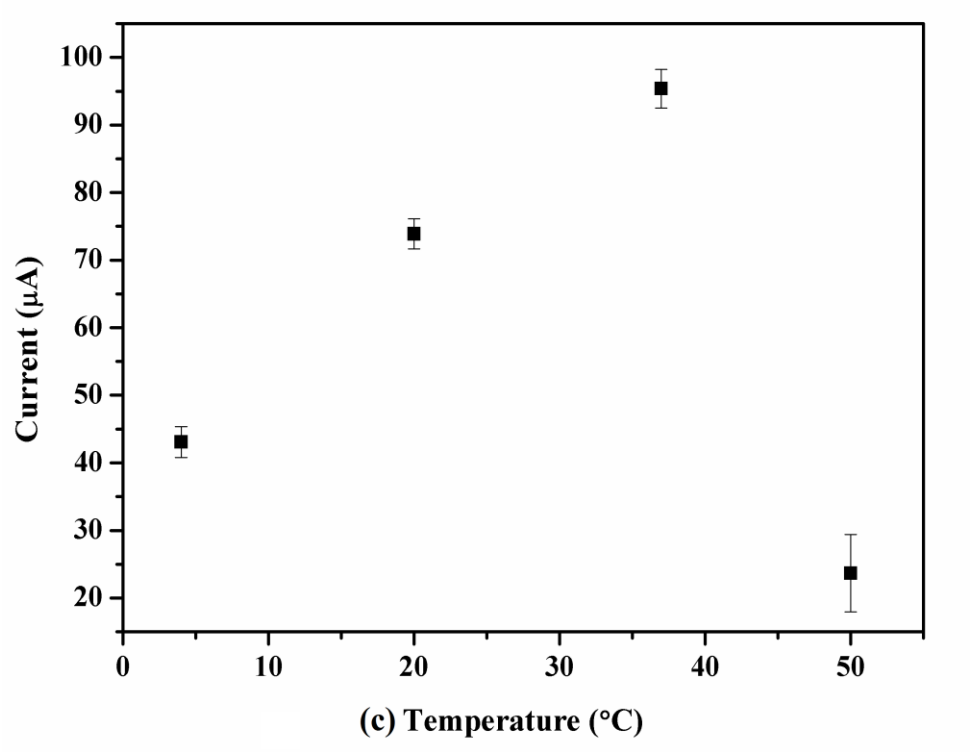

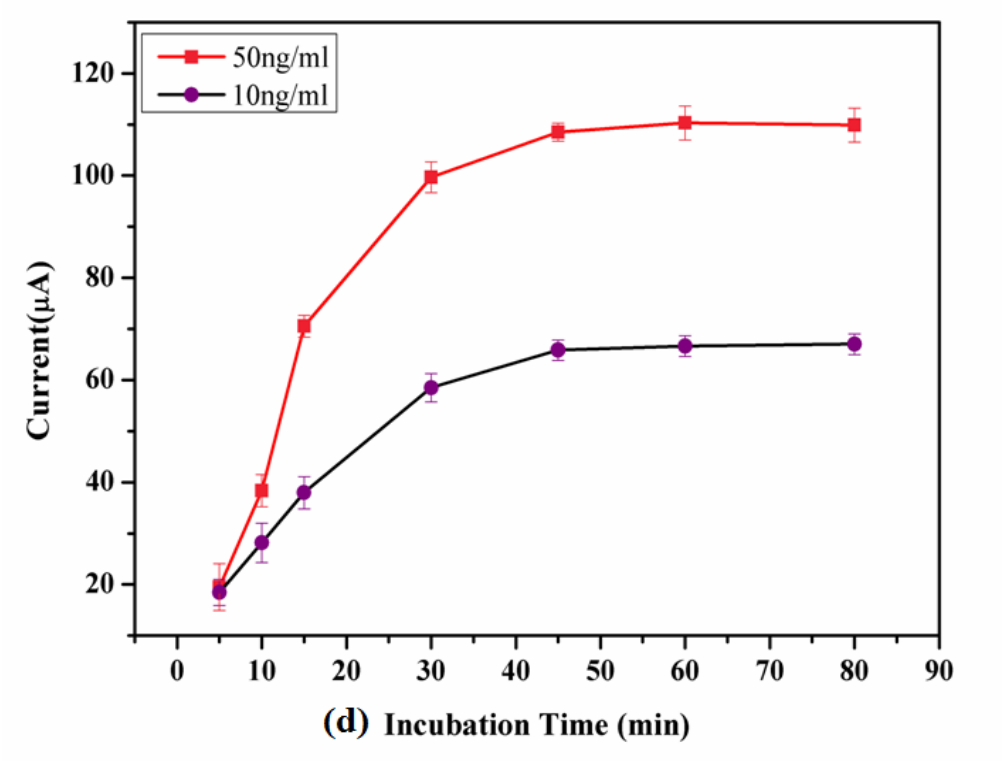

Figure 4.8: Influence of (a) pH value; (b) capture antibody concentration; (c) temperature; (d) incubation time on the immunosensor.

4.3.7 Calibration curve of the cTnI immunosensor

After the optimization experiments, the calibration curves were established under the optimized conditions to determine cTnI using PDDA-MWCNT and chitosan-AuNPs modified electrodes. The oxidation peak currents occur between 0.9 to 1.0 V, as shown in Figure 4.9 (a), 4.10 (a) , and 4.11 (a). The reaction between antibody and antigen was based on sandwich ELISA mechanism. The antigen first react with detection antibody conjugated with ALP label, and then react with immobilized capture antibody. The ALP label increase will lead to current response elevated which is owing to the increasing amount of antigen, cTnI. As shown in Figure 4.9 (a), 4.10 (a) , and 4.11 (a), the peak current increases along with the concentration increasing. Then the dependence of the CV oxidation peak current on the cTnI concentration is linear ranging from 1.0 ng ml^{-1} to 100ng ml^{-1} on bare gold electrode, 0.01 to 300 ng /ml on PDDA-MWCNT electrode, and 0.02 to 200 ng ml^{-1} on chitosan-AuNPs electrode, with a correlation coefficient of 0.978, 0.983, and 0.971 respectively.

In terms of detection linear range and the correlation coefficient, the PDDA-MWCNT electrodes have the widest range comparing to chitosan-AuNPs electrodes and bare electrodes. It can be caused by the unique properties of carbon nanotube such as chemical stability, high surface-volume ratio, capacity of electron transferring and etc. Furthermore, speaking to the AuNPs modified electrodes, comparing to bare electrodes, with relatively low r^2 (correlation coefficient), it might be explained by the biocompatibility of chitosan and AuNPs, which can help absorb more capture antibody and more non-specific binding, which further indication the non-selective properties between chitosan and AuNPs to biomolecules. The sensitivity of three electrodes will be discussed in the following session.

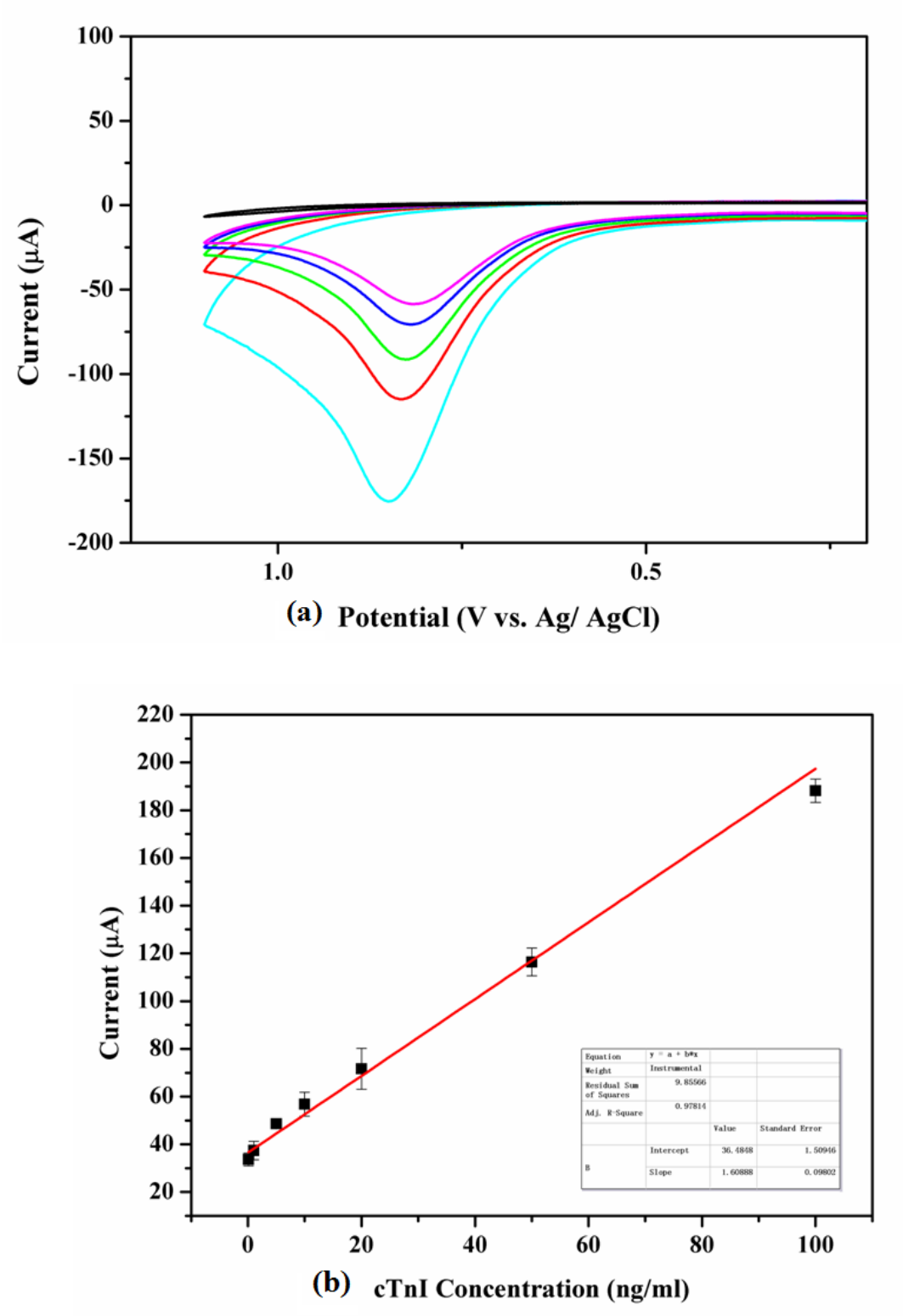

Figure 4.9: (a) The current-voltage response curves (b) calibration curve of bare gold electrodes.

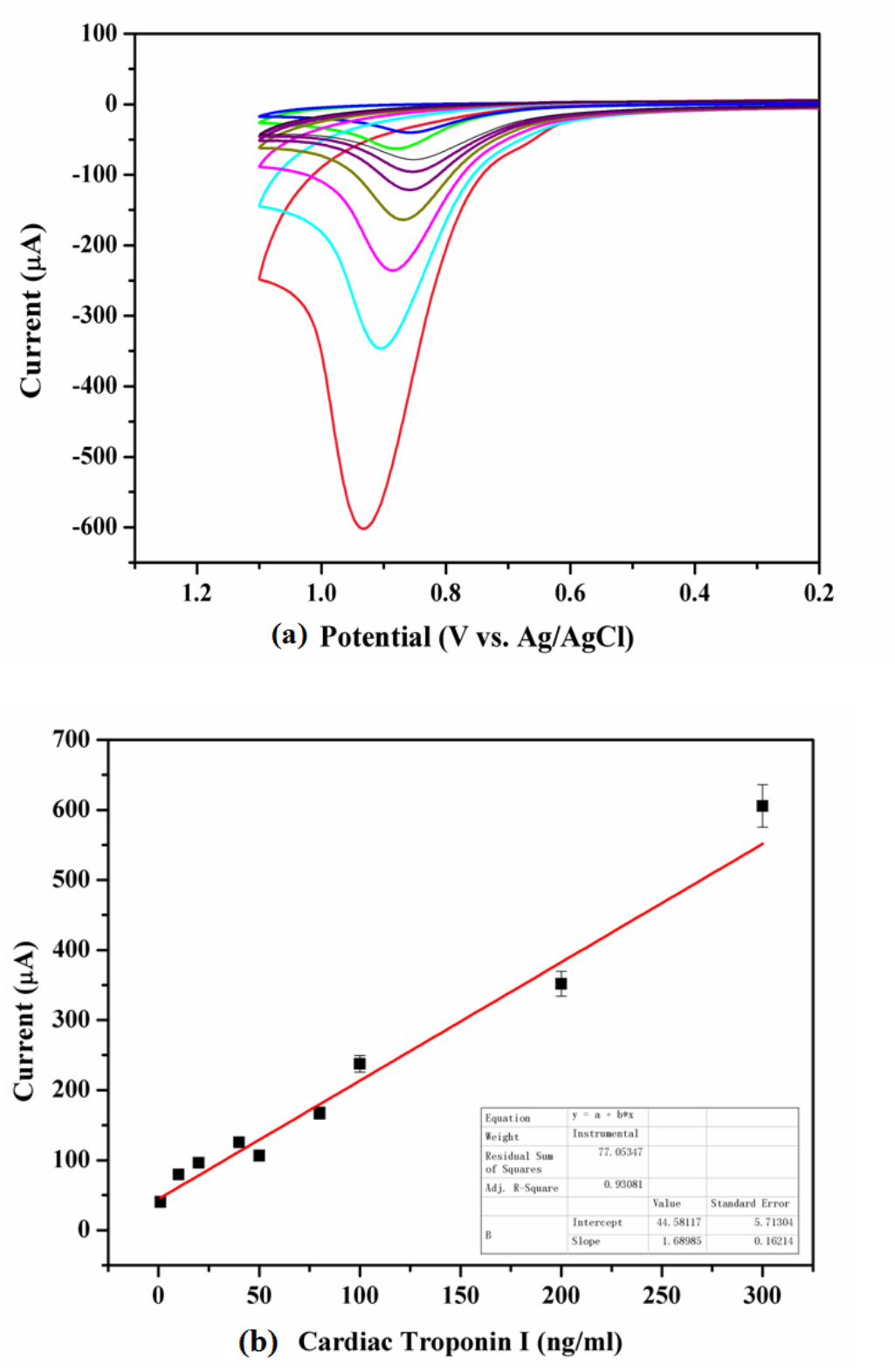

Figure 4.10: (a) The current-voltage response curves (b) calibration curve of chitosan-AuNPs modified gold electrodes.

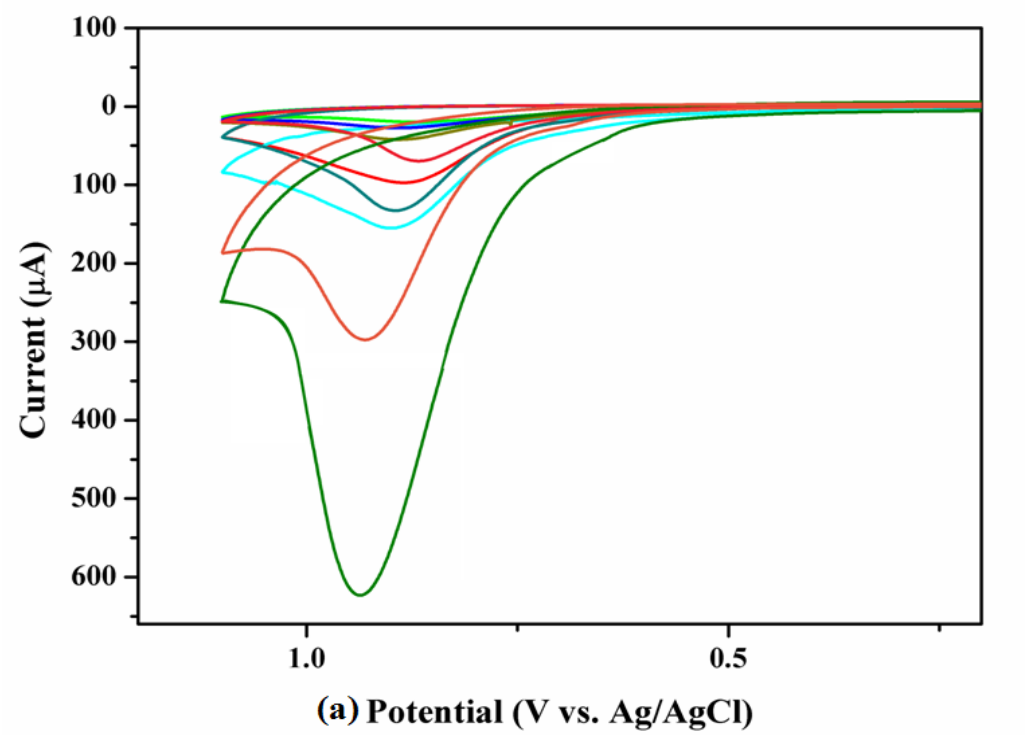

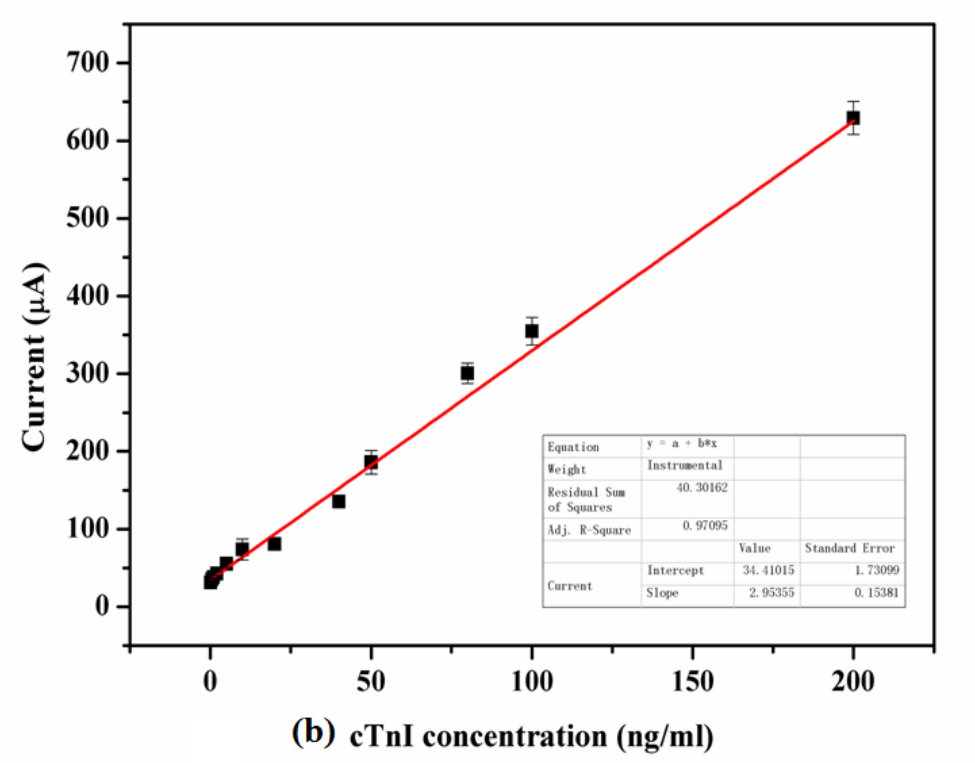

Figure 4.11: (a) The current-voltage response curves (b) calibration curve of PDDA-MWCNT modified gold electrodes.

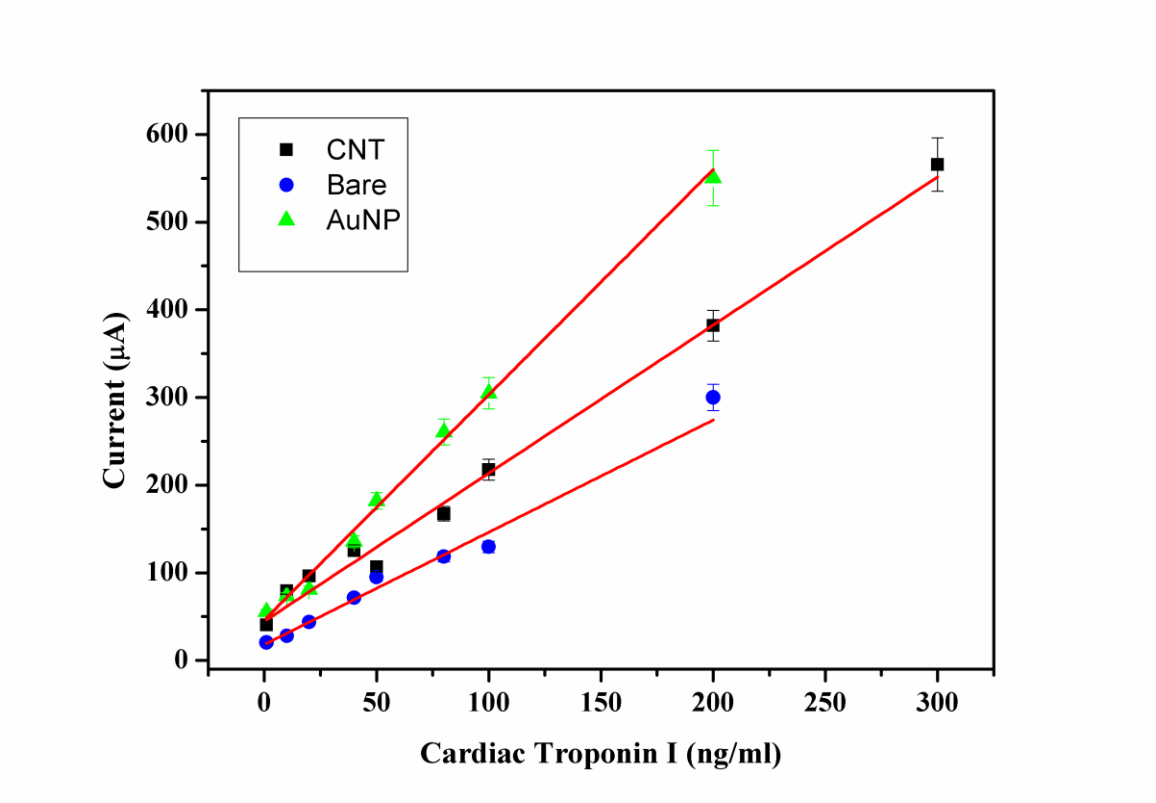

Figure 4.12: Calibration curve of PDDA-MWCNT, AuNPs, and bare electrode.

The detection limits were obtained by triplicate measurements of blank detection and then was calculated to be 0.1 ng ml^{-1}on bare gold, 0.001 ng ml^{-1} on PDDA-MWCNT, and 0.003 on chitosan-AuNP respectively, which was compared with current POCT device detection limit as shown in the Table 4.1. The sensitivity stands for the slope of the calibration curve, (Katus et al., 1989), in our case, the sensitivity is 18.32 µA $mg^{-1}mL^{-1}$ on bare gold, 32.17 µA $mg^{-1}mL^{-1}$ on PDDA-MWCNT, and 40.15 µA $mg^{-1}mL^{-1}$ on chitosan-AuNP respectively (Figure 4.12). When the concentration of cTnI reached over the range higher limits, then it will need to be diluted prior to the experiments. It consists with the relative literature indicated that the application of AuNP and CNT can enhance the catalytic reaction and enhance the sensitivity (Burlina et al., 1994). The enhanced sensitivity is perhaps due to the synergistic effect of AuNP or CNT.

Table 4.1: Characteristics of current cTnI POC assays. Adapted from (Christenson and Azzazy, 2009)

Assay	Lower detection limit(ng ml^{-1})	99th percentile cutoff value (ng ml^{-1})	Receiver- operating characteristic curve cutoff
Abbott i-STAT	0.02	0.08	—
Dade CS	0.03	0.07	0.6-1.5
Response	0.03	< 0.05	—
Biosite Triage	0.19	<0.19	0.4

4.3.8 Stability and reproducibility of the cTnI immunosensor

We investigated the storage stability of the current project. The electrodes were stored in the refrigerator at 4 ℃ and then examined every day for the activity. The electrodes include PDDA-MWCNT, AuNPs, and bare electrodes. The results as shown in Figure 4.12, for all the three electrodes, there were no significant signal decrease being observed before first 20 days. However, the bare electrodes started to decrease immediately after 20 days. The activities of PDDA-MWCNT and AuNPs remained the same response with a few fluctuations between day 20 till day 27, then both of responses of the PDDA-MWCNT and AuNPs drop sharply.

Besides the stability of storage, the stability of operation, the interassay variation coefficient is critical as well. We investigated the interassay variation coefficient by measuring the same sample by five sets of PDDA-MWCNT and AuNPs electrodes, respectively. The results illustrated that the interassay variation coefficient was 20 ng ml^{-1} was 5.8% of PDDA-MWCNT and 20 ng ml^{-1} was 6.4 % AuNPs, which indicating both PDDA-MWCNT and AuNPs has considerable potential for fabrication stability and enduring storage stability.

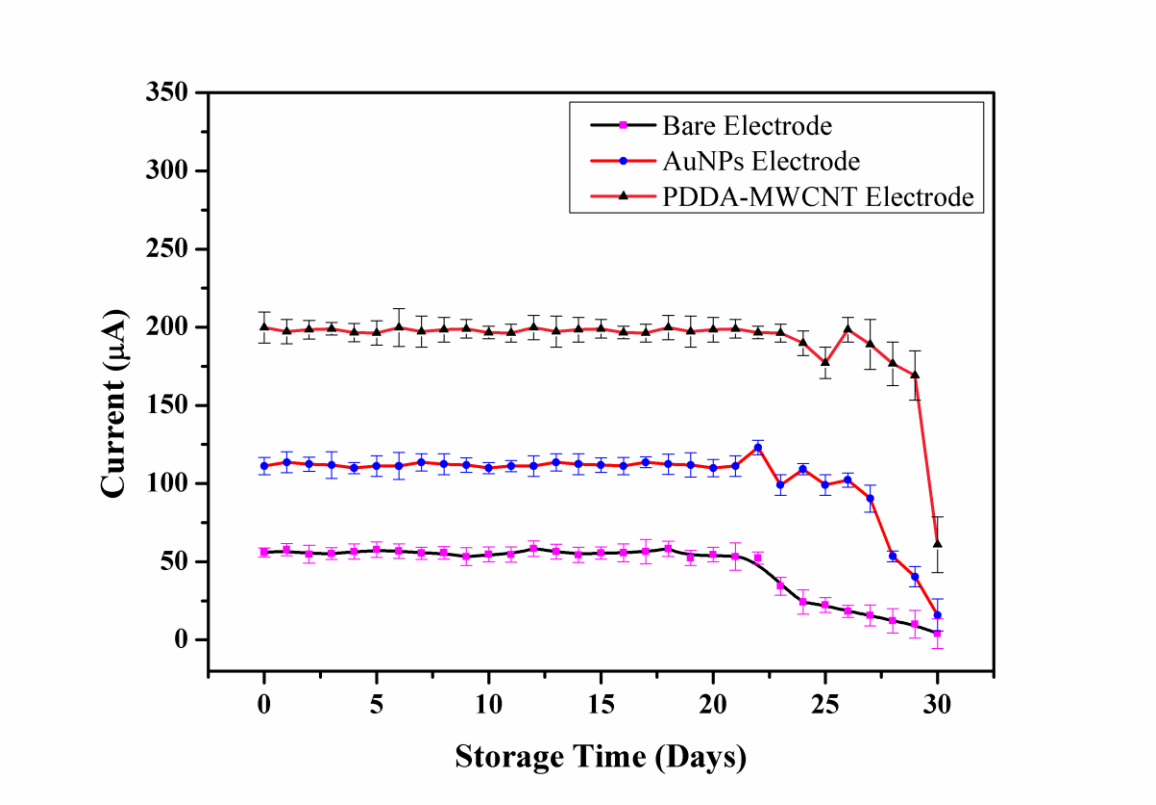

Figure 4.13: Storage stability of the PDDA-MWCNT, AuNPs and bare electrodes.

4.3.9 Accuracy and clinical application

Herein, we study the accuracy of the cTnI immunosensor by comparing the results by determining cTnI in human serum (diluted by PBS buffer pH 7.4 (v: v=1:10)) with PDDA-MWCNT electrochemical immunoassay (EIA) and with spectrophotometric ELISA. As presented in Figure 4.14, the mean values of evaluations in 5 serum samples were performed at five different concentrations, and the error bar stands for the degree of the measurement uncertainty. In addition, as shown in Table 4.2, the relative standard deviation (%), square root of the variances, of PDDA-MWCNT is in the range of 2.94 to 8.56%, and the difference between Chitosan-AuNPs is from 3.92 to 6.86% in extent. Both the figure and the data demonstrated that the measured value of cTnI concentration by spectrophotometric methods shows satisfying agreements with both modified immunosensor based electrochemical methods.

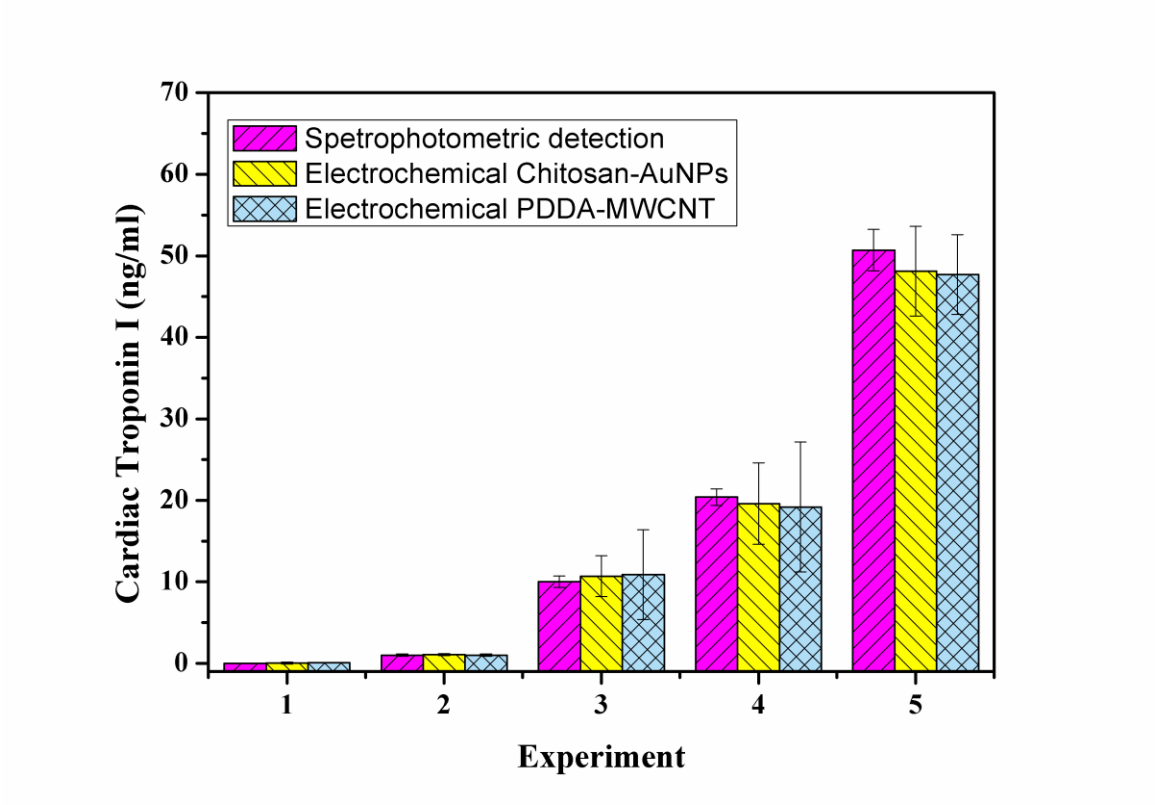

Figure 4.14: Measurement of cTnI with spectrophotometric, the electrochemical with chitosan-AuNPs, PDDA-MWCNT methods in various concentration: 0, 1, 10, 20, 50 ng ml^{-1}.

Table 4.2: Comparison of Measured cTnI levels between two methods.

Samples (ng ml^{-1})	Spectrophotometric (ng ml^{-1})	PDDA-MWCNT Electrochemical (ng ml^{-1})	RSD (%)	Chitosan-AuNPs Electrochemical (ng ml^{-1})	RSD (%)
0	0.01 ±0.02	0.06 ±0.03	-	0.04 ±0.02	-
1	1.02 ±0.15	0.99 ±0.15	2.94	1.09 ±0.16	6.86
10	10.04 ±0.70	10.9 ± 5.50	8.56	10.7 ±2.51	6.57
20	20.40 ±1.02	19.2 ±7.96	5.88	19.6 ±5.01	3.92
50	50.7 ±2.54	47.7 ±4.89	5.92	48.1 ±5.51	5.13

4.4 Conclusions

We designed and developed an amperometric cardiac Troponin I immunosensor based on PDDA-MWCNT and AuNPs, respectively. The electrochemical immunosensor was based on sandwich type ELISA, which employs two antibodies and leads to high sensitivity. The substrate utilizing in the experiment is commercially available and have relatively high stability. The immunosensor presents good sensitivity, positive bioactivity, low detection limit and quick response time and tolerable stability. The immunosensor not only can be utilized on serum to determine cTnI values but also can be applied of different protein molecules.

Chapter 5

5 HRP- and ALP-label enzyme comparison study

This chapter will study characteristic of two enzyme label and various liquid substrate for electrochemical signal response. TMB and HQ for horseradish peroxide enzyme was studies in pH value 5.0 and 7.4, respectively; PNPP and PAPP in Tris buffer and DEA buffer was investigated in alkaline system. HRP-based electrochemical biosensor along with glucose biosensor can be integrated together to accomplish a cardiac-blood chemistry sensor in POCT device. Also, a concept of multiplex cardiac biomarker detection was presented.

5.1 Introduction

As discussed before, the immunoassay herein is to detect the antigen (cTnI) between two antibodies. One of the antibodies was labeled with certain enzyme, which can catalyze redox reaction of the corresponding substrates. Among all the enzyme-based electrochemical biosensor, there are two most commonly used as the enzyme label for signal amplification and catalytic reactions: horseradish peroxidase (HRP) and alkaline phosphatase (ALP). In general, as in HRP-based biosensors (Crew et al., 2007; Fanjul-Bolado et al., 2005; Ionescu et al., 2005; Ionescu et al., 2004; Sun et al., 2001; Volpe et al., 1998), the signal responses generate by substrates electroreduced by the existence HRP. In contrast, in ALP-based biosensors (Aziz et al., 2007; Aziz et al., 2008; Das et al., 2007; Fanjul-Bolado et al., 2007; Hwang et al., 2005; Kwon et al., 2008; Preechaworapun et al., 2008; Wilson and Rauh, 2004), the electrochemical responses were induced by the electrooxidation of the ALP.

Since both HRP-based biosensor and ALP-based biosensors have quite long history as the catalyzing label in ELISA immunoreaction, the overall performance of HRP-based sensors have distinguishable disadvantages from the ALP-based sensors during the electrochemical detections. Comparing to the ALP-based sensors, most HRP-based

sensors have higher background-current levels and less reproducible, which contributes to more difficulty in achieving low detection limits. One the one hand, the majority of the liquid substrates of HRP (such like hydroquinone (HQ)) is unstable and highly electroactive under an narrow electrochemical potential window (Crew et al., 2007; Fanjul-Bolado et al., 2005; Ionescu et al., 2005; Ionescu et al., 2004; Sun et al., 2001; Volpe et al., 1998), while the substrate for ALP is less electroactive (Gyurcsanyi et al., 2002; Preechaworapun et al., 2008), for instance, the PNPP liquid substrates discussed in Chapter 4. Therefore, the interference caused by electroactive substrates will dramatically elevated the background-current level of the HRP-based sensors. On the other hand, the hydrogen peroxide (H_2O_2) is the critical and necessary oxidizing element in HRP catalysis sensor, which is prone to be electroreduced under a certain level of electrochemical potential window. Consequently, the presence of H_2O_2 electroreduction will potentially enhancing the background-current levels.

However, the relatively poor performance of HRP can be overcome by electrochemical strategy in terms of lowing the background-current (Kang et al., 2009). In addition, the unique merit of HRP-based biosensor instead of ALP-based biosensor is the great potential to combine with Glucose or other blood chemistry biosensor (applicable to all the analytes share with the same detection principle with glucose), using hydrogen peroxide (H_2O_2) as the bridge. Over the past several decades, the enzymatic amperometric glucose biosensor has drawn significant from the merchants and scholars owing to the significant sensitivity, robust, and cost-efficient (Heller and Feldman, 2008). Regardless of the various formats or detection methodology, the fundamental format of the glucose biosensor is that the glucose biosensor is using the enzyme glucose oxidise (GOx) immobilization to catalyze the reaction between oxygen and of β-D-glucose, which will generate hydrogen peroxide (H_2O_2) and by-product gluconolactone (Weibel and Bright, 1971). Therefore, in theory, the hydrogen peroxide (H_2O_2) generated by glucose biosensor can be utilized as the oxidizing element in HRP catalysis sensor. Then the investigation and discussion about the cTnI-glucose biosensor is depicted as follows.

5.2 Experimental

5.2.1 Materials and reagents

All the reagents and chemicals are or high than analytical grade without further purification. All the buffers and solution were prepared with deionized water (DI), with resistivity over 18MΩ.

Troponin I from human heart, the rabbit anti-human cTnI polyclonal antibody, and the mouse anti-human cTnI monoclonal antibody were purchased from Sigma-Aldrich. 4-Aminophenyl phosphate monosodium salt hydrate was obtained from Gold Biotechnology (St. Louis, USA). Maleimide alkaline phosphatase and maleimide horseradish peroxide were received from Innova Bioscience (Cambridge, UK). N-Succinimidyl S-acetylthioacetate (SATA), horseradish enzyme stabilizing buffer, sodium aside, diethanolamine (DEA), dimethylsufoxide (DMSO), bovine serum albumin (BSA), p-nitrophenyl phosphate(p-NPP) liquid substrate, Trizma® base (tris-(hydroxylmethyl)-aminomethane(Tris)), TMB liquid substrate, hydroquinone, potassium ferricyanide (III), polyoxyethylenesorbitan manolaurate (Tween™ 20), β-D-glucose, glutaraldehyde and PDDA (20 wt % in water) were all purchased from Sigma-Aldrich.

All these buffers. such like phosphate buffer solution (PBS), blocking buffer (1% BSA in PBS) and etc., were prepared every week. The MWCNT (cylindrical with diameter range in 5-15nm) with 95% purity was purchased from US Research Nanomaterials, Inc.

5.2.2 Preparation of antibody-enzyme conjugates

HRP conjugating with antibody is extremely familiar with the ALP procedures. The process was established through SATA as a crosslink to form a thiol function group and then react with maleimide activated horseradish peroxide (HRP). The antibody-enzyme conjugation process is depicted as follows (Fragoso et al., 2011; O'Regan et al., 2003)

(1) Prepare antibody stock solution. In 2 mL vial, adding 100 μL anti-cTnI polyclonal antibody (1 mg/mL) and then adding 100 μL sodium phosphate buffer (50mM NaH_2PO_4 and 1mM EDTA, pH 7.5).

(2) Prepare SATA stock solution (1.5 mg/mL in DMSO).

(3) Add 5 μL SATA stock solution to antibody stock solution. Then gently shake the vial and set at room temperature for 45 min.

(4) To remove the by-product (residue SATA) by centrifugation using a 30 kDa cut-off ultracentrifuge filter (Sigma) against sodium phosphate buffer.

(5) Prepare deacetylation solution, 20 mL (50 mM NaH_2PO_4, 25 mM EDTA, 0.5M hydroxylamine– HCl, pH 7.5).

(6) Add to the antibody mixture and let it incubate for 2 hours at room temperature to reveal the thoil group.

(7) Dialyse the solution against DPBS (137 mM NaCl, 2.6 mM KCl, 8mM Na_2HPO_4, 1.5 mM NaH_2PO_4, 1 mM EDTA, pH 6.6) at room temperature for 12 h/ overnight.

(8) Add maleimide activated HRP to antibody solution based on molar ration 2:1 (1:1(w/w)) and then left in 4 °C for 12 hours.

(9) Dialyze conjugates against Tris buffer (50 mM Trizma base, 50 mM NaCl, 1 mM $MgCl_2$, pH 7.4) for overnight at room temperature.

(10) Add HRP stabilizing buffer (Tris buffer, pH 8.0, 1% (w/v) BSA and 0.05% (w/v) sodium azide) to adjusted to a final volume of 500 mL. Then store the conjugates at 4 ^{0}C.

5.2.3 Construction of PB-PDDA-MWCNT Glucose Biosensor

To construct the PB-PDDA-MWCNT glucose biosensor includes the following steps:

(1) Electrodes pretreatment and activated and construct PDDA-MWCNT sensor: follow the same procedures in Chapter 4, as shown in Figure 5.1 (a).

(2) PB film deposition: to electropolymerize PB by immersing the electrodes in a solution comprised of 5 mM $K_3[Fe(CN)_6]$, 5 mM $FeCl_3$, 0.01 M HCl and 0.1 M KCl, and scan from -0.1 to 0.4 V at 20 mV/s for 20 cycles (Figure 5.2 (b)) (Karyakin, 2001; Karyakin et al., 1995; Karyakin et al., 1996, 2000; Karyakin et al., 2004), and then washed with double diluted water.

(3) PB activation: immerse the electrode into a solution with 0.1 M KCl and 0.01 M HCl as the support electrolyte solution and activated by scan from -0.1 to 0.4 V at 50 mV/s till the CV curve stable (Figure 5.1 (c)) (de Mattos et al., 2003; MATTOS et al., 2000; Ricci et al., 2003). Then the electrode was cleaned by deionized and heated at 110 °C for 1 h.

(4) Glucose biosensor: this step is to immobilize enzyme GOx on the electrodes, which can be immobilized in two different ways. In order to be a control experiment for cTnI-glucose sensor, the electrodes was with the presence of capture antibody. Namely, combine μL GOx (10 mg/mL) with 10 μL chitosan (0.5%) to obtain the GOx-chitosan mixture and then drop 5 μL mixture on the surface of PB-PDDA-MWCNT electrode, wait till the mixture evaporate at room temperature. As shown in Figure 5.1 (d), the CV difference between with or without glucose presence.

(5) Immobilization of GOx: besides immobilizing with chitosan, also the GOx can be mix with BSA solution (1%, w/V) first, and dropped the mixture on the surface of working electrode and then immerse into 0.25% glutaraldehyde for 10 minutes to generate a cross-link.

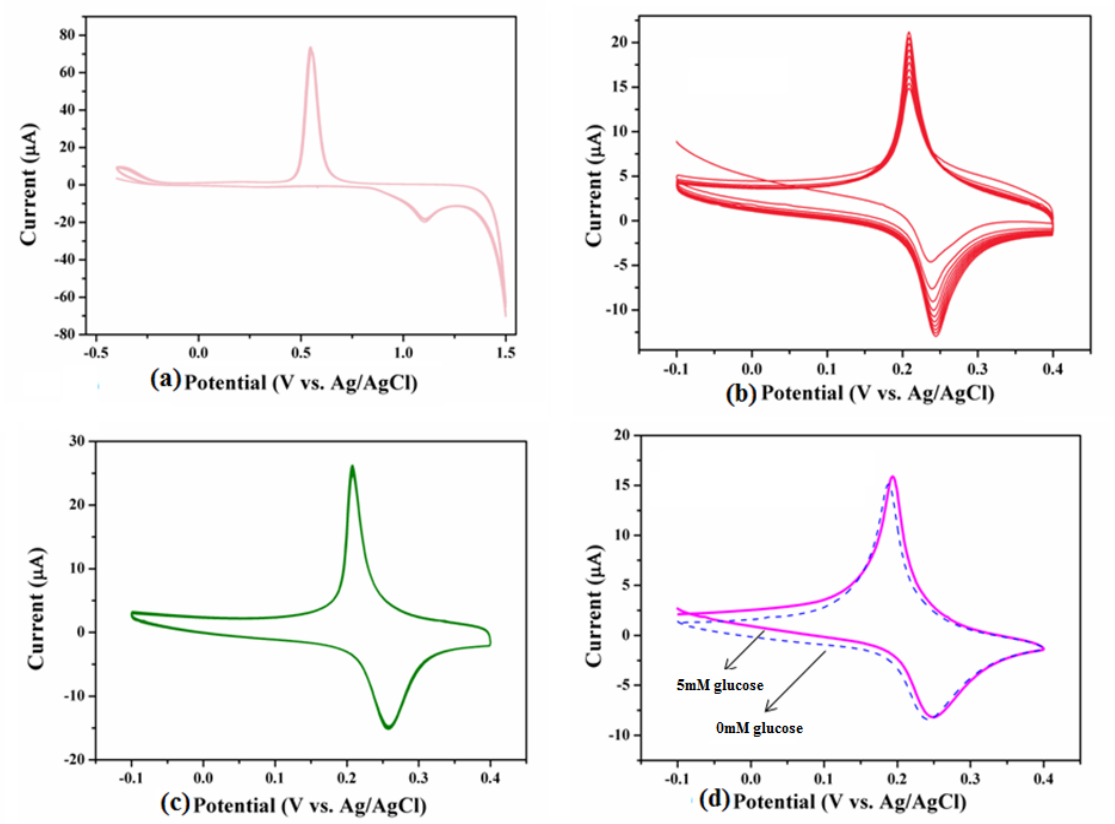

Figure 5.1: Cyclic voltammograms of the electrode pretreatment and PB-glucose sensor construction. (a)Electrode cleaned and activated in 0.5M sulfuric acid; (b) Pb electropolymerization; (c) Pb activation; (d) Biosensor in the null and 5mM glucose.

5.2.4 Electrochemical and immunosensing experiments

The immunoassay utilised in the current work is 2-site enzyme-linked-immunosorbent serologic assay (ELISA), also called as sandwich type ELISA. Therefore, the immunoassay protocol includes three major procedures: incubate first antibody, blocking, and incubation antigen-antibody-HRP. First, incubate the capture antibody. Add 5 μL capture antibody solution (anti-cTnI monoclonal in PBS solution, pH 6.0) and incubate for 60 minutes at 37 °C. Then rinsing thoroughly with washing buffer (0.05% Tween® in PBS, pH 6.4) to remove the unbound antibodies, and add a drop of 5 μL 10% (w/v) BSA-GOx in PBS (pH 6.0) and incubate for 60 minutes at 37 °C, to block the non-specific bounding. Afterwards, repeat washing by 0.05% Tween® in PBS. Finally, incubate the premixed antigen-antibody-HRP a drop of 5 μL, incubate for 60 minutes at 37 °C. Then the electrode would be ready to move on the electrochemical experiments. For the bulk electrodes, after each immunoassay run, immerse the electrode into 0.1 M glycine-HCl (pH 2.0) for 5 min and rinse by double dilute water. Then start from electrode pre-treatment to carry out another sensing cycle (Gao et al., 2003).

All electrochemical experiments were performed by a computer- interfaced CHI1200a (CHI Instruments, Inc., USA). Electrochemical measurements were done in a conventional electrochemical cell or on a flat chip, which is the macroscale prototype of at the room temperature. Firstly, Cyclic voltammograms (CVs) were performed 2 mM PBS (pH 6.5) containing 5.0 mM $K_3[Fe(CN)_6]/K_4[Fe(CN)_6]$ (1:1) mixture and 0.1 M KCl from 0.6 to −0.2 V (vs. Ag/ AgCl) at the scan rate of 50 mV s^{-1} to monitor the current variation (ΔI) before or after nanomaterial modification because PDDA-MWCNT and chitosan-AuNPs will increase the electron transferring and lead to current response enlarged (Gao et al., 2003). Secondly, the immunoreaction was monitored by cyclic voltammograms performed in TMB liquid substrate (pH 5.0) or HQ in PBS (pH 7.4) along with a small concentration of H_2O_2 purchased from Sigma. When the antigen was bound with both antibodies: capture antibody coated on the surface of the electrode and the second antibody (labelled with HRP) catalyzing the substrate to generating current response, then there was current response of the immunoreactions. All the electrochemical experiment was carried at the room temperature.

5.3 Results and discussion

5.3.1 Principle of the glucose- cTnI immunosensor

As shown in Figure 5.2, schematics indicate the concept of the glucose-cTnI immunosensor with the surface modified electrodes. In the scenario of without antigen, the sensor was modified by PDDA-MWCNT, Prussian blue, monoclonal anti-cTnI antibody and BSA-GOx with glutaraldehyde as the cross-link, from the bottom (the bare electrode surface) to the top. When the solution without cTnI was added in the reaction chambers, the glucose oxidize will catalyze the reaction of glucose and oxygen, generation hydrogen peroxide (H_2O_2) and gluconolactone. The product H_2O_2 will be detectable by Prussian blue, which is the quantization of the amount of glucose. While, in the scenario of with antigen cTnI, the glucose oxide (GOx) will first catalyze the reaction of glucose and oxygen to generate hydrogen peroxide (H_2O_2). Subsequently, the hydrogen peroxide will participate in the immunoassay reaction, acting as the oxidizing reagent to electrooxidized the horseradish peroxide (HRP) substrate under the canalization of HRP. Then the results will be used to calculate the amount of cTnI.

The reaction happened in chambers without antigen is shown as follows:

$$\text{Glucose} + O_2 \xrightarrow{\text{GOD}} \text{Gluconolactone} + H_2O_2$$

Besides the glucose reaction with oxygen, the following reaction can be happening depending on the adding substrates:

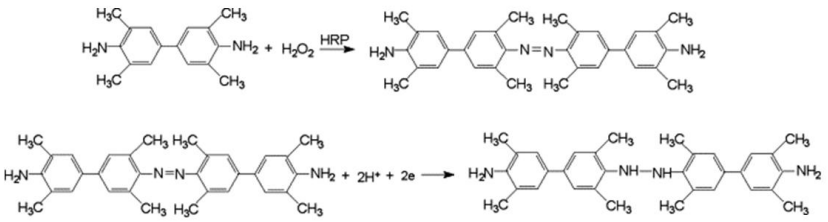

or

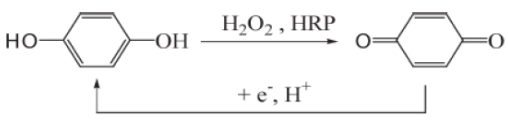

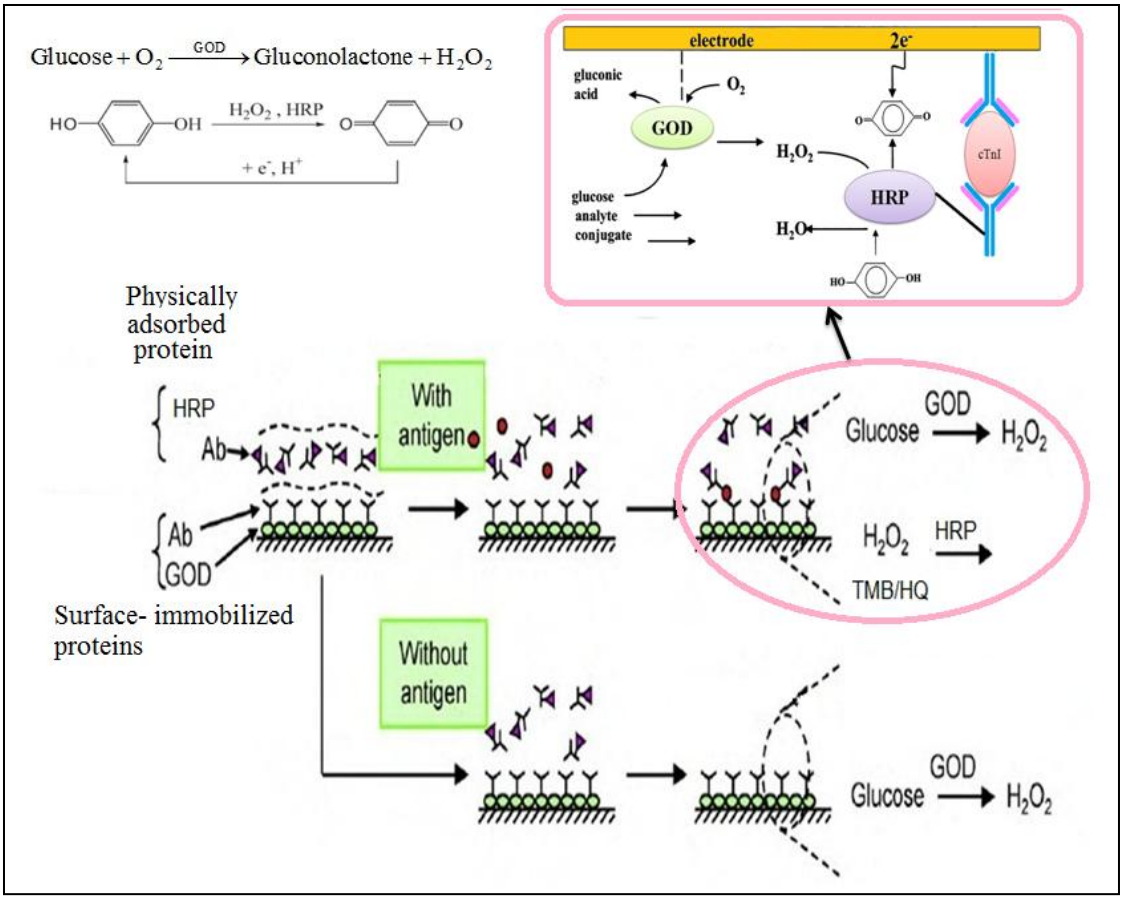

Figure 5.2: Schematics and principle of the cTnI- glucose biosensor. Reprinted with permission from (Henares et al., 2010)

5.3.2 Glucose deterimination

5.3.2.1 Electrochemical behavior of PB-PDDA-MWCNT electrode

Cyclic voltammograms of PB-PDDA-MWCNT electrode in PBS (pH 6.78) illustrates that the existent of PB introduced a standard redox peaks at the potential 0.27 and 0.2 V respectively, which was generated by the redox reaction from PB to Prussian white (PW) (Zeng et al., 2008). Figure 5.3 (a) displays the CV response of PB electrode under increasing scan rate. When the value of scan rate increases, the anodic, cathodic peak currents, and the difference value between peak currents rise. Figure 5.3 (b) presents that the redox peak current is linear to the square root of the scan rate from from 30 mV/s to 300 mV/s. It demonstrates that the redox reaction of PB on PDDA-MWCNT electrodes is a diffusion controllable redox process.

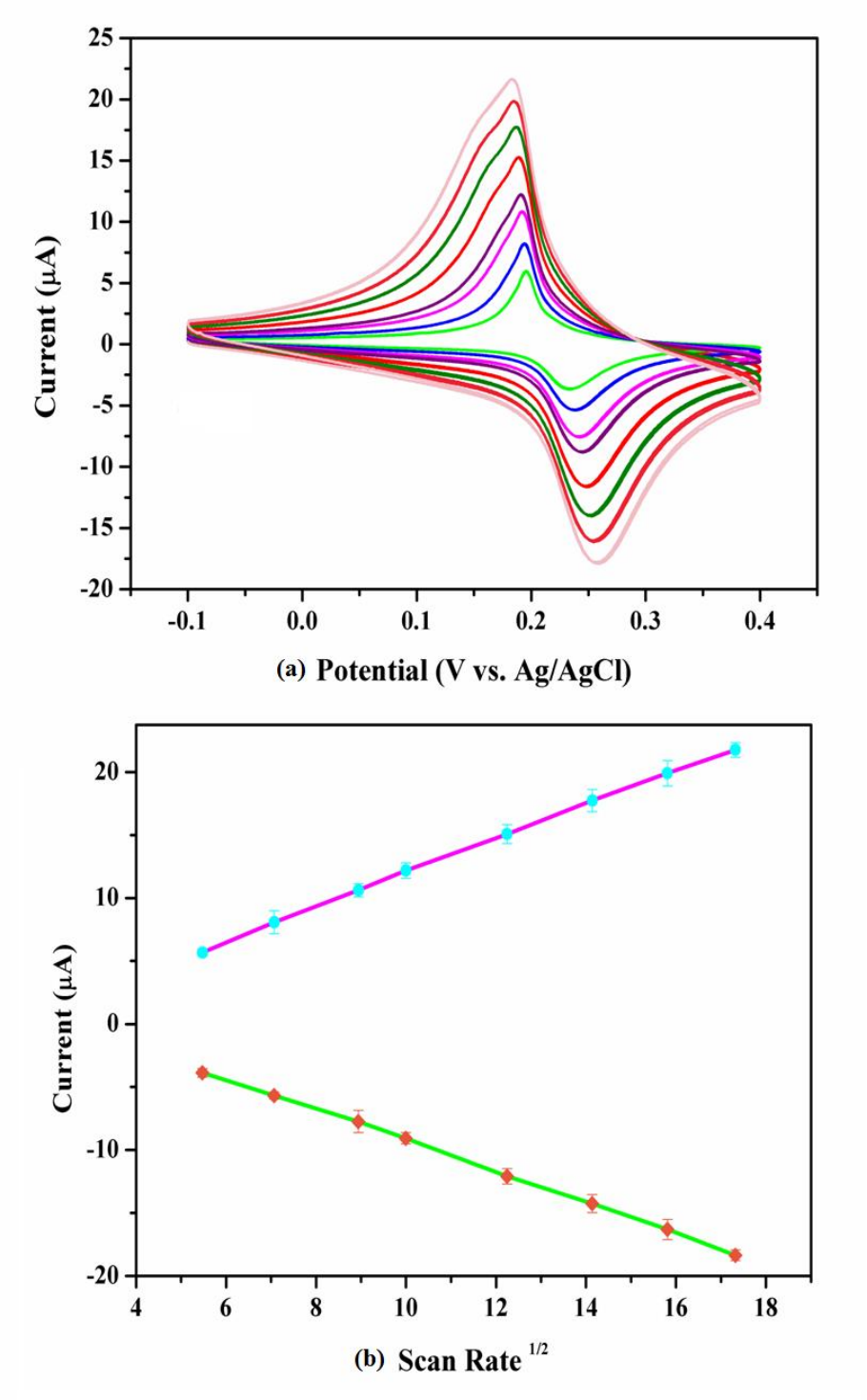

Figure 5.3: (a)Cyclic voltammograms of PB-PDDA-MWCNT electrodes at various scan rates from 30 to 300 Mv S in PBS (pH 6.78). (b) The dependence of the current of redox peaks over the square root of the scan rate.

5.3.2.2 GOx immobilization

Immobilization of glucose oxidize is a critical step in the experiments. Two different methods were used in this case to investigate the influence of GOx immobilization in terms of sensitivity and the dynamic range of the linearity. First, the GOx was mixed with chitosan immobilization matrix and dropped on the electrode surface by physical adsorption, and then coated with capture antibody. Even though, the matrix of chitosan-GOx only being attached on the electrode surface by non-specific physical interaction, but the surface tension of chitosan is strong enough to hold the matrix with the electrode surface. That is also explained the superiority of chitosan in molecule immobilization. But in this scenario, the electron transfer will be hindered by the antibody coverage, since the chitosan- GOx was constructed beneath the capture antibody layer.

Another method to immobilized GOx is to mix with BSA first and then use glutaraldehyde as the cross-link to form a gel texture increasing the surface tension, which will proving stable and insoluble binding.

As shown in Figure 5.4 (a), the current and time response curves of chitosan- GOx and GOx-BSA. Chitosan- GOx has high sensitivity and larger range of detection linearity, which can be cause by the amount of GOx, since the GOx-BSA only exists in the blocking buffer.

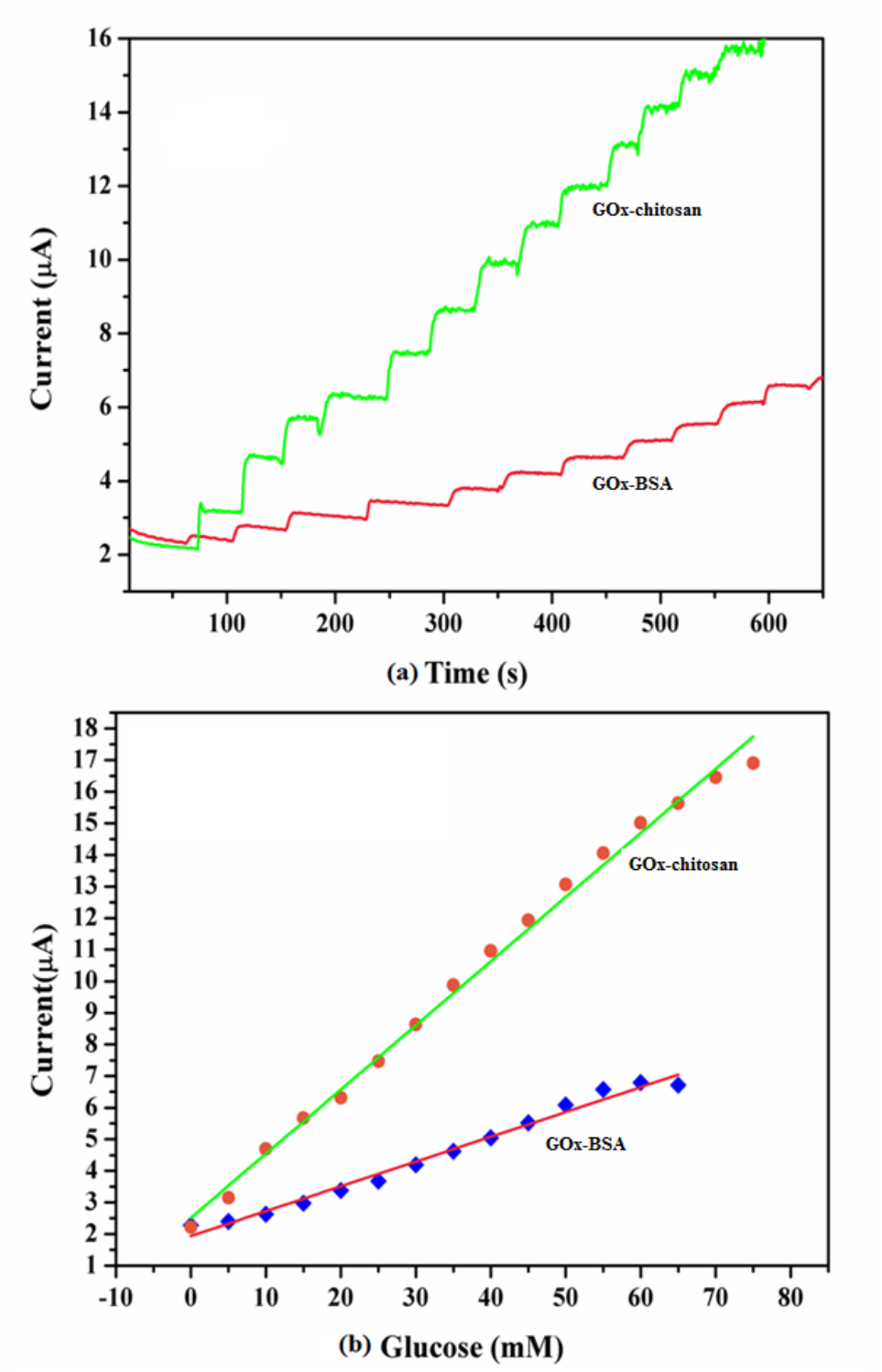

Figure 5.4 (a) Glucose current-time current response curves (b) standard calibration curve.

5.3.3 Feasibility study: HRP determination

5.3.3.1 Cyclic voltammetry study of TMB and HQ for HRP

As shown in Figure 5.5, HRP catalyze the reaction between TMB and H_2O_2 will consume H_2O_2 and Hydrogen ions. The same theory of HQ based immunoassay. However, as shown in the Figure 5.6 and Figure 5.7, there is not obvious current change in peak current when adding glucose in the immunosensor. It might be caused by the following possible reason: First, the pH range may not suitable for both GOx and HRP, either of them lost bioactivity can cause no response. Secondly, the sandwich type of antibody-antigen-antibody complex will hinder the electron transferring, which will cause the blank response.

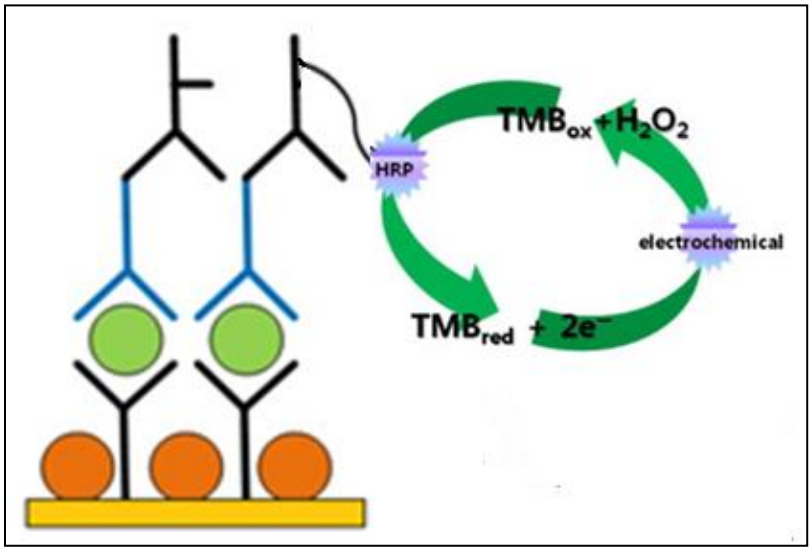

Figure 5.5: Schematic of Horseradish peroxidase catalysis TMB.

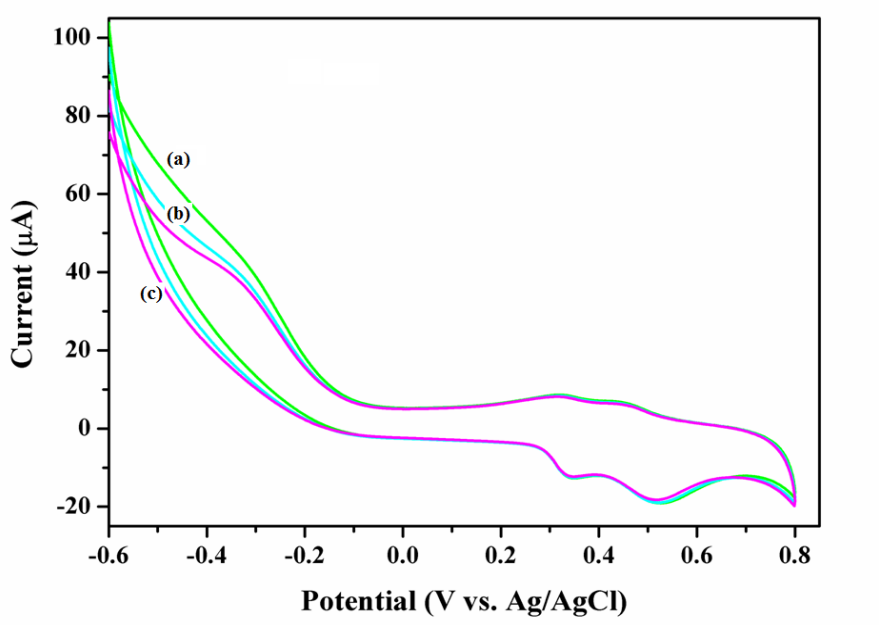

Figure 5.6 : Cyclic voltammograms of 0.2 Mm TMB in citrate-phosphatase buffer (pH 5.0). (a) 10 mM glucose; (b) 5 mM glucose; (C) 0 mM glucose.

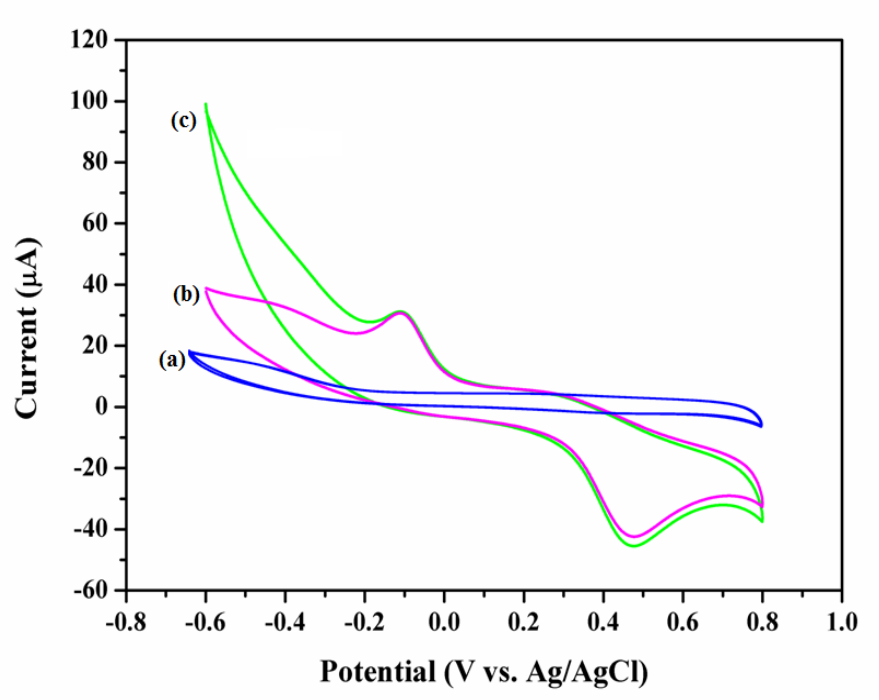

Figure 5.7: Cyclic voltammograms of 0.3 Mm HQ in PBS buffer (pH 7.0) + 0.1 M KCl. (a) PBS-KCl; (b) PBS-KCl-HQ; (c) PBS-KCl-HQ- glucose (5mM).

A preliminary calibration plot was established of HRP-based immunosensor in TMB liquid substrate (pH 5.3) purchased form Sigma. The triangle and dot stands for adding H_2O_2 instead of glucose and the square is the signal generated by adding glucose. The triangle also without any GOx coating involved, and presents the best sensitivity among all the three. Therefore, to combine with glucose sensor and immunosensor will need further discussion or improvements.

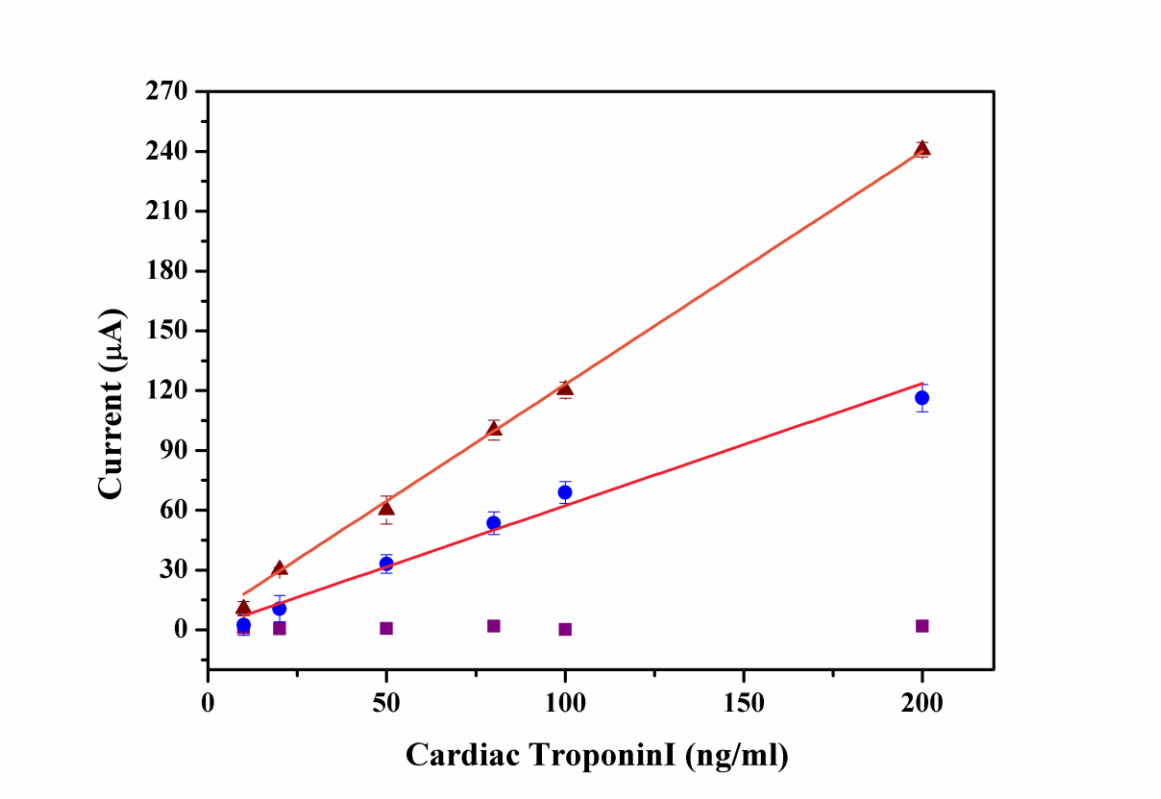

Figure 5.4: HRP-labeled enzyme in HQ-PBS liquid substrate. (Triangle) H_2O_2 of TMB reaction detection cTnI PDDA-MWCNT (Dot)) H_2O_2 of TMB reaction detection cTnI on chitosan-GOx. (Square) Glucose in immunoassay.

5.3.4 Multimarker concept

Multianalyte is the new trend in diagnostic technology development due to the comprehensive results, cost effective (comparing to several consumable in one package), ease-to-use, and labor efficiency.

Simultaneously immunoassay, the multianalyte immunoassay uses arrays of immunosensing electrodes, each capable of performing an independent electrochemical immunoassay for a specific analyte. Each electrode contains immobilized antibodies and uses an AP-based enzyme-linked immunosorbent assay (ELISA) to measure analyte concentration. Amperometric responses are produced at the electrodes due to the electrochemical oxidization of redox mediator, and the size of the response enables the quantification of analytes. (Wilson, 2005).

Successively assay, the multianalyte assay uses arrays of immunosensing electrodes and enzyme sensor, the electroactive substrate produced by enzyme sensor can be utilized in immunoassay. For example, the HRP-based immunosensor can the integrated with glucose sensor or lactase sensor, which relying on detection H_2O_2 concentration to establish linear proportional relationship between electrochemical signal and glucose concentration. However, H_2O_2 also plays a significant role in immunoassay for HRP-based biosensor: neither TMB nor HQ detecting systems can be functional without H_2O_2.

5.4 Conclusion

Based on sandwich ELISA and glucose biosensor, we tried to integrate these enzyme biosensors into one chip. But the results may not show as promising as expected; the sensitivity was limited by the electron transferring by the inactive layer. In order to improvement the experiments, we design to utilize high concentration of the glucose oxidize along with the spatial arrangement of the immunosensor.

Chapter 6

6 Summary and outlook

6.1 Summary

The object of this thesis is to design and develop an electrochemical immunosensor for the specific and sensitive detection of cardiac troponin I with low cost, robustness, time-efficiency and easy-to-operate.

Because amperometric response was obtained through four critical procedures including electrode modification, immunoreaction, signal amplification and amperometric detection, then the immunosensor was investigated by procedures.

First, carbon nanotube (CNT), chitosan and gold nanoparticle (AuNP) were used to modify electrode and to explore the variation in electrochemical behaviors. Experiment conditions were optimized and interferences were investigated. The detection range investigated using cyclic voltammetry (CV) was 0.01 ng/ml to 300 ng/ml on PDDA-MWCNT sensor, 0.001 ng/ml to 500 ng/ml on chitosan-AuNP sensor, respectively. Also, the recorded behavior was linear in the signal versus cTnI concentration, indicating great potential for clinical application.

Second, enzyme labels for signal amplification, ALP and HRP, were studied respectively. Hydrogen peroxide (H_2O_2) is not only the product of glucose oxidize (GOx) catalyzing the oxidation of β-D-glucose by oxygen, but also the needful oxidizing agent in HRP catalysis. Therefore, potentially, HRP-based immunosensor is suitable to integrate immunosensor and enzyme sensor to realize multianalyte detection compacted on one chip. The feasibility was verified by the influence of H_2O_2 concentration of HRP-based biosensor and H_2O_2 quantification on immunosensor with blocking by GOx-BSA.

6.2 Thesis contributions

The immunosensor developed here is an cost-effective, robust and simple-to-use approach to detect cardiac troponin I concentration for cardiac condition diagnostics, especially for point-of-care settings.

A comprehensive investigation has been carried out for experimental variables including nanomaterials modification, experimental condition (temperature, incubation time, pH value and etc.), labeled enzyme, signal generating substrates, and simplifying the detection procedures.

In addition, a concept has been proposed for simultaneously and successively multiplex platform immunosensor. The feasibility was investigated by cTnI immunosensor blocked by GOx-BSA

6.3 Recommendation for future work

One of the most critical objects of this research is to design and develop a CD-platform electrochemical immunosensor for the multiple cardiac biomarkers detection over a wide concentration range along with low detection limits and high sensitivity.

The work showed cTnI immunosensor to be ready for further integrating: Firstly, it can be adapted cTnI immunosensor with blood separation device for an automated whole cardiac diagnostic chip. Secondly, it can be combined with other cardiac biomarkers, such like myoglobin, C - reactive protein (CRP), CK-MB and etc., for diagnosing certain type or stage of cardiac conditions. Thirdly, it can be processed together with glucose, carbamide or lactose sensor for cardiac postoperative vital signs monitoring.

Reference

Adams, J.E., Bodor, G.S., Davilaroman, V.G., Delmez, J.A., Apple, F.S., Ladenson, J.H., and Jaffe, A.S. (1993). Cardiac Troponin I: a marker with high specificity for cardiac injury. Circulation *88*, 101-106.

Ahammad, A.J.S., Choi, Y.H., Koh, K., Kim, J.H., Lee, J.J., and Lee, M. (2011). Electrochemical Detection of Cardiac Biomarker Troponin I at Gold Nanoparticle-Modified ITO Electrode by Using Open Circuit Potential. International Journal of Electrochemical Science *6*, 1906-1916.

Allender S, S.P., Peto V, Raymer M, Leal J, Luengo-Fernandez R. (2008). European cardiovascular disease statistic, 2008 edition. London *British Heart Foundation*.

Alpert, J.S., Antman, E., Apple, F., Armstrong, P.W., Bassand, J.P., de Luna, A.B., Beller, G., Breithardt, G., Chaitman, B.R., Clemmensen, P., *et al.* (2000). Myocardial infarction redefined - A consensus Document of the Joint European Society of Cardiology/American College of Cardiology Committee for the Redefinition of Myocardial Infarction. Journal of the American College of Cardiology *36*, 959-969.

Alpert, J.S., Thygesen, K., Antman, E., Bassand, J.P., Apple, F., Armstrong, P.W., de Luna, A.B., Beller, G., Breithardt, G., Chaitman, B.R., *et al.* (2001). Myocardial infarction redefined - A consensus document of the joint European Society of Cardiology/American College of Cardiology Committee for the redefinition of myocardial infarction (Reprinted from J Am Coll Cardiol, vol 36, pg 959-69, 2000). Clinical Chemistry *47*, 382-392.

Aziz, M.A., Park, S., Jon, S., and Yang, H. (2007). Amperometric immunosensing using an indium tin oxide electrode modified with multi-walled carbon nanotube and poly(ethylene glycol)-silane copolymer. Chemical Communications, 2610-2612.

Aziz, M.A., Patra, S., and Yang, H. (2008). A facile method of achieving low surface coverage of Au nanoparticles on an indium tin oxide electrode and its application to protein detection. Chemical Communications, 4607-4609.

Azzazy, H.M.E., and Christenson, R.H. (2002). Cardiac markers of acute coronary syndromes: is there a case for point-of-care testing? Clinical Biochemistry *35*, 13-27.

Azzazy, H.M.E., and Mansour, M.M.H. (2009). In vitro diagnostic prospects of nanoparticles. Clinica Chimica Acta *403*, 1-8.

Babuin, L., and Jaffe, A.S. (2005). Troponin: the biomarker of choice for the detection of cardiac injury. Can. Med. Assoc. J. *173*, 1191-1202.

Bakker, E. (2004). Electrochemical sensors. Analytical Chemistry *76*, 3285-3298.

Balasubramanian, K., and Burghard, M. (2006). Biosensors based on carbon nanotubes. Analytical and Bioanalytical Chemistry *385*, 452-468.

Bange, A., Tu, J., Zhu, X., Ahn, C., Halsall, H.B., and Heineman, W.R. (2007). Electrochemical detection of MS2 age using a bead-based immunoassay and a NanoIDA. Electroanalysis *19*, 2202-2207.

benjamin Y. part, R.Z., and Marc J. Madou Fabrication of Microelectrode using the lift-off technique. Methods in Molecular Biology *321*, 23-26.

Bertinchant, J.P., Larue, C., Pernel, I., Ledermann, B., FabbroPeray, P., Beck, L., Calzolari, C., Trinquier, S., Nigond, J., and Pau, B. (1996). Release kinetics of serum cardiac troponin I in ischemic myocardial injury. Clinical Biochemistry *29*, 587-594.

Bi, S., Zhou, H., and Zhang, S. (2009). Multilayers enzyme-coated carbon nanotubes as biolabel for ultrasensitive chemiluminescence immunoassay of cancer biomarker. Biosensors and Bioelectronics *24*, 2961-2966.

Birkhahn, R.H., Haines, E., Wen, W.D., Reddy, L., Briggs, W.M., and Datillo, P.A. (2011). Estimating the clinical impact of bringing a multimarker cardiac panel to the bedside in the ED. American Journal of Emergency Medicine *29*, 304-308.

Blick, K.E. (1999). Current trends in automation of immunoassays. Journal of Clinical Ligand Assay *22*, 6-12.

Bodor, G.S., Porter, S., Landt, Y., and Ladenson, J.H. (1992). Development of Monoclonal- antibodies for An Assay of Cardiac Troponin I and Preliminary Results in Suspected Cases of Mypcardial Infarction. Clinical Chemistry *38*, 2203-2214.

Braunwald, E. (2008). Biomarkers in heart failure. New England Journal of Medicine *358*, 2148-2159.

Brieger, D., Eagle, K.A., Goodman, S.G., Steg, P.G., Budaj, A., White, K., Montalescot, G., and Investigators, G. (2004). Acute coronary syndromes without chest pain, an underdiagnosed and undertreated high-risk group - Insights from the Global Registry of Acute Coronary Events. Chest *126*, 461-469.

Brogan, G.X., and Bock, J.L. (1998). Cardiac marker point-of-care testing in the Emergency Department and Cardiac Care Unit. Clinical Chemistry *44*, 1865-1869.

Buhrer-Sekula, S., Smits, H.L., Gussenhoven, G.C., van Leeuwen, J., Amador, S., Fujiwara, T., Klatser, P.R., and Oskam, L. (2003). Simple and fast lateral flow test for classification of leprosy patients and identification of contacts with high risk of developing leprosy. Journal of Clinical Microbiology *41*, 1991-1995.

Burlina, A., Zaninotto, M., Secchiero, S., Rubin, D., and Accorsi, F. (1994). Troponin T-as a marker of ischemic myocardial injury. Clinical Biochemistry *27*, 113-121.

Cabrera, H.A. (1969).A comprehensive evaluation of pregnancy test. American Journal of Obstetrics and Gynecology *103*, 32-&.

Carpenter, C., Shepard, C., and Stevenson, M. (2004). Gate Electrode Formation Process Optimization in a GaAs FET Device.

Cavalcanti, I.T., Silva, B.V.M., Peres, N.G., Moura, P., Sotomayor, M.D.P.T., Guedes, M.I.F., and Dutra, R.F. (2012). A disposable chitosan-modified carbon fiber electrode for dengue virus envelope protein detection. Talanta *91*, 41-46.

CDC Home (2009). Center for disease control and prevention faststats: Heart Disease. http://www.cdc.gov/nchs/fastats/heart.htm.

Chan, C.P.Y., Sanderson, J.E., Glatz, J.F.C., Cheng, W.S., Hempel, A., and Renneberg, R. (2004). A superior early myocardial infarction marker - Human heart-type fatty acid-binding protein. Zeitschrift Fur Kardiologie *93*, 388-397.

Cheng, C.M., Martinez, A.W., Gong, J.L., Mace, C.R., Phillips, S.T., Carrilho, E., Mirica, K.A., and Whitesides, G.M. (2010). Paper-Based ELISA. Angewandte Chemie-International Edition *49*, 4771-4774.

Christenson, R.H., and Azzazy, H.M.E. (1998). Biochemical markers of the acute coronary syndromes. Clinical Chemistry *44*, 1855-1864.

Christenson, R.H., and Azzazy, H.M.E. (2009). Cardiac point of care testing: A focused review of current National Academy of Clinical Biochemistry guidelines and measurement platforms. Clinical Biochemistry *42*, 150-157.

Christenson, R.H., Duh, S.H., Sanhai, W.R., Wu, A.H.B., Holtman, V., Painter, P., Branham, E., Apple, F.S., Murakami, M., and Morris, D.L. (2001). Characteristics of an albumin cobalt binding test for assessment of acute coronary syndrome patients: A multicenter study. Clinical Chemistry *47*, 464-470.

Chua, J.H., Chee, R.-E., Agarwal, A., Wong, S.M., and Zhang, G.-J. (2009). Label-Free Electrical Detection of Cardiac Biomarker with Complementary Metal-Oxide Semiconductor-Compatible Silicon Nanowire Sensor Arrays. Analytical Chemistry *81*, 6266-6271.

Collinson PO (1999). The need for point of care testing: an evidence-based appraisal. Scand J Clin Lab Invest Suppl *230*, 67-73.

Collinson, P.O., Jorgensen, B., Sylven, C., Haass, M., Chwallek, F., Katus, H.A., Muller-Bardorff, M., Derhaschnig, U., Hirschl, M.M., and Zerback, R. (2001). Recalibration of the point-of-care test for CARDIAC T Quantitative with Elecsys Troponin T 3rd generation. Clinica Chimica Acta *307*, 197-203.

Corgier, B.P., Marquette, C.A., and Blum, L.J. (2005). Diazonium-protein adducts for graphite electrode microarrays modification: Direct and addressed electrochemical immobilization. Journal of the American Chemical Society *127*, 18328-18332.

Corgier, B.P., Marquette, C.A., and Blum, L.J. (2007). Direct electrochemical addressing of immunoglobulins: Immuno-chip on screen-printed microarray. Biosensors & Bioelectronics *22*, 1522-1526.

Crew, A., Alford, C., Cowell, D.C.C., and Hart, J.P. (2007). Development of a novel electrochemical immuno-assay using a screen printed electrode for the determination of secretory immunoglobulin A in human sweat. Electrochimica Acta *52*, 5232-5237.

D'Orazio, P. (2011). Biosensors in clinical chemistry-2011 update. Clinica Chimica Acta *412*, 1749-1761.

Daniels, J.S., and Pourmand, N. (2007). Label-free impedance biosensors: Opportunities and challenges. Electroanalysis *19*, 1239-1257.

Das, J., Jo, K., Lee, J.W., and Yang, H. (2007). Electrochemical immunosensor using p-aminophenol redox cycling by hydrazine combined with a low background current. Analytical Chemistry *79*, 2790-2796.

Davis, J.J., Coleman, K.S., Azamian, B.R., Bagshaw, C.B., and Green, M.L.H. (2003). Chemical and biochemical sensing with modified single walled carbon nanotubes. Chemistry-a European Journal *9*, 3732-3739.

de Lemos, J.A., Morrow, D.A., Bentley, J.H., Omland, T., Sabatine, M.S., McCabe, C.H., Hall, C., Cannon, C.P., and Braunwald, E. (2001). The prognostic value of B-type natriuretic peptide in patients with acute coronary syndromes. New England Journal of Medicine *345*, 1014-1021.

de Mattos, I.L., Gorton, L., and Ruzgas, T. (2003). Sensor and biosensor based on Prussian Blue modified gold and platinum screen printed electrodes. Biosensors and Bioelectronics *18*, 193-200.

Delaney, J.L., Hogan, C.F., Tian, J., and Shen, W. (2011). Electrogenerated Chemiluminescence Detection in Paper-Based Microfluidic Sensors. Analytical Chemistry *83*, 1300-1306.

Di Serio, F., Lovero, R., Leone, M., De Sario, R., Ruggieri, V., Varraso, L., and Pansini, N. (2006). Integration between the Tele-Cardiology Unit and the central laboratory: methodological and clinical evaluation of point-of-care testing cardiac marker in the ambulance. Clinical Chemistry and Laboratory Medicine *44*, 768-773.

Dong, H., Li, C.M., Zhang, Y.F., Cao, X.D., and Gan, Y. (2007). Screen-printed microfluidic device for electrochemical immunoassay. Lab on a Chip *7*, 1752-1758.

Doron, A., Katz, E., and Willner, I. (1995). Organization of Au colloids as monolayer films onto ITO glass surfaces- application of the metal colloid films as base interfaces to construct redox-active monolayers. Langmuir *11*, 1313-1317.

Drummond, T.G., Hill, M.G., and Barton, J.K. (2003). Electrochemical DNA sensors. Nature Biotechnology *21*, 1192-1199.

Du Clos, T.W. (2000). Function of C-reactive protein. Annals of Medicine *32*, 274-278.

Duan, X.F., and Lieber, C.M. (2000). General synthesis of compound semiconductor nanowires. Advanced Materials *12*, 298-302.

Elliott, J.M., Birkin, P.R., Bartlett, P.N., and Attard, G.S. (1999). Platinum microelectrodes with unique high surface areas. Langmuir *15*, 7411-7415.

Fanjul-Bolado, P., Gonzalez-Garia, M.B., and Costa-Garcia, A. (2005). Amperometric detection in TMB/HRP-based assays. Analytical and Bioanalytical Chemistry *382*, 297-302.

Fanjul-Bolado, P., Hernandez-Santos, D., Gonzalez-Garcia, M.B., and Costa-Garcia, A. (2007). Alkaline phosphatase-catalyzed silver deposition for electrochemical detection. Analytical Chemistry *79*, 5272-5277.

Fragoso, A., Latta, D., Laboria, N., von Germar, F., Hansen-Hagge, T.E., Kemmner, W., Gartner, C., Klemm, R., Drese, K.S., and O'Sullivan, C.K. (2011). Integrated microfluidic platform for the electrochemical detection of breast cancer markers in patient serum samples. Lab on a Chip *11*, 625-631.

Fraser, C.G. (2001). Optimal analytical performance for point of care testing. Clinica Chimica Acta *307*, 37-43.

Galla, J.M., Mahaffey, K.W., Sapp, S.K., Alexander, J.H., Roe, M.T., Ohman, E.M., Granger, C.B., Armstrong, P.W., Harrington, R.A., White, H.D., *et al.* (2006). Elevated creatine kinase-MB with normal creatine kinase predicts worse outcomes in patients with acute coronary syndromes: Results from 4 large clinical trials. American Heart Journal *151*, 16-24.

Gao, M., Dai, L., and Wallace, G.G. (2003). Glucose sensors based on glucose-oxidase-containing polypyrrole/aligned carbon nanotube coaxial nanowire electrodes. Synthetic Metals *137*, 1393-1394.

Ge, L., Wang, S.M., Song, X.R., Ge, S.G., and Yu, J.H. (2012). 3D Origami-based multifunction-integrated immunodevice: low-cost and multiplexed sandwich chemiluminescence immunoassay on microfluidic paper-based analytical device. Lab on a Chip *12*, 3150-3158.

Gibler, W.B., Lewis, L.M., Erb, R.E., Makens, P.K., Kaplan, B.C., Vaughn, R.H., Biagini, A.V., Blanton, J.D., and Campbell, W.B. (1990). Early detection of acute myocardial infarction in patients presenting with chest pain and nondiagnostic ECGs - serial CK-MB sampling in the emergency department. Annals of Emergency Medicine *19*, 1359-1366.

Glatz, J.F.C., van der Voort, D., and Hermens, W.T. (2002). Fatty acid-binding protein as the earliest available plasma marker of acute myocardial injury. Journal of Clinical Ligand Assay *25*, 167-177.

Godfrey, C., Harrison, M.B., Medves, J., and Tranmer, J.E. (2006). The symptom of pain with heart failure: A systematic review. Journal of Cardiac Failure *12*, 307-313.

Golden, J., Miller, H., Nawrocki, D., and Ross, J. (2009). Optimization of Bi-layer Lift-Off Resist Process. CS Mantech Technical Digest.

Guo, Z., Fan, X., Liu, L., Bian, Z., Gu, C., Zhang, Y., Gu, N., Yang, D., and Zhang, J. (2010). Achieving high-purity colloidal gold nanoprisms and their application as biosensing platforms. Journal of Colloid and Interface Science *348*, 29-36.

Gyurcsanyi, R.E., Bereczki, A., Nagy, G., Neuman, M.R., and Lindner, E. (2002). Amperometric microcells for alkaline phosphatase assay. Analyst *127*, 235-240.

Ha, S.-M., Cho, W., and Ahn, Y. (2009). Disposable thermo-pneumatic micropurnp for bio lab-on-a-chip application. Microelectronic Engineering *86*, 1337-1339.

Hedges, J.R., Gibler, W.B., Young, G.P., Hoekstra, J.W., Slovis, C., Aghababian, R., Smith, M., and Rubison, M. (1996). Multicenter study of creatine kinase-MB use: Effect on chest pain clinical decision making. Acad. Emerg. Med. *3*, 7-15.

Heller, A., and Feldman, B. (2008). Electrochemical glucose sensors and their applications in diabetes management. Chemical reviews *108*, 2482-2505.

Henares, T.G., Tsutsumi, E., Yoshimura, H., Kawamura, K., Yao, T., and Hisamoto, H. (2010). Single-step ELISA capillary sensor based on surface-bonded glucose oxidase, antibody, and physically-adsorbed PEG membrane containing peroxidase-labeled antibody. Sensors and Actuators B: Chemical *149*, 319-324.

Hoekstra, J.W., Hedges, J.R., Gibler, W.B., Rubison, R.M., and Christensen, R.A. (1994). Emergency department CK-MB: a predictor of ischemic complications. National cooperative CK-MB project group. Academic emergency medicine : official journal of the Society for Academic Emergency Medicine *1*, 17-27.

Hong, B., and Kang, K.A. (2006). Biocompatible, nanogold-particle fluorescence enhancer for fluorophore mediated, optical immunosensor. Biosensors & Bioelectronics *21*, 1333-1338.

Hunt, S.A., Baker, D.W., Chin, M.H., Cinquegrani, M.P., Feldman, A.M., Francis, G.S., Ganiats, T.G., Goldstein, S., Gregoratos, G., Jessup, M.L., *et al.* (2001). ACC/AHA guidelines for the evaluation and management of chronic heart failure in the adult: Executive summary - A report of the American College of Cardiology/American Heart Association Task Force on Practice Guidelines (Committee to revise the 1995 Guidelines for the Evaluation and Management of Heart Failure). Journal of the American College of Cardiology *38*, 2101-2113.

Hwang, S., Kim, E., and Kwak, J. (2005). Electrochemical detection of DNA hybridization using biometallization. Analytical Chemistry *77*, 579-584.

Ionescu, R.E., Gondran, C., Cosnier, S., Gheber, L.A., and Marks, R.S. (2005). Comparison between the performances of amperometric immunosensors for cholera antitoxin based on three enzyme markers. Talanta *66*, 15-20.

Ionescu, R.E., Gondran, C., Gheber, L.A., Cosnier, S., and Marks, R.S. (2004). Construction of amperometric immunosensors based on the electrogeneration of a permeable biotinylated polypyrrole film. Analytical Chemistry *76*, 6808-6813.

Jeremias, A., and Gibson, C.M. (2005). Narrative review: Alternative causes for elevated cardiac troponin levels when acute coronary syndromes are excluded. Annals of Internal Medicine *142*, 786-791.

Jernberg, T., James, S., Lindahl, B., Stridsberg, M., Venge, P., and Wallentin, L. (2004). NT-proBNP in unstable coronary artery disease - experiences from the FAST, GUSTO IV and FRISC II trials. European Journal of Heart Failure *6*, 319-325.

Justino, C.I.L., Rocha-Santos, T.A., and Duarte, A.C. (2010). Review of analytical figures of merit of sensors and biosensors in clinical applications. Trac-Trends in Analytical Chemistry *29*, 1172-1183.

Kang, H.J., Aziz, M.A., Jeon, B., Jo, K., and Yang, H. (2009). Strategy for Low Background-Current Levels in the Electrochemical Biosensors Using Horse-Radish Peroxidase Labels. Electroanalysis *21*, 2647-2652.

Kannan, R., Parthasarathy, M., Maraveedu, S.U., Kurungot, S., and Pillai, V.K. (2009). Domain size manipulation of perflouorinated polymer electrolytes by sulfonic acid-functionalized MWCNTs to enhance fuel cell performance. Langmuir *25*, 8299-8305.

Karyakin, A.A. (2001). Prussian blue and its analogues: electrochemistry and analytical applications. Electroanalysis *13*, 813-819.

Karyakin, A.A., Gitelmacher, O.V., and Karyakina, E.E. (1995). Prussian Blue-based first-generation biosensor. A sensitive amperometric electrode for glucose. Analytical Chemistry *67*, 2419-2423.

Karyakin, A.A., Karyakina, E.E., and Gorton, L. (1996). Prussian-Blue-based amperometric biosensors in flow-injection analysis. Talanta *43*, 1597-1606.

Karyakin, A.A., Karyakina, E.E., and Gorton, L. (2000). Amperometric biosensor for glutamate using Prussian blue-based "artificial peroxidase" as a transducer for hydrogen peroxide. Analytical Chemistry *72*, 1720-1723.

Karyakin, A.A., Puganova, E.A., Budashov, I.A., Kurochkin, I.N., Karyakina, E.E., Levchenko, V.A., Matveyenko, V.N., and Varfolomeyev, S.D. (2004). Prussian blue based nanoelectrode arrays for H2O2 detection. Analytical Chemistry *76*, 474-478.

Katus, H.A., Remppis, A., Looser, S., Hallermeier, K., Scheffold, T., and Kubler, W. (1989). Enzyme Linked Immunoassay of Cardiac Troponin T for the Detection of Acute Myocardial Infarction in Patients. Journal of Molecular and Cellular Cardiology *21*, 1349-1353.

Kemp, B.E., Rylatt, D.B., Bundesen, P.G., Doherty, R.R., McPhee, D.A., Stapleton, D., Cottis, L.E., Wilson, K., John, M.A., Khan, J.M., *et al.* (1988). Autologous red-cell agglutination assay for HIV-1 antibodies-simplified test with whole blood. Science *241*, 1352-1354.

Kerman, K., Saito, M., Yamamura, S., Takamura, Y., and Tamiya, E. (2008). Nanomaterial-based electrochemical biosensors for medical applications. Trac-Trends in Analytical Chemistry *27*, 585-592.

Kim, B., Park, H., and Sigmund, W.M. (2003). Electrostatic interactions between shortened multiwall carbon nanotubes and polyelectrolytes. Langmuir *19*, 2525-2527.

Kim, B., and Sigmund, W.M. (2003). Self-alignment of shortened multiwall carbon nanotubes on polyelectrolyte layers. Langmuir *19*, 4848-4851.

Kost, G.J., and Tran, N.K. (2005). Point-of-care testing and cardiac biomarkers: The standard of care and vision for chest pain centers. Cardiology Clinics *23*, 467-+.

Kurita, R., Yokota, Y., Sato, Y., Mizutani, F., and Niwa, O. (2006). On-chip enzyme immunoassay of a cardiac marker using a microfluidic device combined with a portable surface plasmon resonance system. Analytical Chemistry *78*, 5525-5531.

Kurkina, T., and Balasubramanian, K. (2012). Towards in vitro molecular diagnostics using nanostructures. Cell. Mol. Life Sci. *69*, 373-388.

Kwon, S.J., Yang, H., Jo, K., and Kwak, J. (2008). An electrochemical immunosensor using p-aminophenol redox cycling by NADH on a self-assembled monolayer and ferrocene-modified Au electrodes. Analyst *133*, 1599-1604.

Ladue JS, Wroblewski F, and Karmen A (1954). Serum glutamic xoaloacetic transaminase activity in human acute transmural mypcardial infarction. Science *120*, 497-499.

Lahann, J., Balcells, M., Lu, H., Rodon, T., Jensen, K.F., and Langer, R. (2003). Reactive polymer coatings: A first step toward surface engineering of microfluidic devices. Analytical Chemistry *75*, 2117-2122.

Lee-Lewandrowski, E., Corboy, D., Lewandrowski, K., Sinclair, J., McDermot, S., and Benzer, T.I. (2003). Implementation of a point-of-care satellite laboratory in the emergency department of an academic medical center - Impact on test turnaround time and patient emergency department length of stay. Archives of Pathology & Laboratory Medicine *127*, 456-460.

Lewandrowski, K., Chen, A., and Januzzi, J. (2002). Cardiac markers for myocardial infarction. A brief review. American journal of clinical pathology *118 Suppl*, S93-99.

Licka, M., Zimmermann, R., Zehelein, J., Dengler, T.J., Katus, H.A., and Kubler, W. (2002). Troponin T concentrations 72 hours after myocardial infarction as a serological estimate of infarct size. Heart *87*, 520-524.

Life Technologies Chemical Crosslinking Reagents- Section 5.2. http://www.invitrogen.com/site/us/en/home/References/Molecular-Probes-The-Handbook/Crosslinking-and-Photoactivatable-Reagents/Chemical-Crosslinking-Reagents.html.

Lin, C.-C., Wang, J.-H., Wu, H.-W., and Lee, G.-B. (2010a). Microfluidic Immunoassays. Jala *15*, 253-274.

Lin, C.C., Wang, J.H., Wu, H.W., and Lee, G.B. (2010b). Microfluidic Immunoassays. Jala *15*, 253-274.

Lin, D.H., Taylor, C.R., Anderson, W.F., Scherer, A., and Kartalov, E.P. (2010c). Internally calibrated quantification of VEGF in human plasma by fluorescence immunoassays in disposable elastomeric microfluidic devices*. Journal of Chromatography B-Analytical Technologies in the Biomedical and Life Sciences *878*, 258-263.

Lin, J., He, C., Pang, X., and Hu, K. (2011). Amperometric Immunosensor for Prostate Specific Antigen Based on Gold Nanoparticles Ionic Liquid Chitosan Hybrid Film. Analytical Letters *44*, 908-921.

Liu, G., and Lin, Y. (2007). Nanomaterial labels in electrochemical immunosensors and immunoassays. Talanta *74*, 308-317.

Liu, H., and Crooks, R.M. (2011). Three-Dimensional Paper Microfluidic Devices Assembled Using the Principles of Origami. Journal of the American Chemical Society *133*, 17564-17566.

Liuzzo, G., Biasucci, L.M., Gallimore, J.R., Grillo, R.L., Rebuzzi, A.G., Pepys, M.B., and Maseri, A. (1994). The prognostic value of C-reaction protein and serum amyloid- a protein in servere unstable angina. New England Journal of Medicine *331*, 417-424.

Luckham, R.E., and Brennan, J.D. (2010). Bioactive paper dipstick sensors for acetylcholinesterase inhibitors based on sol-gel/enzyme/gold nanoparticle composites. Analyst *135*, 2028-2035.

Luo, X.L., Morrin, A., Killard, A.J., and Smyth, M.R. (2006). Application of nanoparticles in electrochemical sensors and biosensors. Electroanalysis *18*, 319-326.

Mabey, D., Peeling, R.W., Ustianowski, A., and Perkins, M.D. (2004). Diagnostics for the developing world. Nature Reviews Microbiology *2*, 231-240.

Mair, J., Artnerdworzak, E., Lechleitner, P., Morass, B., Smidt, J., Wagner, I., Dienstl, F., and Puschendorf, B. (1992). Early diagnosis of acute myocardial infarction by a newly developed rapid immunoturbidimetric assay for myoglobin. British Heart Journal *68*, 462-468.

Males, R.G., Stephenson, J., and Harris, P. (2001). Cardiac markers and point-of-care testing: a perfect fit. Critical care nursing quarterly *24*, 54-61.

Manesh, K., Kim, H.T., Santhosh, P., Gopalan, A., and Lee, K.P. (2008). A novel glucose biosensor based on immobilization of glucose oxidase into multiwall carbon nanotubes–polyelectrolyte-loaded electrospun nanofibrous membrane. Biosensors and Bioelectronics *23*, 771-779.

Mao, H.B., Yang, T.L., and Cremer, P.S. (2002). Design and characterization of immobilized enzymes in microfluidic systems. Analytical Chemistry *74*, 379-385.

Martins, J.T., Li, D.J., Baskin, L.B., Jialal, I., and Keffer, J.H. (1996). Comparison of cardiac troponin I and lactate dehydrogenase isoenzymes for the late diagnosis of myocardial injury. American journal of clinical pathology *106*, 705-708.

MATTOS, I.L., Gorton, L., Ruzgas, T., and Karyakin, A.A. (2000). Sensor for hydrogen peroxide based on Prussian Blue modified electrode: improvement of the operational stability. Analytical Sciences *16*, 795-798.

McBride JD, C.M., . (2008). A high sensitivity assay for the inflammatory marker C-reactive protein employing acoustic biosensing. J Nanobiotechnol *6*.

McDonnell, B., Hearty, S., Leonard, P., and O'Kennedy, R. (2009). Cardiac biomarkers and the case for point-of-care testing. Clinical Biochemistry *42*, 549-561.

Merkoci, A. (2007). Electrochemical biosensing with nanoparticles. Febs Journal *274*, 310-316.

MicroChem Corp (2001). MicroChem LOR Lift-off Resist http://microchem.com/pdf/PMGI-Resists-data-sheetV-rhcedit-102206.pdf.

Mizuno, K., Satomura, K., Miyamoto, A., Arakawa, K., Shibuya, T., Arai, T., Kurita, A., Nakamura, H., and Ambrose, J.A. (1992). Angioscopic Evaluation of Coronary- artery Thrombi in Acute Coronary Syndromes. New England Journal of Medicine *326*, 287-291.

Mohammed, M.I., and Desmulliez, M.P.Y. (2011). Lab-on-a-chip based immunosensor principles and technologies for the detection of cardiac biomarkers: a review. Lab on a Chip *11*, 569-595.

Morrow, D.A. (2004). Evidence-based decision limits for cardiac troponin: Low-level elevation and prognosis. American Heart Journal *148*, 739-742.

Morrow, D.A., Cannon, C.P., Jesse, R.L., Newby, L.K., Ravkilde, J., Storrow, A.B., Wu, A.H.B., Christenson, R.H., Apple, F.S., Francis, G., *et al.* (2007). National Academy of Clinical Biochemistry Laboratory Medicine Practice Guidelines: Clinical characteristics and utilization of biochemical markers in acute coronary syndromes. Clinical Chemistry *53*, 552-574.

Nam, J.M., Stoeva, S.I., and Mirkin, C.A. (2004). Bio-bar-code-based DNA detection with PCR-like sensitivity. Journal of the American Chemical Society *126*, 5932-5933.

Nam, J.M., Thaxton, C.S., and Mirkin, C.A. (2003). Nanoparticle-based bio-bar codes for the ultrasensitive detection of proteins. Science *301*, 1884-1886.

Newby, L.K., Goldmann, B.U., and Ohman, E.M. (2003). Troponin: An important prognostic marker and risk-stratification tool in non-ST-segment elevation acute coronary syndromes. Journal of the American College of Cardiology *41*, 31S-36S.

O'Regan, T., Pravda, M., O'Sullivan, C.K., and Guilbault, G.G. (2003). Development of biosensor array for rapid detection of cardiac markers: Immunosensor for detection of free cardiac troponin I. Analytical Letters *36*, 1903-1920.

O'Regan, T.M., Pravda, M., O'Sullivan, C.K., and Guilbault, G.G. (2002). Development of a disposable immunosensor for the detection of human heart fatty-acid binding protein in human whole blood using screen-printed carbon electrodes. Talanta *57*, 501-510.

Panteghini, M. (1998). Diagnostic application of CK-MB mass determination. Clinica Chimica Acta *272*, 23-31.

Panteghini, M., Cuccia, C., Bonetti, G., Giubbini, R., Pagani, F., and Bonini, E. (2002). Single-point cardiac troponin T at coronary care unit discharge after myocardial infarction correlates with infarct size and ejection fraction. Clinical Chemistry *48*, 1432-1436.

Panteghini, M., Pagani, F., Yeo, K.T.J., Apple, F.S., Christenson, R.H., Dati, F., Mair, J., Ravkilde, J., Wu, A.H.B., and Comm Standardization Markers, C. (2004). Evaluation of imprecision for cardiac troponin assays at low-range concentrations. Clinical Chemistry *50*, 327-332.

Payne, D. (1988). Use and limitations of light-microscopy for diagnosing malaria at the primary health-care level. Bulletin of the World Health Organization *66*, 621-626.

Pelsers, M., Hermens, W.T., and Glatz, J.F.C. (2005). Fatty acid-binding proteins as plasma markers of tissue injury. Clinica Chimica Acta *352*, 15-35.

Penney, M.D. (2005). Natriuretic peptides and the heart: current and future implications for clinical biochemistry. Annals of Clinical Biochemistry *42*, 432-440.

Pfister, R., and Schneider, C.A. (2004). Natriuretic peptides BNP and NT-pro-BNP: established laboratory markers in clinical practice or just perspectives? Clinica Chimica Acta *349*, 25-38.

Pham, M.X., Whooley, M.A., Evans, G.T., Liu, C., Emadi, H., Tong, W., Murphy, M.C., and Fleischmann, K.E. (2004). Prognostic value of low-level cardiac troponin-1 elevations in patients without definite acute coronary syndromes. American Heart Journal *148*, 776-782.

Piao, M.H., Yang, D.S., Yoon, K.R., Lee, S.H., and Choi, S.H. (2009). Development of an Electrogenerated Chemiluminescence Biosensor using Carboxylic acid-functionalized MWCNT and Au Nanoparticles. Sensors *9*, 1662-1677.

Preechaworapun, A., Dai, Z., Xiang, Y., Chailapakul, O., and Wang, J. (2008). Investigation of the enzyme hydrolysis products of the substrates of alkaline phosphatase in electrochemical immunosensing. Talanta *76*, 424-431.

Punukollu, H., Khan, I.A., Punukollu, G., Gowda, R.M., Mendoza, C., and Sacchi, T.J. (2005). Acute pulmonary embolism in elderly: clinical characteristics and outcome. International Journal of Cardiology *99*, 213-216.

Remme, W.J., Swedberg, K., and European Soc, C. (2001). Guidelines for the diagnosis and treatment of chronic heart failure. European Heart Journal *22*, 1527-1560.

Ricci, F., Amine, A., Tuta, C.S., Ciucu, A.A., Lucarelli, F., Palleschi, G., and Moscone, D. (2003). Prussian Blue and enzyme bulk-modified screen-printed electrodes for hydrogen peroxide and glucose determination with improved storage and operational stability. Analytica chimica acta *485*, 111-120.

Ridderhof, J.C., van Deun, A., Kam, K.M., Narayanan, P.R., and Aziz, M.A. (2007). Roles of laboratories and laboratory systems in effective tuberculosis programmes. Bulletin of the World Health Organization *85*, 354-359.

Rivas, G.A., Rubianes, M.D., Rodriguez, M.C., Ferreyra, N.E., Luque, G.L., Pedano, M.L., Miscoria, S.A., and Parrado, C. (2007). Carbon nanotubes for electrochemical biosensing. Talanta *74*, 291-307.

Rochette, J.F., Sacher, E., Meunier, M., and Luong, J.H.T. (2005). A mediatorless biosensor for putrescine using multiwalled carbon nanotubes. Analytical Biochemistry *336*, 305-311.

Roesch, W.J., and Hamada, D.J.M. (2004). Studying yield and reliability relationships for metal defects. In ROCS Workshop, 2004.[Reliability of Compound Semiconductors] (IEEE), pp. 121-133.

Rosen S (2004). Market outlook for IVDs. IVD Tech *10*, 39-43.

Saito, T., Matsushige, K., and Tanaka, K. (2002). Chemical treatment and modification of multi-walled carbon nanotubes. Physica B: Condensed Matter *323*, 280-283.

Sluss, P.M. (2006). Cardiac Markers: Current Technologies for Their Measurement at Points of Care. Point of Care *5*, 38-46.

St-Louis, P. (2000). Status of point-of-care testing: Promise, realities, and possibilities. Clinical Biochemistry *33*, 427-440.

Stedtfeld, R.D., Tourlousse, D.M., Seyrig, G., Stedtfeld, T.M., Kronlein, M., Price, S., Ahmad, F., Gulari, E., Tiedje, J.M., and Hashsham, S.A. (2012). Gene-Z: a device for point of care genetic testing using a smartphone. Lab on a Chip *12*, 1454-1462.

Storrow, A.B., and Gibler, W.B. (1999). The role of cardiac markers in the emergency department. Clinica Chimica Acta *284*, 187-196.

Sun, W., Jiao, K., Zhang, S.S., Zhang, C.L., and Zhang, Z.F. (2001). Electrochemical detection for horseradish peroxidase-based enzyme immunoassay using p-aminophenol as substrate and its application in detection of plant virus. Analytica Chimica Acta *434*, 43-50.

Suprun, E., Bulko, T., Lisitsa, A., Gnedenko, O., Ivanov, A., Shumyantseva, V., and Archakov, A. (2010). Electrochemical nanobiosensor for express diagnosis of acute myocardial infarction in undiluted plasma. Biosensors & Bioelectronics *25*, 1694-1698.

Suprun, E.V., Shilovskaya, A.L., Lisitsa, A.V., Bulko, T.V., Shumyantseva, V.V., and Archakov, A.I. (2011). Electrochemical Immunosensor Based on Metal Nanoparticles for Cardiac Myoglobin Detection in Human Blood Plasma. Electroanalysis *23*, 1051-1057.

Tang, H.T., Lunte, C.E., Halsall, H.B., and Heineman, W.R. (1988). P-Aminophenyl Phosphate- An Improved Substrate for Electrochemical Enzyme Immunoassay. Analytica Chimica Acta *214*, 187-195.

Tang, J., Tang, D., Su, B., Huang, J., Qiu, B., and Chen, G. (2011). Enzyme-free electrochemical immunoassay with catalytic reduction of p-nitrophenol and recycling of p-aminophenol using gold nanoparticles-coated carbon nanotubes as nanocatalysts. Biosensors & Bioelectronics *26*, 3219-3226.

Thevenot, D.R., Toth, K., Durst, R.A., and Wilson, G.S. (2001). Electrochemical biosensors: recommended definitions and classification. Biosensors & Bioelectronics *16*, 121-131.

Tomonaga, Y., Gutzwiller, F., Luscher, T.F., Riesen, W.F., Hug, M., Diemand, A., Schwenkglenks, M., and Szucs, T.D. (2011). Diagnostic accuracy of point-of-care testing for acute coronary syndromes, heart failure and thromboembolic events in primary care: a cluster-randomised controlled trial. Bmc Family Practice *12*.

Volpe, G., Compagnone, D., Draisci, R., and Palleschi, G. (1998). 3,3 ',5,5 '-tetramethylbenzidine as electrochemical substrate for horseradish peroxidase based enzyme immunoassays. A comparative study. Analyst *123*, 1303-1307.

von Lode, P. (2005). Point-of-care immunotesting: Approaching the analytical performance of central laboratory methods. Clinical Biochemistry *38*, 591-606.

Wanekaya, A.K., Chen, W., Myung, N.V., and Mulchandani, A. (2006). Nanowire-based electrochemical biosensors. Electroanalysis *18*, 533-550.

Wang, C., Chen, S., Xiang, Y., Li, W., Zhong, X., Che, X., and Li, J. (2011). Glucose biosensor based on the highly efficient immobilization of glucose oxidase on Prussian blue-gold nanocomposite films. Journal of Molecular Catalysis B: Enzymatic *69*, 1-7.

Wang, J. (2005). Carbon-nanotube based electrochemical biosensors: A review. Electroanalysis *17*, 7-14.

Wei, J.Y., Mu, Y., Song, D.Q., Fang, X.X., Liu, X., Bu, L.S., Zhang, H.Q., Zhang, G.Z., Ding, J.H., Wang, W.Z., *et al.* (2003). A novel sandwich immunosensing method for measuring cardiac troponin I in sera. Analytical Biochemistry *321*, 209-216.

Weibel, M.K., and Bright, H.J. (1971). Glucose oxidase mechanism- interpretation of Ph dependence. Journal of Biological Chemistry *246*, 2734-&.

Wen, D., Liu, Y., Yang, G.C., and Dong, S.J. (2007). Electrochemistry of glucose oxidase immobilized on the carbon nanotube wrapped by polyelectrolyte. Electrochimica Acta *52*, 5312-5317.

Wilson, M.S. (2005). Electrochemical immunosensors for the simultaneous detection of two tumor markers. Analytical Chemistry *77*, 1496-1502.

Wilson, M.S., and Rauh, R.D. (2004). Hydroquinone diphosphate: an alkaline phosphatase substrate that does not produce electrode fouling in electrochemical immunoassays. Biosensors & Bioelectronics *20*, 276-283.

Wu, A.H.B. (2005). Markers for early detection of cardiac diseases. Scandinavian Journal of Clinical & Laboratory Investigation *65*, 112-121.

Wu, A.H.B., Apple, F.S., Gibler, W.B., Jesse, R.L., Warshaw, M.M., and Valdes, R. (1999). National Academy of Clinical Biochemistry standards of laboratory practice: Recommendations for the use of cardiac markers in coronary artery diseases. Clinical Chemistry *45*, 1104-1121.

Xue, M.H., Xu, Q., Zhou, M., and Zhu, J.J. (2006). In situ immobilization of glucose oxidase in chitosan-gold nanoparticle hybrid film on Prussian Blue modified electrode for high-sensitivity glucose detection. Electrochemistry Communications *8*, 1468-1474.

Yager, P., Domingo, G.J., and Gerdes, J. (2008). Point-of-care diagnostics for global health. In Annual Review of Biomedical Engineering (Palo Alto: Annual Reviews), pp. 107-144.

Yang, H., Yuan, R., Chai, Y., and Zhuo, Y. (2011). Electrochemically deposited nanocomposite of chitosan and carbon nanotubes for detection of human chorionic gonadotrophin. Colloids and Surfaces B-Biointerfaces *82*, 463-469.

Yang, Z., and Zhou, D.M. (2006). Cardiac markers and their point-of-care testing for diagnosis of acute myocardial infarction. Clinical Biochemistry *39*, 771-780.

Young, G.P., Hedges, J.R., Gibler, W.B., Green, T.R., and Swanson, R. (1991). Do CK-MB Results Affect Chest Pain Decision- making in the Emergency Department. Annals of Emergency Medicine *20*, 1220-1228.

Zang, D.J., Ge, L., Yan, M., Song, X.R., and Yu, J.H. (2012). Electrochemical immunoassay on a 3D microfluidic paper-based device. Chemical Communications *48*, 4683-4685.

Zaytseva, N.V., Goral, V.N., Montagna, R.A., and Baeumner, A.J. (2005). Development of a microfluidic biosensor module for pathogen detection. Lab on a Chip *5*, 805-811.

Zeng, J.X., Wei, W.Z., Liu, X.Y., Wang, Y., and Luo, G.M. (2008). A simple method to fabricate a Prussian Blue nanoparticles/carbon nanotubes/poly(1,2-diaminobenzene) based glucose biosensor. Microchimica Acta *160*, 261-267.

Zhou, F., Lu, M., Wang, W., Bian, Z.P., Zhang, J.R., and Zhu, J.J. (2010). Electrochemical Immunosensor for Simultaneous Detection of Dual Cardiac Markers Based on a Poly(Dimethylsiloxane)-Gold Nanoparticles Composite Microfluidic Chip: A Proof of Principle. Clinical Chemistry *56*, 1701-1707.

Curriculum Vitae

Name:	Yang Cheng
Post-secondary Education and Degrees:	Donghua University Shanghai, China 2004-2008 B.Sc. The University of Western Ontario London, Ontario, Canada 2010-2012 M.Sc
Honours and Awards:	Western Graduate Research Scholarship The University of Western Ontario, Canada 2011-2012 Undergraduate Student Scholarship Donghua University Shanghai, China
Related Work Experience	Teaching Assistant The University of Western Ontario 2011-2012